

Effect of maternal diabetes on the β -cell health in the offspring –
lessons from offspring of MIDY pigs

von Libera Valla

Inaugural-Dissertation zur Erlangung der Doktorwürde
(Dr. rer. biol. vet.)
der Tierärztlichen Fakultät der Ludwig-Maximilians-
Universität München

Effect of maternal diabetes on the β -cell health in the offspring -
lessons from offspring of MIDY pigs

von Libera Valla
aus Bitonto, Italien

München 2024

Aus dem Veterinärwissenschaftlichen Department
der Tierärztlichen Fakultät
der Ludwig-Maximilians-Universität München

Lehrstuhl für Molekulare Tierzucht und Biotechnologie

Arbeit angefertigt unter der Leitung von:

Univ.-Prof. Dr. Eckhard Wolf

Mitbetreuung durch:

Priv.-Doz. Dr. Elisabeth Kemter

Gedruckt mit Genehmigung der Tierärztlichen Fakultät
der Ludwig-Maximilians-Universität München

Dekan: Univ.-Prof. Dr. Reinhard K. Straubinger, Ph.D.

Berichterstatter: Univ.-Prof. Dr. Eckhard Wolf

Korreferent: Univ.-Prof. Dr. Gabriela Knubben

Tag der Promotion: 6. Juli 2024

Posters, presentations and paper

DZD German Centre for Diabetes Research (Dresden - 11th-12th October 2022) – poster

Title: The effect of maternal diabetes on β -cell health in offspring

The Swine in Biomedical Research Conference (Madison, WI (USA) - 10th-14th of June 2022) – poster

Title: The effect of maternal diabetes on β -cell health in offspring: lesson from MIDY pigs

Gene Centre Seminar Retreat (30th-31st of May and 1st of June 2022) – poster

Title: The effect of maternal diabetes on β -cell health in offspring: lesson from MIDY pigs

Gene Centre Seminar Meeting (online - 24th January 2022) – presentation

Title: The effect of maternal diabetes on β -cell health in offspring

Paper: **Maternal hyperglycaemia induces alterations in hepatic amino acid, glucose and lipid metabolism of neonatal offspring: Multi-omics insights from a diabetic pig model**

Bachuki Shashikadze, **Libera Valla**, Salvo Danilo Lombardo, Cornelia Prehn, Mark Haid, Fabien Riols, Jan Bernd Stöckl, Radwa Elkhateib, Simone Renner, Birgit Rathkolb, Jörg Menche, Martin Hrabě de Angelis, Eckhard Wolf, Elisabeth Kemter, Thomas Fröhlich

DOI: 10.1016/j.molmet.2023.101768 (Shashikadze, Valla et al. 2023)

TABLE OF CONTENTS

| | |
|---|-----------|
| I. INTRODUCTION | 1 |
| II. REVIEW OF THE LITERATURE | 3 |
| 1. Maternal diabetes mellitus and effects on offspring: what is known in humans? | 3 |
| 1.1. The concept of the “Pedersen’s Hypothesis” | 4 |
| 1.2. Impact of aberrant intrauterine environment beyond maternal glucose levels on offspring health | 4 |
| 1.3. Macrosomia vs. low birth weight in offspring of diabetic mothers | 5 |
| 1.4. Maternal diabetes affects the offspring’s insulin secretion in adulthood..... | 6 |
| 2. Models to study the effect of maternal diabetes | 8 |
| 2.1. Methods used on rodents to mimic the diabetes in human | 9 |
| 2.2. The pig as a model for diabetes research | 12 |
| 3. The sow’s placenta and insulin absorption: similarities and differences with human | 13 |
| 3.1. Physiological mode of glucose transition between mother and foetus: the GLUT family | 15 |
| 3.2. Placental alterations during maternal diabetes | 17 |
| 4. Maternal diabetes affects offspring in a sex-dependent manner | 18 |
| 5. Pancreas and β-cell development..... | 20 |
| 5.1. Differences in islet architecture between mice, pigs, and humans..... | 20 |
| 5.2. Islet maturation and proliferation | 22 |
| 5.3. β -cell dedifferentiation as a mechanism of failure in hyperglycaemic environment..... | 25 |
| 5.3.1. Major causes of the β -cell dedifferentiation: ROS production | 26 |
| 5.3.2. Major causes of the β -cell dedifferentiation: ER stress | 27 |
| 6. Regulation of the insulin secretion and techniques to study | 29 |
| 6.1. Biorep Perifusion System..... | 29 |
| 6.2. Study of insulin secretion on porcine pancreatic tissue slices | 30 |
| III. ANIMALS, MATERIALS AND METHODS..... | 32 |
| 1. Animals..... | 32 |

| | | |
|-----------|---|-----------|
| 2. | Materials | 32 |
| 2.1. | Chemicals | 32 |
| 2.2. | Perifusion materials | 33 |
| 2.3. | Consumables | 34 |
| 2.4. | Devices | 35 |
| 2.5. | Drugs | 36 |
| 2.6. | Kits | 36 |
| 2.7. | Software | 36 |
| 2.8. | Buffers and solutions..... | 37 |
| 2.8.1. | Solutions for perifusion system..... | 37 |
| 2.8.2. | Fixatives and other solutions..... | 38 |
| 2.8.3. | Buffer for PCR | 39 |
| 3. | Methods | 39 |
| 3.1. | Reproduction management of the sows | 40 |
| 3.2. | Oral glucose tolerance test (OGTT) of new-born piglets..... | 40 |
| 3.3. | Blood sampling from the sows..... | 41 |
| 3.4. | Clinical-chemical analysis of blood samples | 41 |
| 3.5. | Ultrasensitive Insulin-ELISA immunoassay (Merckodia®)..... | 42 |
| 3.6. | Identification of piglets' genotype using polymerase chain reaction (PCR) | 42 |
| 3.7. | Necropsy..... | 44 |
| 3.8. | Sampling of the pancreas | 45 |
| 3.8.1.1. | Processing of the pancreas | 46 |
| 3.8.2. | Sampling of the other organs | 46 |
| 3.9. | Immunofluorescence staining and stereological quantification of endocrine cell volume ratio..... | 48 |
| 3.9.1. | Processing of fixated tissue | 48 |
| 3.9.2. | Immunofluorescence (IF) staining | 48 |
| 3.9.3. | Image acquisition and digital image analysis..... | 49 |
| 3.10. | <i>In situ</i> dynamic glucose stimulation insulin secretion (GSIS) on pancreatic tissue slices..... | 50 |
| 3.10.1. | Pancreas processing and vibratome slices..... | 51 |
| 3.10.2. | Samples equilibration and perifusion experiment..... | 52 |
| 3.10.3. | HTRF assay for determination of insulin of tissue slice GSIS | 55 |

| | | |
|------------|---|-----------|
| 3.11. | scRNA sequencing on porcine β -cells | 55 |
| 3.11.1. | Generation of scRNA-seq samples from pigs | 55 |
| 3.11.2. | Flow cytometry | 55 |
| 3.11.3. | Single-cell sequencing..... | 56 |
| 3.11.4. | Improved genome annotation for <i>Sus scrofa</i> | 56 |
| 3.11.5. | Pre-processing of droplet-based scRNA-seq data..... | 57 |
| 3.11.5.1. | Data preparation | 57 |
| 3.11.5.2. | Ambient gene detection..... | 57 |
| 3.11.5.3. | Empty Droplets | 57 |
| 3.11.5.4. | Quality Control..... | 57 |
| 3.11.5.5. | Doublet detection | 58 |
| 3.11.5.6. | Concatenation and normalization..... | 58 |
| 3.11.5.7. | Integration | 58 |
| 3.11.5.8. | Single-cell manifolds and visualization | 58 |
| 3.11.5.9. | Doublet Removal..... | 58 |
| 3.11.5.10. | Clustering and Cell Type annotation..... | 59 |
| 3.11.5.11. | Differential gene expression between offspring of healthy and diabetic mom..... | 59 |
| 3.12. | Holistic proteomic analysis by LC/MS-MS | 59 |
| 3.12.1. | Sample processing and LC/MS-MS | 59 |
| 3.12.2. | Data analysis | 60 |
| 3.13. | Statistical analysis | 61 |
| IV. | RESULTS | 62 |
| 1. | First observation during the pregnancy and immediately after the birth | 62 |
| 1.1. | General aspects..... | 62 |
| 1.2. | Pregnancy rate between healthy vs hyperglycaemic sows..... | 62 |
| 1.3. | Hyperglycaemia caused reduced litter size, increases the number of stillborn and occasionally malformations in offspring..... | 63 |
| 1.4. | Pre-gestational diabetes led to reduced birth weight in offspring..... | 64 |
| 2. | Phenotypic characterization of the glucose metabolism in PHG piglets | 66 |
| 2.1. | Piglets born from diabetic mothers exhibited hyperglycaemia, hyperinsulinemia and altered glucose and insulin metabolism with gender | |

| | |
|---|------------|
| effect upon OGTT | 66 |
| 2.2. Clinical-Chemical Parameters..... | 68 |
| 2.3. Dynamic GSIS assay with pancreatic tissue slices showed an impaired insulin secretion in PHG offspring..... | 70 |
| 3. Omics studies for the insight characterization of the β-cells..... | 73 |
| 3.1. Holistic proteomics revealed alterations in both exocrine and endocrine compartment of the pancreas in PHG | 73 |
| 3.2. Findings of scRNAseq on β -cells..... | 76 |
| 4. Immunofluorescence analysis for the validation of the alterations of the β-cells..... | 81 |
| V. DISCUSSION..... | 84 |
| 1. The MIDY <i>INS</i>^{C94Y} pig model as adequate model for the study of maternal diabetes' effect on the offspring..... | 85 |
| 1.1. Pregnancy rate and malformations in offspring | 85 |
| 1.2. Low body weight at birth | 86 |
| 1.3. Clinical chemical parameters of offspring born in diabetic mothers | 87 |
| 2. Intrauterine glucotoxic environment impaired insulin sensitivity in new-born healthy piglets..... | 88 |
| 2.1. The PHG piglets show an impaired glucose tolerance 30 minutes after the birth | 89 |
| 2.2. Impaired insulin response after OGTT in PHG compared to PNG piglets | 90 |
| 2.3. Sex specific effect in the PHG group due to the hyperglycaemic intrauterine environment | 92 |
| 3. Omics studies for the molecular characterization of the β-cells | 94 |
| VI. CONCLUSION | 99 |
| VII. SUMMARY..... | 102 |
| VIII. ZUSAMMENFASSUNG | 104 |
| IX. REFERENCE LIST | 107 |
| X. INDEX OF FIGURES | 146 |
| XI. INDEX OF TABLES | 147 |

XII. ANNEX.....148

INDEX OF ABBREVIATIONS

| | | | |
|--------------|--|----------------|--|
| - | Negative | MAFA | MAF BZIP transcription factor A |
| + | Positive | MIDY | Mutant <i>INS</i> gene induced diabetes of youth |
| µg | Micrograms | min | Minutes |
| µL | Microliters | mL | Milliliters |
| µm | Micrometres | mm | Millimeters |
| Abs | Antibodies | mM | Millimolar |
| ADA | American diabetes association | NEFA | Non-esterified fatty acids |
| AldoB | Aldolase B | NeuroG3 | Neurogenin-3 |
| AUC | Area under the curve | OGTT | Oral glucose tolerance test |
| BGC | Blood glucose concentration | PCR | Polymerase chain reaction |
| BW | Body weight | PDX1 | Pancreatic and duodenal homeobox 1 |
| DDIT3 | DNA damage-inducible transcript 3 | PGDM | Pre-gestational diabetes mellitus |
| DM | Diabetes mellitus | pH | Potential of hydrogen |
| DNA | Deoxyribonucleic acid | PHG | Healthy piglets from hyperglycaemic mother |
| ELISA | Enzyme-linked immunosorbent assay | PNG | Healthy piglets from normoglycemic mother |
| f | Female | RBP4 | Retinol binding protein 4 |
| GDM | Gestational diabetes mellitus | SE | Standard Error |
| Glc | Glucose | SI | Stimulation Index |
| GLUT | Glucose transporter | SOX9 | SRY-Box transcription factor |
| GSIS | Glucose stimulation insulin secretion | T1DM | Type 1 diabetes mellitus |
| INS | Insulin | T2DM | Type 2 diabetes mellitus |
| eGFP | enhanced green fluorescent protein | vs | Versus |
| IR | Insulin receptor | WT | Wild type |
| kg | Kilogram | scRNA | Single cell RNA sequencing |
| LMU | Ludwig-Maximilians-Universität München | seq | |
| m | Male | RNA | Ribonucleic acid |
| MW | Molecular weight | | |

I. INTRODUCTION

Diabetes is one of the most common metabolic complications during pregnancy and the number of cases is steadily increasing worldwide (Diabetes 2022). Numerous studies were enrolled in humans, such as ‘Hyperglycaemia and Adverse Pregnancy Outcome’ (HAPO), HAPO Follow-up Study (HAPO FUS), or clinical trials of the ‘Maternal-Foetal Medicine Units (MFMU) Network’ (Bloom, Belfort et al. 2016, Lowe, Scholtens et al. 2019) and complemented by studies in animal models, to understand the broad range of adverse short- and long-term outcomes on the offspring caused by an aberrant intrauterine environment in diabetic mothers (Fetita, Sobngwi et al. 2006, Lowe, Scholtens et al. 2019, Shashikadze, Flenkenthaler et al. 2021). Short-term effects on the offspring encompass a higher risk of stillbirth, aberrant intrauterine growth, and malformations, but also metabolic alterations in new-borns. Epigenetic modifications due to adverse *in utero* environment programs, also named developmental programming, were identified to mediate the long-term effects of maternal diabetes in offspring, such as increased risk of type 2 diabetes (T2DM), obesity, or cardiovascular disease.

The key feature of metabolic alterations in new-born offspring of diabetic mothers is hyperinsulinemia. The hyperglycaemia-hyperinsulinemia hypothesis - also known as Pedersen hypothesis, which was formulated already more than 60 years ago - recognized changes of glucose metabolism in babies of diabetic mothers. As maternal glucose can pass the placenta but insulin not, maternal hyperglycaemia leads also to foetal hyperglycaemia, upon which the foetus responds with increased insulin production. Bush et al. showed in children aged 5–10 years that maternal gestational glucose concentration negatively affected offspring insulin sensitivity and β -cell response (Bush, Chandler-Laney et al. 2011). To understand the alterations in β -cells in offspring of diabetic mothers, several studies were performed mainly in streptozotocin-induced diabetic rodent models or after high-fat diet (HFD) feeding.

Although mouse models for diabetes research are widely developed and studied, their physiology, anatomy and pharmacokinetics do not fully reflect the human situation, unlike other animal models such as the pig model (Kleinert, Clemmensen et al. 2018, Ludwig, Wolf et al. 2020).

The pig is one of the most studied models for translational research because of its advantages: it is similar in size and physiology of many organs to humans, genetic tools are widely available (as for rodents), pharmacokinetics and the pancreas and islet architecture are similar to humans (Renner, Dobenecker et al. 2016, Bakhti, Bottcher et al. 2019). A former study carried by our institute, demonstrated how piglets' metabolism can be affected when exposed to mild hyperglycaemia in the intrauterine life (Renner, Martins et al. 2019).

In this study, we aim to demonstrate and to clarify the adverse outcomes of the severe hyperglycaemic intrauterine environment on the offspring, focusing on the β -cells, using a severely diabetic pig model (Renner, Braun-Reichhart et al. 2013).

II. REVIEW OF THE LITERATURE

1. Maternal diabetes mellitus and effects on offspring: what is known in humans?

In recent years, the number of babies that have developed in a hyperglycaemic intrauterine environment is increasing. In 2021, it was estimated that 16.7% of alive-born babies were from mothers that showed hyperglycaemia during pregnancy (Diabetes 2022). The increase of affected offspring, which were exposed to maternal hyperglycaemia during their foetal life, could be in line with the increasing number of (pre-)diabetic women worldwide. Women with hyperglycaemia during pregnancy could be suffering from pre-existing diabetes mellitus (PGDM), when the mother had type 1 or type 2 diabetes (T1DM and T2DM) prior the pregnancy, or they can be affected by gestational diabetes mellitus (GDM) that spontaneously develops during the pregnancy and usually occurs during the 5th month of pregnancy. Obesity, high maternal age, and the absence of physical activity could be some of the risk factors that contribute to the increasing cases of maternal diabetes. Poorly managed PGDM with elevated blood sugar levels before conception and in the first trimester can lead to major birth defects in 5–10% of pregnancies and spontaneous abortions in 15–20% of pregnancies (Reece 2012).

That the intrauterine environment has an important role on the health and in disease susceptibility in offspring in post-natal life was already recognized 60 years ago by Pedersen. In his studies on babies that were born from diabetic mothers, he recognized that these babies were hyperglycaemic and showed hyperinsulinemia at birth. He summarized his findings in the “Pedersen’s Hypothesis”. Up to date, numerous studies were enrolled in humans, such as ‘Hyperglycaemia and Adverse Pregnancy Outcome’ (HAPO), HAPO Follow-up Study (HAPO FUS), or clinical trials of the ‘Maternal-Foetal Medicine Units (MFMU) Network’ to understand the broad range of adverse short- and long-term outcomes on the offspring caused by an aberrant intrauterine environment in diabetic mothers (Fetita, Sobngwi et al. 2006, Lowe, Scholtens et al. 2019) (reviewed in: (Shashikadze, Flenkenthaler et al. 2021)).

1.1. The concept of the “Pedersen’s Hypothesis”

Pedersen (1967) studied the birth weight, length, organ size, and state of maturity of infants born to mothers with PGDM and observed increased adipose tissue and overweight (macrosomia) (Pedersen 1954). He suggested that the high maternal glucose levels increase the transplacental passage of nutrients to the foetus, resulting in macrosomia. The foetus responds to maternal hyperglycaemia by hyperinsulinemia that reduces blood glucose levels but may lead to enhanced infant’s growth. Greco et al. (Greco, Vimercati et al. (2003) found that the gestational age when macrosomia can first be diagnosed is around week 24 of pregnancy when a significant difference in abdominal circumference between macrosomic offspring and offspring of normal birth weight could be observed. The foetuses then maintained their growth profile throughout pregnancy.

1.2. Impact of aberrant intrauterine environment beyond maternal glucose levels on offspring health

Globally, around 8 million babies, constituting 6% of all births, face complications from congenital defects by early school age, with roughly half of these issues identified immediately post-birth. Annually, at least 3.3 million children under the age of 5 succumb to severe birth defects, with congenital heart defects and neural tube defects being the primary culprits (Murphy, Xu et al. 2013, Walani and Biermann 2017).

Offspring born to mothers with PGDM experience birth defects in 5–10% of live births, with an estimated 8,000 such cases recorded in the United States in 2010 (Correa, Gilboa et al. 2012). Elevated levels of maternal glycated haemoglobin (HbA1c), indicating hyperglycaemia, particularly in the first trimester, are associated with increased rates of birth defects, spontaneous abortions, stillbirths, and other pregnancy complications (Burlina, Dalfrà et al. 2019).

More than half of all perinatal deaths stem from major congenital malformations in infants of diabetic mothers (Greene 2001). Diabetic embryopathy can affect various organ systems during development, with neural tube defects and cardiovascular malformations being the most prevalent and severe anomalies linked to diabetic pregnancies. Clinical studies have identified atrioventricular septal (AVS) defects, hypoplastic left heart syndrome, and persistent truncus arteriosus as the most common cardiac malformations (Martinez-Frias 1994, Correa, Gilboa et al. 2008,

Corrigan, Brazil et al. 2009). Aberrations in maternal/foetal fuel metabolism, including hyperglycaemia, hyperketonaemia, and disrupted metabolism of arachidonic acid, myoinositol, and prostaglandins, along with heightened oxidative stress, contribute to embryonic developmental changes (Reece, Homko et al. 1998, Ornoy, Zaken et al. 1999). Elevated glucose levels during critical morphogenesis periods emerge as the primary teratogen in diabetic pregnancies. Another possible mechanism is diabetes-induced hypoxia, likely due to hyperglycaemia (Ornoy, Tsadok et al. 2009). Epigenetic modifications due to adverse *in utero* environment programs, also named as developmental programming, were identified to mediate the long-term effects of maternal diabetes in offspring, such increased risk of T2DM, obesity, or cardiovascular disease.

Diabetic embryopathy exhibits a phenotype of incomplete penetrance, meaning not all individuals exposed to the diabetic environment manifest birth defects. However, the precise way how maternal metabolic alterations lead to developmental defects, particularly targeting specific tissues, remains uncertain (Greene 2001).

A wide variety of prenatal and postnatal factors were assumed that may influence the growth of the offspring of diabetic mothers, and include the severity and onset of diabetes, the degree of diabetic control, and the mode of treatment of the mother.

1.3. Macrosomia vs. low birth weight in offspring of diabetic mothers

Maternal hyperglycaemia and elevated plasma amino acid concentrations have also been linked with foetal macrosomia. Greco et al. (Greco, Vimercati et al. 2003) discovered that macrosomia could first be detected using ultrasound around week 24 of gestation, evidenced by a notable difference in abdominal circumference between macrosomic and normal birth weight offspring. Lampl and Jeanty (Lampl and Jeanty 2004) compared intrauterine growth between 37 fetuses of diabetic mothers and 29 fetuses of non-diabetic, non-smoking mothers, revealing asymmetric growth patterns in fetuses of diabetic mothers across various stages of pregnancy, affecting the head, limbs, and abdomen differently. Scholl and colleagues (Scholl, Sowers et al. 2001) investigated the impact of maternal blood glucose levels in non-diabetic women on their offspring's birth weight, noting a 200 g increase in weight with blood glucose levels exceeding 130 mg/dL, while maternal hypoglycaemia was associated with reduced birth weight in term infants.

These studies collectively underscore the correlation between hyperglycaemia and increased foetal weight, highlighting the critical importance of optimal glycaemic control during pregnancy.

Beside macrosomia, another effect of maternal diabetes on the newborn can also be a low birth weight (LBW) (Petersen, Pedersen et al. 1988). In the era before insulin therapy, most infants born to diabetic mothers were of low birth weight (LBW), either due to maternal starvation—an approach used to lower serum glucose levels and prevent intrauterine foetal death—or because of severe diabetic complications leading to placental damage. Since the advent of insulin treatment, LBW in infants of mothers with PGDM typically indicates severe diabetic vascular complications and is increasingly observed in women with PGDM and comorbid conditions such as hypertension, renal disease, or in malformed infants (Kliegman and Gross 1985, Kitzmiller and Combs 1996, Biesenbach, Grafinger et al. 2000).

Like macrosomia, LBW serves as a risk factor for various diseases including hypertension, cardiovascular diseases, and diabetes (Barker 1997, Eriksson, Forsen et al. 2000, Ornoy 2011, Ornoy, Livshitz et al. 2011). With improved treatment for PGDM and better pregnancy outcomes, more LBW infants are being born to mothers with diabetic complications, potentially subjecting the offspring to the complications associated with LBW.

The studies indicated that low birth weight was related to T2DM in adulthood; however, the mechanism by which low birth weight increases the risk of T2DM remains unclear. Some research has suggested that it may be a compensatory adaptation to an adverse intrauterine environment during foetal development. The smaller foetus and structural and functional change of important organs lead to insulin resistance and abnormal islet development, which could cause diabetes in adults (Mi, Fang et al. 2017).

1.4. Maternal diabetes affects the offspring's insulin secretion in adulthood

After delivery, children born from mothers with maternal diabetes show hypoglycaemia, due to an excess of insulin secretion (hyperinsulinemia) (Fetita, Sobngwi et al. 2006).

In fact, several studies have shown how the predisposition of an individual to develop metabolic diseases, linked to the dysfunction of pancreatic β -cells, begins in intrauterine life (Dorner and Plagemann 1994, Reusens and Remacle 2001, Vaiserman and Lushchak 2019). These situations can disrupt the maternal-foetal environment and this causes adaptive changes during the organogenesis, leading to a decreased β -cell mass and reduced insulin secretion (Vaiserman and Lushchak 2019).

Beyond mere associations with body weight, offspring exposed to diabetes during pregnancy face an elevated risk of metabolic diseases. Indigenous communities, characterized by higher rates of pregnancies complicated by diabetes, have served as focal points for studies revealing correlations between maternal diabetes during pregnancy and increased occurrences of childhood obesity and early-onset T2DM, notably observed in Pima Indian populations in Arizona (Pettitt, Knowler et al. 1987, Pettitt, Aleck et al. 1988). Recent investigations have further underscored these findings, revealing a positive correlation not only between maternal diabetes but also third-trimester glucose tolerance and higher offspring birth weight, along with an increased incidence of youth-onset T2DM in the Pima Indians (Franks, Looker et al. 2006). In a ground-breaking study, Dabelea et al. (Dabelea, Hanson et al. 2000) identified a heightened risk of T2DM in offspring exposed to maternal diabetes during pregnancy compared to siblings from previous pregnancies not exposed to diabetes, with an odds ratio for T2DM of 3.7.

In Canada, the Manitoba First Nations people have demonstrated a significant link between gestational diabetes mellitus (GDM) and the onset of obesity, non-alcoholic fatty liver disease, hypertension, renal, and cardiac conditions later in life (Sellers, Dean et al. 2016). Notably, maternal pre-existing T2DM throughout pregnancy increased the risk of childhood onset T2DM by 14 times (Young, Martens et al. 2002), while exposure to GDM elevated a child's risk of developing youth-onset T2DM by four times compared to children not exposed to diabetes during gestation. While Indigenous communities exhibit higher rates of pregnancies complicated by diabetes, studies involving primarily Caucasians also confirm the positive association between maternal diabetes exposure and adverse metabolic health outcomes. Offspring of mothers with GDM displayed higher fasting blood glucose levels during adolescence, although insulin levels did not differ significantly (Patel, Fraser et al. 2012). Moreover, these offspring had an eight-fold increased risk of developing T2DM later in life (Clausen, Mathiesen et al. 2008).

Evidence of insulin resistance and impaired pancreatic β -cell function was evident in offspring as young as age 7 born to mothers with diabetes during pregnancy, including both GDM and pre-pregnancy T1DM, as well as in adult offspring (Kelstrup, Damm et al. 2013). The comprehensive SEARCH for Diabetes in Youth study supported these findings, revealing that maternal diabetes exposure (encompassing pre-existing T1DM and T2DM along with GDM) or maternal obesity accounted for 47% of the risk of developing T2D before 22 years of age in offspring (Dabelea, Mayer-Davis et al. 2008).

Sibling studies suggested that the heightened body mass index (BMI) and risk of T2D in offspring exposed to diabetes during pregnancy were unlikely to be attributed to shared lifestyle factors or genetic polymorphisms, but rather to intrauterine exposure to diabetes.

Many studies focused on the epigenetic programming pattern that change in children exposed to maternal diabetes, compared to babies raised in a normoglycemic environment, that lasts also in adulthood (Shashikadze, Flenkenthaler et al. 2021). Many alterations were associated with DNA methylation in genes involved in metabolic functions of the babies' genome, such as the leptin gene, adiponectin, lipoprotein lipase (Bouchard, Hivert et al. 2012, Houde, St-Pierre et al. 2014, Lesseur, Armstrong et al. 2014). Finally, other studies were conducted looking at the proteome of the cord blood cells of offspring born from diabetic mothers, where several proteins were associated with abnormalities in glucose and lipid metabolism (Shashikadze, Flenkenthaler et al. 2021).

2. Models to study the effect of maternal diabetes

Despite this pathological situation can cause several problems to the offspring's health, with short-term and long-term consequences, many studies have been conducted on maternal diabetes and its effect on the mother, as most of them are conducted in a retrospective way. For this reason, the molecular mechanisms how maternal diabetes affects the offspring's health are still unknown, especially how maternal diabetes influences the health of the offspring's β -cells of the islets of Langerhans remains unclear. Due to ethical reasons, studies in humans are limited to clinical observations (such as macrosomia and body weight at birth (LeMay-Nedjelski, Butcher et al. 2020)) or readily available biological samples such as placenta or fluid samples from offspring and mothers, such as blood (peripheral and

umbilical cord), milk, urine, or amniotic fluid (Ruchat, Houde et al. 2013, Yuksel, Oncul et al. 2014, Ma, Tutino et al. 2015, Wawrusiewicz-Kurylonek, Telejko et al. 2015, de Souza, Hara et al. 2016, Powe 2017, Carrasco-Wong, Moller et al. 2020, Lee, Barr et al. 2020, Peila, Gazzolo et al. 2020); different human studies refer to clinical trials carried in close groups (such as families and/or small populations) (Thomas, Balkau et al. 1994, Damm, Houshmand-Oeregaard et al. 2016, Mandy and Nyirenda 2018), or they are based on the lifestyle of the mother and how to improve the outcome of the future babies (Barua and Junaid 2015) (Zhang and Rawal 2017, Peters and Brazeau 2019).

However, these data and biological samples are not suitable to address the question of what happens *in situ* at the molecular and physiological level to the pancreatic islets of offspring from diabetic mothers. For this reason, various animal models have been developed to carry out more specific and targeted studies on the islets of Langerhans. The most widely used models are murine models, due to their vast benefits from a practical point of view: excellent characterization of genetically modified and pharmacologically induced models (e.g. with streptozotocin) for the study of maternal diabetes, possibility of having a considerable amount of data in a short time, reduced gestation times, excellent cost-benefit ratio (Brelje, Scharp et al. 1993, Dorner and Plagemann 1994, Dunn and Bale 2009, Ding, Wang et al. 2012, Szlapinski, King et al. 2019, Zhu, Chen et al. 2019). Nevertheless, rodent models have certain limitations for human translational medicine from an anatomical, physiological, and metabolic point of view.

2.1. Methods used on rodents to mimic the diabetes in human

Several animal models have been developed for studying diabetes mellitus (reviewed in (Kleinert, Clemmensen et al. 2018)) and various methods are used to induce hyperglycaemia, before or during pregnancy, aiming to replicate aspects of PGDM or GDM (Renner, Dobenecker et al. 2016, Lin, Cheng et al. 2020). Early methods like pancreatectomy, involving surgical removal of the pancreas, have been largely replaced by less invasive techniques such as chemical ablation of β -cells (using streptozotocin or alloxan), diet-induced diabetes, and genetic engineering. Pancreatectomy is not used anymore because it involves the partial or total removal of the pancreas by surgery, depending on the different degree of

diabetes, but it anyway remains an invasive procedure, generating a high degree of inflammation with high post-surgical mortality rates (Pasek and Gannon 2013).

The utilization of animal models, particularly rodents, is essential for understanding the mechanisms underlying human birth defects associated with diabetes during pregnancy. Various mouse strains are commonly employed in research focusing on diabetic pregnancy, including those genetically predisposed to diabetes, chemically induced to mimic diabetic characteristics, and those administered exogenous glucose to induce hyperglycaemia (Grupe and Scherneck 2023). In these animal models of diabetic embryopathy, elevated glucose levels are adequate to induce dysmorphism in embryos, either through direct injection of glucose into pregnant dams or in whole embryo culture (Grupe and Scherneck 2023). While some studies have investigated heart defects induced by diabetes, neural tube defects are the primary structural abnormalities assessed due to their detectability during mid-gestation and later stages. It is noteworthy that only a fraction of embryos in diabetic pregnancies exhibit defects, and despite significant maternal hyperglycaemia, some pregnancies yield normal offspring (Agarwal, Morriseau et al. 2018). This phenomenon underscores the complexity of diabetic embryopathy and the need for further research to elucidate its underlying mechanisms. The variability in outcomes of diabetic pregnancies among outbred mouse strains may stem from genetic disparities among individual dams (Pani, Horal et al. 2002). Conversely, distinctions observed in inbred strains are attributed to non-genetic factors contributing to pathogenesis. Consequently, it has been suggested that malformations observed in human diabetic pregnancies may be influenced at the epigenetic level, involving mechanisms such as DNA methylation, chromatin modification (e.g., histone methylation and acetylation), transcriptional regulation (e.g., production of microRNAs, RNA stability, protein synthesis, and localization), and oxidative stress (Zangen, Ryu et al. 2006, Salbaum and Kappen 2011). Experiments conducted in animal models of diabetic pregnancies have revealed that hyperglycaemia triggers oxidative stress within the developing cells and tissues of the embryo and foetus (Morgan, Relaix et al. 2008, Ornoy, Tsadok et al. 2009, Zhao, Yang et al. 2009, Cao, Zhao et al. 2012). As maternal glucose concentration rises, so does the concentration of reactive oxygen species (ROS) within the embryo and foetus. Elevated ROS levels diminish the natural antioxidant capacity of foetal cells, leading to at least three biomolecular events that contribute to birth defects: membrane alterations, mitochondrial dysfunction, and the initiation of abnormal

programmed cell death (apoptosis) (Reece, Ma et al. 2002, Ornoy, Tsadok et al. 2009). Evidence illustrating how maternal hyperglycaemia triggers these events leading to birth defects has been elucidated in animal models, particularly through the induction of type 1 diabetes by administering streptozotocin (STZ), a compound targeting and destroying pancreatic β -cells.

The pancreas, in fact, is an organ which is very sensitive to external changes during organogenesis, especially if they relate to inadequate nutritional status, and can cause structural or functional changes in pancreatic tissue. Indeed, in mouse models, a caloric deficiency in the nutritional status of mothers can cause a reduction in β -cell mass (Tarry-Adkins and Ozanne 2011).

Examination of murine embryos from diabetic dams has uncovered that elevated glucose levels induce membrane alterations, manifested by changes in the yolk sac, premature aging, abnormal morphology of the endoplasmic reticulum, and prevention of neural tube closure (Reece, Pinter et al. 1985, Reece, Ma et al. 2002, Cao, Zhao et al. 2012). Furthermore, researchers have observed that maternal glucose excess leads to increased oxidative phosphorylation in the mitochondria, resulting in the accumulation of reactive oxygen species (ROS) that can damage foetal tissues and cells (Wang, Ratchford et al. 2009). Studies investigating the expression levels of pro-apoptotic proteins in murine models of diabetic pregnancy have demonstrated that maternal hyperglycaemia can trigger abnormal cell death signalling pathways within the developing embryo, potentially leading to malformations or foetal death (Yang, Zhao et al. 2007).

Transgenic rodents are largely used for creating specific diabetic models. This is, nowadays, the most reliable way to mimic the human diabetes using animal models (Otani, Tanaka et al. 1991, Yoshioka, Kayo et al. 1997) (King 2012). More recent studies also suggest how these rodent models can be used for the study of the maternal diabetes, even showing a gender effect as it is seen in human studies (Grasemann, Devlin et al. 2012). Other animal models were focusing on the β -cell expansion during pregnancy in the mother, a physiological mechanism that occurs during normoglycemic pregnancies (Plank, Frist et al. 2011) (Demirci, Ernst et al. 2012). Even if these studies were fundamental to understand the pathophysiology of the maternal status during the pregnancy, they do not give a clear overview of what happens in the offspring.

2.2. The pig as a model for diabetes research

As mentioned above, in contemporary biomedical research, the utilization of porcine models is gaining momentum, with notable advantages highlighted over traditional murine models in the study of diabetes pathophysiology and therapeutic interventions (Wolf, Braun-Reichhart et al. 2014) (Renner, Blutke et al. 2020).

Unlike murine models, which possess inherent physiological and anatomical differences from humans, porcine models exhibit greater similarities in size, pharmacokinetics and pancreas architecture, rendering them more reflective of human physiology (Rees and Alcolado 2005, Graham and Schuurman 2015, Kleinert, Clemmensen et al. 2018, Ludwig, Wolf et al. 2020).

Porcine models offer several advantages. Their physiological resemblance to humans, coupled with the availability of genetic tools akin to those in rodent models, facilitates comprehensive investigations into diabetes aetiology and treatment (Dufrane and Gianello 2012, Hoang, Matsunari et al. 2014, Renner, Dobenecker et al. 2016, Bakhti, Bottcher et al. 2019). Furthermore, the economic feasibility of utilizing mini pigs mitigates the high costs associated with larger animal models like non-human primates (Kleinert, Clemmensen et al. 2018).

Moreover, the pig represents a valid model thanks to the architecture and morphology of its pancreatic islets, and for this reason, a large usage of this animal is in the development of new therapeutic approaches such as xenotransplantation of the Langerhans islets (Dufrane and Gianello 2012).

Pigs have a shorter gestational cycle than other large animals and can give birth to up to 15 offspring (depending on the species and the individual physiology of the animal). They have a similar circadian rhythm as humans, unlike rodents, and similar eating habits to humans. The gastrointestinal tract is similar between pigs and humans (Renner, Dobenecker et al. 2016). Porcine insulin differs from human insulin only in one amino acid, as porcine insulin was used to treat diabetes in humans before recombinant human insulin was synthesized.

Moreover, thanks to the possibility of surgical intervention and genetic modification, the pig model is one of the most promising models for diabetes research. Furthermore, pigs are possible future donors of Langerhans islets for the treatment of T1DM (Klymiuk, van Buerck et al. 2012).

Just as with rodents, there are several methods for the development of diabetic pig models. Generally, it is possible to induce diabetes in these animals by several methods: partial or total pancreatectomy by surgery, pharmacological induction, using

streptozotocin (STZ) or alloxan, which are two selective toxic substances for β -cells (Wilson, Dhall et al. 1986, Grussner, Nakhleh et al. 1993, King 2012). Other methods are induction through diet or genetic modification.

Although, as in rodents, induction of diabetes by high-fat diets is still widely used, it has disadvantages: it is very expensive (prices are higher compared with rodents), does not always result in significant hyperglycaemia (Feng, Yang et al. 2015) and is often used in conjunction with STZ to develop diabetes (Koopmans, Mroz et al. 2006).

For this reason, more and more diabetic models with genetic modification are being developed. Two different models with permanent diabetes have been developed, the *INS^{C94Y}* and *INS^{C93S}* models (Renner, Braun-Reichhart et al. 2013, Renner, Martins et al. 2019).

Mutations in the insulin gene result in the accumulation of misfolded pro-insulin, which causes endoplasmic reticulum (ER) stress that leads to β -cell apoptosis. In particular, *INS^{C94Y}* pigs are characterized by impaired insulin secretion that increases blood glucose levels and decreases β -cell mass and growth in the transgenic diabetic pig (Renner, Braun-Reichhart et al. 2013). *INS^{C93S}* pigs show lower expression of the mutated protein than the *INS^{C94Y}* transgenic pigs and therefore also lower hyperinsulinemia and hyperglycaemia. This model was used to study the effects of maternal diabetes on offspring, showing that litters born to *INS^{C93S}* sows showed impaired glucose tolerance and insulin resistance compared to piglets born to non-diabetic mothers (Renner, Martins et al. 2019).

In addition, to study β -cell growth and function, a pig model expressing a green fluorescent protein (eGFP) was developed and this reporter gene was inserted under the control of the insulin promoter, demonstrating that its presence within the insulin gene does not affect insulin secretion (Kemter, Cohrs et al. 2017).

3. The sow's placenta and insulin absorption: similarities and differences with human

In mammalian biology, the placenta plays a pivotal role as the interface between the mother and the foetus, orchestrating foetal development by efficiently transporting essential nutrients and oxygen into the offspring's bloodstream. Throughout a typical pregnancy, the mother's metabolism adapts in a series of ways

to ensure an ample supply of nutrients not just for herself but also for the growing baby. The foetus's growth correlates directly with the availability of maternal nutrients and how these traverses the placenta into the foetal bloodstream. This exchange of nutrients in mammals occurs via a complex mechanism that maintains a selective barrier between the mother's and foetus's blood circulation (Brett, Ferraro et al. 2014). Several factors govern this exchange, including morphological aspects such as the type of placenta, vascular system, and molecular components like transporter distribution (as reviewed in (Fowden, Forhead et al. 2008)), along with the capacity and availability of nutrients.

The most informative way to delineate placental function is through the histological structure, particularly evident in human and rodent placentas.

In humans and rodents, the placenta is haemochorial, denoting an invasive type where the haemochorion is degraded and the maternal circulation directly contacts the trophoblast cells. Notably, the human haemochorion features a single layer of trophoblast cells (syncytiotrophoblast), while rodents possess three trophoblast layers (syncytiotrophoblast II, syncytiotrophoblast I, and cytotrophoblast). The syncytiotrophoblast serves as the primary barrier regulating nutrient supply from the mother to the developing foetus, expressing numerous nutrient transporters (Brett, Ferraro et al. 2014). This barrier comprises two polarized membranes: the microvillus membrane (MVM), interfacing with the maternal blood circulation, and the basal membrane (BM), in contact with the foetal circulation (Brett, Ferraro et al. 2014, Blundell, Tess et al. 2016).

The expression of nutrient transporters in the syncytiotrophoblast is intricately regulated by various factors stemming from the foetus, mother, and placenta. The type and quantity of each transporter largely depend on the nutrients, amino acids, and hormones released by both the mother and the foetus. Notably, crucial maternal influences on trophoblast transporters encompass hormones and nutrients from the maternal circulation (Lager and Powell 2012). Particularly, the MVM plays a significant role in expressing transporters for various maternal hormones, such as insulin receptors (IRs), insulin like grow factor receptors (IGF1R and IGF2R), NNAT, which is an activator of the PI3-AKT pathway that promotes the expression of GLUT-1, and leptin receptors. Throughout pregnancy, the MVM consistently expresses transporters for amino acids, fatty acids, and glucose (Sferruzzi-Perri, Owens et al. 2011).

In contrast, the porcine placenta is defined as epitheliochorial, representing a non-invasive type composed of six layers that maintain the separation between maternal and foetal blood circulation. These layers are the maternal endothelial vessels, connective tissue, intact endometrial epithelium on the maternal side and trophoblast epithelium on the foetal side, connective tissue, and foetal endothelial vessels (Furukawa, Kuroda et al. 2014). The pig placenta is complete during the 60th-70th day of gestation, when the uterine-placental interface develops several folding and maturate the areolae, to maximize the exchange surface between the mother and foetus. As well as in human and rodents, also in pigs there are studies and findings of the presence of IRs, NNAT, IGF1 and IGF2 in the trophoctoderm, which suggest that pigs use the same pathways to control and lead the developing of the foetus (Fiorimanti, Cristofolini et al. 2022).

3.1. Physiological mode of glucose transition between mother and foetus: the GLUT family

In humans, maternal glucose serves as the primary energy source for foetal development and is transported across the placenta through facilitated diffusion facilitated by transporters expressed on the placental surface throughout pregnancy (Illsley 2000, Baumann, Deborde et al. 2002, Ruiz-Palacios, Ruiz-Alcaraz et al. 2017). These transporters belong to the GLUT protein family, acting independently of insulin, although insulin receptors (IRs) have been observed on the placenta, activating signalling pathways for this hormone (Desoye, Hofmann et al. 1992) and contributing to placental nutrient metabolism (Hiden, Maier et al. 2006). Given minimal gluconeogenesis in the foetus, maternal glucose becomes pivotal for foetal energy needs, thus highlighting the significance of GLUT receptors (Hay 1991, Kalhan and Parimi 2000).

The human placenta exhibits different isoforms of GLUT transporters: GLUT-1, 3, 4, 8, 9, 10, and 12. These isoforms are distributed across various sites along the placental layers, with their expression changing throughout gestation. Among these isoforms, GLUT-1 stands out as the predominant glucose transporter throughout pregnancy, showing ubiquitous expression across all placental compartments and high specificity for glucose (Sibiak, Ozegowska et al. 2022).

In human, the asymmetrical distribution of GLUT-1 within the placenta is significant in regulating glucose distribution. It is notably more represented in the

microvillus membrane (MVM) on the maternal side than in the basal membrane (BM) on the foetal side, indicating a higher degree of glucose transport selection. The foetal bloodstream's adequate glucose maintenance relies on the gradient established between the MVM and BM. This gradient facilitates glucose influx to the foetus, constituting approximately one-third of the total processed glucose by the placenta. This selective mechanism orchestrated by the MVM and BM ensures sufficient glucose reaches the growing foetus, crucial for its development (Illsley and Baumann 2020).

In pigs, glucose passes through the endometrial epithelium using GLUT-1 and then through GLUT-3 to foetal blood via the chorioallantois. GLUT-1 and GLUT-3 stand out as the predominant glucose transporter isoforms in pig placenta, similar to humans and mice. However, unlike humans and mice, where GLUT-1 is more abundant in the MVM throughout pregnancy, in pigs, its expression decreases during pregnancy, replaced by GLUT-3 (Mathew 2020).

Notably, in humans and rodents, GLUT-3 is predominantly expressed in the syncytiotrophoblast, displaying its highest expression during early gestation, and decreasing throughout pregnancy. In pigs, it serves as the primary glucose transporter from the trophoctoderm to the chorion throughout pregnancy, primarily present in the areolae where significant nutrient exchange between mother and foetus is higher (Wright, Miles et al. 2016, Mathew 2020).

The reason for this difference may lie in the fact that GLUT-1 handles the basal glucose uptake, while GLUT-3 is a high-affinity and high-capacity transporter, that usually increased during hypoxia status in human. This suggests that despite having a more efficient placenta compared to humans and mice, pig placentas develop folds and areolae to maximize nutrient transport between mother and foetus. Moreover, it mostly exposes GLUT-3 in the areolae, to increase the glucose uptake that fuel to the foetus (Friess, Sinowatz et al. 1981, Mathew 2020, Almeida and Dias 2022).

In fact, despite the different placenta types, it was calculated that the amount of glucose that fuel from the mother to the foetus during the pregnancy, is around the 50-70% of the total glucose circulating. Moreover, it seems that, in human and rodents, the mother utilizes the 30-50% of glucose during the pregnancy, while in pigs, maternal bloodstream glucose uses the 40-70% of (Pere 2003).

Recent studies conducted in pigs (Almeida and Dias 2022, Johnson, Seo et al. 2023) show that the trophoctoderm utilizes glucose via the aerobic glycolytic pathway and its metabolic intermediates like the formate, obtained from the conversion of the

serine via the 1C metabolic pathway, are used for the novo synthesis of amino acid and nucleotides. This synthesis of ATP, amino acid and nucleotides is fundamental for the support of the pregnancy and conceptus elongation, hormone synthesis and foetus development.

3.2. Placental alterations during maternal diabetes

Studies show altered molecular pathways in placentae of diabetic mothers, indicating reduced protein expression of insulin signalling components, independently of disease control. DM primes the placenta to overstimulate insulin signalling in response to sustained hyperglycaemia, affecting glucose uptake and contributing to a hyperglycaemic state (reviewed: (Bedell, Hutson et al. 2021)).

The Insulin-like Growth Factor (IGF) axis, comprising IGF1, IGF2, and their receptors, shares similarities with insulin signalling and plays a crucial role in intrauterine development. IGF1 exhibits hypoglycaemic effects, while IGF2 has hyperglycaemic potential (LeRoith and Yakar 2007), and both are expressed in the placenta. Dysregulated IGF signalling contributes to excessive foetal growth, a common complication in GDM pregnancies, alongside increased glucose transporters favouring heightened placental and foetal glucose uptake.

Alterations in serum components of the IGF axis in GDM patients, such as increased maternal IGF1 levels and decreased IGF1R, indicate activated IGF1 signalling in GDM placentae. Increased phosphorylation patterns of IGF1R in placentae from metabolic uncontrolled GDM and T2DM mothers support persistent activation of IGF1 signalling in GDM placentae, potentially contributing to macrosomia in new-borns. The same was observed in pigs, where the foetal glucose and *IGF1* mRNA concentrations were increased in foetal tissue by maternal diabetes (166% and 34%). The foetal tissues where it was increased were skeletal muscle, liver, heart, kidney, and placenta and depressed in adipose tissue and brain (Ramsay, Wolverson et al. 1994).

Overall, dysregulated insulin and IGF signalling pathways contribute to altered placental functioning in GDM pregnancies, impacting glucose uptake, inflammatory responses, insulin resistance, and ultimately foetal growth (Olmos-Ortiz, Flores-Espinosa et al. 2021).

It was observed, in hyperglycaemic intrauterine environment, an increment of the GLUT-1 transporter at the BM level, leading to an increase of foetal glucose level

that potentially stimulate the β -cell maturity in response to high glucose level in the foetal circulation (Illsley and Baumann 2020). Several studies have also observed that in sows made diabetic during pregnancy to study gestational diabetes, the adipose tissue of piglets born to diabetic mothers was greater (Hausman, Kasser et al. 1982), suggesting that diabetic pregnancy in pigs stimulates *de novo* synthesis of fatty acids, glucose uptake within the foetus and lipogenesis in adipose tissue (Ezekwe and Martin 1980, Kasser, Martin et al. 1981). In line with this, recent studies *in vitro* using human trophoblast cell line indicated affections in high glucose conditions and they indicate that high glucose leads to increased placental triglyceride levels, indicating decreased placental β -oxidation in a subset of women with DM and obesity, which could lead to an increase in lipid transfer and potentially excessive foetal growth (Hulme, Nicolaou et al. 2019).

4. Maternal diabetes affects offspring in a sex-dependent manner

As previously mentioned, it is demonstrated that the human offspring born from obese and hyperglycaemic mothers, have short-term and long-term consequences, and, regarding the long-term consequences, they have higher risk to develop obesity and insulin resistance compared to offspring born from normoglycemic mothers. Moreover, recent studies have shown that exposure to a hyperglycaemic intrauterine environment can have varying consequences depending on the sex of the offspring (Casasnovas, Damron et al. 2021).

For instance, offspring of obese dams developed sex-differences in glucose intolerance and insulin secretion. Indeed, the prevalence of prediabetic syndromes such as impaired fasting glucose is more prevalent in men, whereas impaired glucose tolerance is more prevalent in women (Mauvais-Jarvis 2015). Whether foetal exposure to maternal diabetes predisposes to alterations in insulin secretion in a sexually dimorphic manner is unknown (Gautier, Fetita et al. 2018). However, there are fundamental aspects of the control of glucose homeostasis that are regulated differently in males and females (Mauvais-Jarvis 2015, Joshi, Azuma et

al. 2020, Akhaphong, Gregg et al. 2021). Most of the studies *in vivo*, conducted in mice, demonstrated how male offspring are more affected than females (Mauvais-Jarvis 2015, Nicholas, Nagao et al. 2020, Casasnovas, Damron et al. 2021, Zhu, Luo et al. 2021). Females showed increased insulin secretion and mitochondrial respiration, reduced markers of apoptosis, and higher oestrogen receptor expression. Conversely, males may respond to these signals in a way that minimizes the risk of neonatal hypoglycaemia and maximizes neonatal survival. They display, in fact, compromised mitochondrial respiration and a reduced number of insulin granules in β -cells. This mechanism becomes a problem in later life due to the onset of obesity and insulin resistance in these male offspring (Nicholas, Nagao et al. 2020).

The intervention of sexual hormones in the insulin secretion is not new and it is highly demonstrated in humans as well. Healthy women have increased insulin secretion for a given glucose load compared to healthy man after a meal. In addition, the disposition index, which reflects insulin secretion for a given level of insulin action, is higher in women than in men, supporting greater insulin secretion in women (Gannon, Kulkarni et al. 2018). In human pancreas biopsies, one study of 19 individuals found that females have an average of 6% more β -cells than males. This is supported by an imaging study using radiolabelled exendin, which binds to the GLP-1 receptor on β -cells, where females showed increased absorbance compared to males. This difference was also confirmed when individuals were exposed to maternal diabetes during intrauterine life. In fact, exposure to hyperglycaemia during pregnancy predisposes both sexes to develop metabolic diseases early in life. Women, however, seem particularly susceptible to developing increased adiposity and impaired glucose homeostasis. The male placenta is particularly vulnerable to damage caused by adverse nutritional states, and this may underlie some of the metabolic phenotypes observed in adulthood (reviewed in: (Dearden, Bouret et al. 2018)). One of the proofs that the incidence of diabetes and metabolic diseases are associated with the different steroid hormones secreted by females and males, is that there is evidence of sex different in manifesting the diabetes in the population.

For instance, the prevalence of T2DM is higher in adolescent females compared to males, potentially due to greater insulin resistance in females during puberty, when offspring was expose to maternal diabetes (Dearden, Bouret et al. 2018). However,

in middle age, T2DM is more common in men, possibly due to differences in fat distribution, with women having more subcutaneous fat and improved insulin sensitivity (Dearden, Bouret et al. 2018).

Moreover, even if it was not associated directly with exposure to maternal diabetes, several are the proof of the intervention of sexual hormones in the insulin secretion. Interestingly, islet transplants performed with female donor islets showed improved clinical outcomes compared with islets obtained from male donors (Marchese, Rodeghier et al. 2015). This is probably true because in women, the ovarian islet axis influences β -cell biology during reproductive years and at menopause. Prolactin and lactogen mediate their actions on β -cell proliferation through HGF, serotonin, and/or osteoprotegerin pathways (Karnik, Chen et al. 2007, Kim, Toyofuku et al. 2010, Allan 2014, De Jesus and Kulkarni 2014).

The deficit of oestrogen during menopause also increases the risk of T2DM. Studies such as the Women's Health Initiative in 2004 confirmed the anti-diabetic effects of oestrogen, showing a decrease in diabetes incidence in women undergoing hormonal replacement therapy (HRT). Other studies have similarly demonstrated a reduction in diabetes incidence with HRT in postmenopausal women (Merino and Garcia-Arevalo 2021). While, studied confirmed that testosterone deficiency predisposes to hyperglycaemia and diabetes in man (Navarro, Allard et al. 2015, Mauvais-Jarvis 2016, Dimitriadis, Randeve et al. 2018).

5. Pancreas and β -cell development

5.1. Differences in islet architecture between mice, pigs, and humans

The interaction among endocrine cells forming the islets of Langerhans plays a crucial role in their function, influenced by homotypic and heterotypic cell-cell contacts within the organ, as proposed by Steinberg's differential adhesion hypothesis (Steinberg 1963, Steinberg 2007). Studies show varying structures of these islets across species, indicating that the spatial arrangement of α -, β -, and δ -cells contributes significantly to their function and may differ among models (Hoang, Matsunari et al. 2014).

The arrangement of cells within the islets of Langerhans is still a source of controversy in the scientific community, indeed, earlier morphological analyses

suggested a random distribution of different cell types within the islets, predominantly with β - and α -cells in heterotypic contact (Cabrera, Berman et al. 2006).

In mice, islets display a shell-core structure, with β -cells centralized and other endocrine cells positioned in the outer layer. Conversely, in pig and human islets, cells are not only located towards the periphery but also within the core, suggesting more diverse heterotypic cell interactions.

Three-dimensional reconstructions of murine and human islets revealed a core of β -cells surrounded by α -cells and non-penetrating blood vessels in murine islets, potentially forming an epithelium that facilitates diverse cell contacts and paracrine signalling (Arrojo e Drigo, Ali et al. 2015).

Comparing cell fractions, human β -cells demonstrate lower fractions than murine cells (P_{β} 0.62-0.78 vs P_{β} 0.91-0.94 respectively), while pig islets show intermediate characteristics between mouse and human islets (P_{β} 0.87-0.91) (Kim, Miller et al. 2009, Arrojo e Drigo, Ali et al. 2015).

Regarding cell contacts, mouse islets exhibit more β - β contacts compared to pig and human islets, which feature more β - α contacts. This difference in cell contacts may influence islet organization.

To understand these cell interactions, the researchers proposed a model that depicted pancreatic islets as dynamic structures. They used two parameters:

1. Cell-attraction (J): This represents the energy required to break contact between two different cells (in this case, β - and α -cells). It quantified the strength of attraction between cells.
2. Motility (T): This factor represents the energy causing fluctuations and dissociating contacts between cells.

When comparing the relative strengths of attraction between different cell types within pancreatic islets, the study found that these attractions were quite similar and didn't surpass the motility factor (T). Specifically, the difference between the attractions of β - β cells and β - α cells remained within the range dictated by the motility factor ($J_{\beta\beta} - J_{\alpha\beta} < T$).

This similarity in the relative strengths of attraction between different cell types, not exceeding the energy threshold for cell dissociation (T), seems to be a significant factor influencing the organizational differences observed in pancreatic islets across species. Particularly, the study noted that this difference in the strength of attraction (J) is markedly lower in human islets, resembling pig islets, while it's

higher in mouse islets. This difference might contribute to the varying arrangements and organization seen in pancreatic islets between species (Hoang, Matsunari et al. 2014).

Different studies have focused on the size of the islets and which of them were more similar to humans by diameter. A review published by Huang et al (Huang, Harrington et al. 2018) aimed to summarize what is known about the islets' diameter in an inter-species prospective. Notably, except for one study that shows strong similarities between pig and human islets (declaring that human and pig islets measure around 50 μ m) compared to mice (approximately 116 μ m) (Kim, Miller et al. 2009), the range of diameters result relatively similar across species, including similarities between humans, mice and pigs. Specifically, adults pig islets can reach average diameter of 154 \pm 8 (Lembert, Wesche et al. 2003, Dufrane, Goebbels et al. 2005), while humans of 108 \pm 6 (Kilimnik, Jo et al. 2012, Wang, Danielson et al. 2013, Ramachandran, Huang et al. 2015).

Differences in the number and location of islets are evident between species (Saito, Iwama et al. 1978), with mice displaying a more significant disparity in islet numbers between the head and tail regions of the pancreas compared to humans (Rahier, Wallon et al. 1979). Additionally, while mouse islets are primarily interlobular, larger mammals show intralobular positioning. This variation might stem from embryonic development, where smaller lobules merge to form larger lobules, thereby affecting the initial placement of islets (Murakami, Fujita et al. 1993, Murakami, Hitomi et al. 1997, Merkwitz, Blaschuk et al. 2013). While in pigs, the differences in the islets' cytoarchitecture between the lobes were negligible (Nagaya, Hayashi et al. 2019).

5.2. Islet maturation and proliferation

Due to ethical reasons, knowledge about the maturation of islets and β -cells during the human pregnancies are limited. For these reasons, these observations are taken considering the maturation and proliferation pathways involved in hyperglycaemic situations as well as T2DM in human.

The PI3K-AKT/PKB pathway stands as a key regulator in managing the function and growth of β -cells, impacting insulin secretion and the expression of crucial genes associated with cell proliferation. In individuals with T2DM, there's often a

noticeable reduction in AKT2 and PI3K expression within islet cells. This decrease suggests a potential correlation with the progression of the disease (Camaya, Donnelly et al. 2022).

The activation of the AKT/PKB pathway occurs via insulin, growth factors, incretins, and glucose. These stimuli play a pivotal role in engaging the IRS2 receptors, which are fundamental in preserving the mass of β -cells. Studies conducted on mice lacking IRS2 receptors revealed reduced proliferation among β -cells, coupled with an inadequate response to external insulin stimulation. Conversely, boosting the expression of IRS2 receptors in β -cells has shown to spur proliferation and decrease cell death, especially in high glucose conditions observed in humans (Mackenzie and Elliott 2014, Camaya, Donnelly et al. 2022).

After a period of prolonged fasting followed by refeeding, the islet's genetic activity undergoes changes. This transition triggers the activation of genes associated with β -cell identity while simultaneously invoking markers linked to pluripotency or immaturity (Talchai, Xuan et al. 2012, Liu, Javaheri et al. 2017).

Glucose plays a crucial role in upregulating MAFA, a transcriptional activator specific to β -cells that controls insulin gene expression. This influence suggests MAFA's involvement in the function, development, and potentially the onset of diabetes within β -cells (Zhang, Moriguchi et al. 2005, Nasteska, Fine et al. 2021).

The maturity level of β -cells, as indicated by PDX1 and MAFA levels, significantly influences islet function. An increase in mature β -cells ($PDX1^{HIGH}/MAFA^{HIGH}$) can lead to islet failure due to disruptions in ionic fluxes, metabolism, and cellular connectivity. Conversely, a decrease in less mature β -cells ($PDX1^{LOW}/MAFA^{LOW}$) results in altered calcium fluxes within the islet, causing broader changes in β -cell function that affect responses to glucose levels and insulin secretion (Nasteska, Fine et al. 2021).

About pigs, new studies (Nagaya, Hayashi et al. 2019, Kim, Whitener et al. 2020) aim to understand pig pancreas development as a complementary experimental system to investigate the development and maturation of pancreatic islets, noting differences between humans, mice, and pigs. Using an integrated approach, genetic and phenotypic analysis was conducted at the foetal and postnatal stages of pig

pancreas development, revealing many similarities in the formation and regulation of β -, α -, and δ -cells in pig pancreatic islets compared to humans. Notably, features absent in mice are highlighted. Specifically, the genetic regulation similarity between pigs and humans, revealing an unexpected dynamic in gene regulation and the presence of native intra-islet GLP-1 signalling, is underscored. Similarities in gene expressions of β - and α -cells during development between pigs and humans, including genes like *MAFA* and *PDX1*, are highlighted as particularly significant. It is noted that both *MAFA* and *PDX1* are expressed in both β - and α -cells in pigs, as also observed in human islets, emphasizing a parallelism in the development of these cells across species. Specifically, *MAFA* shows increased expression in foetal stages of pig β -cells, continuing into postnatal stages. While in humans, *MAFA* expression begins in foetal stages and increases after birth, foetal regulation remains unreported. These findings indicate similarities in the expression of crucial genes like *MAFA* and *PDX1* between pigs and humans during pancreas development, suggesting that pigs could be a reliable animal model to study human islet function and genes related to their regulation.

Moreover, there are similarities between pigs and humans that surpass those between pigs and mice during pancreatic islet development and genetic regulation. While pigs exhibit many similarities to human systems, these are absent in mice. Specifically, genetic regulation in the pig's pancreas seems more akin to humans than that of mice. For instance, the dynamic gene regulation and presence of native intra-islet GLP-1 signalling observed in pigs and humans stand as significant differences from mice. *GLP1R* is known to be highly expressed in human β -cells and involved in β -cell function and like human, *GLP1R* mRNA was highly expressed in pig β -cells, moreover, as in humans (Dai, Hang et al. 2017), *GLP1R* is expressed in pig β -cells but not α -cells, and this expression increases from foetal to neonatal stages. These details emphasize variations in the genetic regulation of pancreatic islet development across different animal models.

While mice are commonly used as a model for studying human diseases, especially diabetes, the findings highlight crucial differences between mice and pigs in genetic regulation and pancreatic islet development. This suggests that, for certain specific aspects, pigs might be a more representative model of human processes compared to mice.

5.3. β -cell dedifferentiation as a mechanism of failure in hyperglycaemic environment

In situations of constant glucotoxicity, such as exposure to maternal hyperglycaemia *in utero*, the decline in β -cell functionality primarily results from apoptosis mechanisms and a loss of differentiation, leading to a gradual decrease in β -cell mass over time (Bensellam, Jonas et al. 2018). Recent findings suggest that β -cell dedifferentiation contributes more significantly to β -cell dysfunction in the early or middle stages of diabetes development, rather than an increase in β -cell death (Khin, Lee et al. 2021). Several studies aimed to clarify this topic, using omics techniques (such as transcriptome or proteome) to build a clear map of what is happening during the passage from the pre-diabetic to the diabetic condition. What is clear is that, one major aspect of glucotoxicity is the downregulation of β -cell-enriched genes, particularly *INS*, mediated by alterations in key transcription factors like PDX1 and MAFA (Guo, Dai et al. 2013). This downregulation of *INS* gene expression is linked to oxidative stress and ER stress, among other mechanisms (Hollien and Weissman 2006). Additionally, glucotoxicity affects the expression of other genes involved in maintaining β -cell phenotype, such as *Nkx6.1*, *Hnf1 α* , and *Glut2*, further contributing to β -cell dedifferentiation. The complex network of transcription factors and regulatory elements involved in β -cell identity maintenance is disrupted under conditions of glucotoxicity. These studies were confirmed using murine models that show a loss of β -cell identity in chronic hyperglycaemia (Jonas, Sharma et al. 1999). Moreover, in diabetic mice and rats with partial pancreatectomy, β -cell dedifferentiation was observed as the decrease in the differentiation markers such as insulin, PDX1, and MAFA (Tellez, Vilaseca et al. 2016, Neelankal John, Morahan et al. 2017). In addition, the expression of pancreatic progenitor-associated transcription factors such as NGN3 and SRY-Box 9 was upregulated in β -cells of middle-aged Wistar rats following partial pancreatectomy (Neelankal John, Morahan et al. 2017).

In recent years, there has been significant interest in FOXO1 as a potential transcription factor that connects metabolic stress to the dedifferentiation of β -cells in T2DM. FOXO1 serves as a versatile transcription factor with both adaptive and detrimental roles in β -cells depending on the circumstances. Studies have demonstrated that under oxidative stress, FOXO1 moves into the nucleus and

stimulates the expression of *Neurod1* and *MafA* genes (Kitamura, Kitamura et al. 2005). Additionally, in transgenic mouse models, FOXO1 has been implicated in compensatory mechanisms in β -cells during insulin resistance by enhancing β -cell proliferation, mass, function, and the expression of antioxidant genes (Zhang, Kim et al. 2016). Intriguingly, the deletion of *Foxo1* specifically in β -cells led to β -cell dedifferentiation in aging male mice and multiparous female mice, accompanied by the upregulation of markers associated with progenitor and pluripotency states (Talchai, Xuan et al. 2012). Throughout the dedifferentiation, obviously, several transcription factors typically expressed in progenitor cells at the embryonic stage and repressed in adult β -cells were upregulated in β -cells of various diabetic animal models, including neurogenin 3 (NeuroG3), nanog homeobox (NANOG), octamer-binding transcription factor 4 (OCT4 also known as POU5F1) (Talchai, Xuan et al. 2012, Wang, York et al. 2014). Lineage tracing studies confirmed that these dedifferentiated cells originate from cells that expressed insulin and also suggested their trans differentiation in other islet non- β -cells, including α -cells (Talchai, Xuan et al. 2012).

The proposed mechanisms that can lead to β -cell dedifferentiation are several, but two major causes have been highlighted in recent studies, which are ROS production and ER stress.

5.3.1. Major causes of the β -cell dedifferentiation: ROS production

Oxidative stress is the consequence of an imbalance between cellular antioxidants and production of reactive oxygen species (ROS) (Robertson, Harmon et al. 2003, Wu, Nicholson et al. 2004). β -cells are particularly sensitive to ROS because of the relatively low presence of antioxidant enzymes. Thus, high ROS levels in β -cells accelerate their dedifferentiation and loss of function. In fact, in immortalised β -cells exposed to high glucose to mimic the glucotoxicity, an increased ROS production but a decreased insulin secretion was observed and attributed to MAFA downregulation (Guo, Dai et al. 2013, Fu, Cui et al. 2017). ROS are produced in different subcellular locations (e.g., mitochondria, peroxisomes, and ER) during cellular metabolism (Guo, Dai et al. 2013). High glucose and palmitate levels activate pathways that increase ROS production, impairing β -cell metabolic

functions. ROS-induced oxidative stress is implicated in β -cell dedifferentiation and functional failure, with potential involvement of inflammatory pathways.

The absence of catalase enzyme in β -cell peroxisomes results in the accumulation of hydrogen peroxide (H_2O_2), contributing to oxidative stress induced by palmitate. Additionally, high levels of glucose and palmitate activate NADPH oxidase, leading to increased cellular superoxide levels (Morgan, Oliveira-Emilio et al. 2007, Ly, Xu et al. 2017). Mitochondria, being the primary site of ROS generation, are crucial for glucose metabolism and insulin secretion in pancreatic β -cells. Any defects in mitochondrial function compromise the metabolic activities of β -cells (Supale, Li et al. 2012). Long-term consumption of oscillating glucose (LOsG) in rodents' triggers ROS stress in β -cells, resulting in dedifferentiation and functional decline by disrupting the FOXO1-thioredoxin interacting protein pathway (Lai, Teodoro et al. 2007).

However, it is unclear whether ROS induces β -cell dedifferentiation without an intermediate role of inflammatory cytokines.

5.3.2. Major causes of the β -cell dedifferentiation: ER stress

The ER has the crucial role in folding and synthesizing proteins and, as previously written, pancreatic β -cells are highly specialised cells that secrete high doses of insulin with every glucose stimulus. When an error occurs, misfolded or unfolded proteins accumulate in the ER, leading to ER stress. To cope with this massive load by the ER, β -cells use compensatory mechanisms to prevent the formation of misfolded proteins, called unfolded protein response (UPR). This compensatory response is triggered by 3 sensors located on the ER membrane, which are pancreatic ER kinase (PERK, also known as EIF2AK3), inositol endoribonuclease/kinase 1 (IRE1, also known as ERN1) and activating transcription factor 6 (ATF6). PERK causes the attenuation of protein translation to reduce the load on the ER by increasing the expression of transcripts such as ATF4. This transcription factor upregulates the expression of antioxidant genes but also pro-apoptotic genes such as *Ddit3*, which contributes to β -cell death after prolonged ER stress (Schroder and Kaufman 2005, Lai, Teodoro et al. 2007,

Karunakaran, Kim et al. 2012, Schwarz and Blower 2016). In pancreatic β -cells, where insulin production is highly dependent on ER function, ER stress occurs under conditions of increased insulin demand, such as in diabetes. The adaptive UPR response is crucial for maintaining β -cell differentiation and function. Failure of this response is associated with dedifferentiation and loss of β -cell function.

Inside pancreatic β -cells, the production and release of insulin rely on the capacity of the ER. It's widely known that almost half of the total protein synthesis in these cells is dedicated to insulin. When someone has diabetes, the need for insulin rises, leading to increased synthesis of proinsulin and causing stress on the ER, in fact, many studies demonstrated that the chronic exposure to high glucose can activate the ER stress in β -cells (Herbert and Laybutt 2016). In response, the UPR is activated as a protective mechanism. This response is crucial for preserving the specialized characteristics of β -cells. However, if the UPR fails to adapt in β -cell ER, it's associated with the dedifferentiation of β -cells and the impairment of their function (Herbert and Laybutt 2016), although it is not clear how it works, although hypoxia and inflammatory signalling have been implicated in the inactivation of UPR in β -cells under diabetic conditions (Kupsco and Schlenk 2015).

In general, the ER-mediated oxidative stress and the inflammation can be associated to the β -cell dedifferentiation. Further studies need to clarify the crosstalk between the ER and mitochondria (Khin, Lee et al. 2021), although it can be assumed that hypoxia and inflammation in the loss of adaptive UPR under chronic hyperglycaemia. Under chronic hyperglycaemia, the acceleration of mitochondrial metabolism and the stimulation of ATP consuming cellular processes, increases β -cell O_2 consumption. On the other hand, chronic hyperglycaemia negatively affects islet vasculature thereby resulting in reduced O_2 supply. These events lead to β -cell hypoxia and activation of downstream PKR and DDIT3. Activation of these effectors plays an important role in the inhibition of the UPR under hypoxia (Bensellam, Jonas et al. 2018).

6. Regulation of the insulin secretion and techniques to study

Physiological insulin secretion is characterized by an inter-prandial and nocturnal basal flow that is overlaid by secretory peaks in response to meals. The main regulator of insulin secretion is glucose (Park, Gautier et al. 2021).

In relative fasting period, the insulin plasma level is maintained at value of around $10 \mu\text{U}/\text{mL}$, whereas, in conjunction with meals reaches values between 50 and $120 \mu\text{U}/\text{mL}$. Under conditions of total fasting or during prolonged exercise, this value decreases by 50%; while, after a normal meal, the plasma insulin level increases 3 to 10 times, with an observable peak 30-60 minutes after the start of the meal (Casella, Soricelli et al. 2016). Several *in vitro* methods exist to study insulin secretion in response to glucose and the presence of secretagogues or inhibitors of secretion.

6.1. Biorep Perifusion System

On a physiological level, cells are continuously subjected to environmental changes, as a result of which they generate responses in relation to the stimuli they receive. In pancreatic tissue, the vascular system is designed to dynamically flush the pancreatic islets through a dense capillary network. In fact, although the total β -cell mass represents less than 5% of the entire pancreatic parenchyma, more than 15% of the total pancreatic blood volume is irrigated daily (Lifson, Lassa et al. 1985). This massive perfusion makes us realize how greedy the pancreatic islets are for metabolites. In fact, β -cells are continuously subjected to respond to different blood glucose concentrations in different time intervals, adjusting an insulin response proportional to blood glucose levels. This process mediates the control of blood glucose homeostasis. To date, there is no artificial endocrine pancreas model capable of mimicking what happens in pancreatic tissue, however, thanks to the Biorep Perifusion system (Biorep Technologies) it is possible to reproduce *in vitro* the microfluidic dynamics that characterize the responses that occur physiologically *in vivo*. This system allows the islets of Langerhans to be sprayed with different solutions containing varying concentrations of glucose and/or secretagogues in a temperature-controlled environment (37°C) according to timings set by the operator.

This system is used by many laboratories research laboratories to assess the insulin secretion of the islets or pseudo-islets in response to different stimuli (such as may be different glucose concentrations, the presence of secretagogues the presence of

drugs or secretion inhibitors) or to assess the goodness of the islets before they go for transplantation (Cabrera, Jacques-Silva et al. 2008, Whitticar, Strahler et al. 2016, Teraoku and Lenzen 2017). The protocol of all these works involves perfusing the islets with solutions at different glucose concentrations to assess the response of insulin secretion which must be proportional to the amount of glucose in the solution (Bentsi-Barnes, Doyle et al. 2011). The cells are, therefore, perfused with a solution that is called 'stimulus', which is the solution that has the concentration of glucose we want to analyse or molecules to be study such as secretagogues, drugs or inhibitors. Subsequently, the cells are perfused with an aqueous solution of KCl (potassium chloride) a membrane depolarizing membrane, which promotes the release of all the insulin granules present in the cells.

6.2. Study of insulin secretion on porcine pancreatic tissue slices

Although the Biorep Perifusion System is the most accurate way to study the GSIS *in vitro*, the use of islets of Langerhans as samples has certain limitations.

For instance, separation of the islets of Langerhans from the surrounding tissue causes a loss in terms of studying the islets in their natural habitat. In addition, the isolation procedure involves physical and mechanical stress that can induce changes in the physiology of the cells, and the separation of the exocrine cells from the endocrine cells does not allow organ-specific studies on the interaction between the two compartments (endocrine and exocrine) (Bhagat, Singh et al. 2000, Ahn, Xu et al. 2007, Negi, Jetha et al. 2012, Irving-Rodgers, Choong et al. 2014). It is essential that this aspect is not lost, especially in this study, where we want to verify the state of β -cells influenced by the external environment, which in our case is the intrauterine environment. Furthermore, this less invasive procedure allows paracrine and autocrine interactions to be preserved (Marciniak, Cohrs et al. 2014). Last but not least, the freshly isolated islets cannot be used immediately for the GSIS experiment but need a resting time some days (Borg, Weigelt et al. 2014, Jun, Lee et al. 2019, Alcazar, Alvarez et al. 2020). Because of these stresses, using Langerhans islets *in vitro* may not reflect what happens *in vivo*.

The study conducted by the University of Dresden also assessed, using *in situ* imaging studies, that islet innervation, calcium dynamics, endocrine and exocrine tissue morphology were intact using the less invasive procedure of producing tissue slices (Marciniak, Cohrs et al. 2014). For these reasons, we used the Biorep

Perifusion System for pancreatic tissue slices, as described in (Panzer, Cohrs et al. 2020) and published from University of Dresden. In this study, we adapted the protocol, that was established for murine pancreas, for the porcine pancreas (see materials and methods).

III. ANIMALS, MATERIALS AND METHODS

1. Animals

In this study, *INS*^{C94Y} transgenic and the *INS-eGFP* transgenic pig lines were used. The *INS*^{C94Y} pig line harbours a mutant *INS* p.C94Y transgene leading to permanent neonatal diabetes due to mutant misfolded insulin expression and represents a large animal model for the human disease MIDY (mutant *INS* gene induced diabetes of youth) (Renner, Braun-Reichhart et al. 2013). *INS-eGFP* transgenic pigs express an eGFP reporter gene selectively in the β -cells (Kemter, Cohrs et al. 2017), enabling β -cell sampling to be flow cytometry. To reduce the genetic variance, the sows used for the project, were themselves littermates of a wild-type (WT) mother and an *INS*^{C94Y}/*INS-eGFP* dual transgenic boar. Moreover, for the project, the sows were mated with the same WT boar or an *INS-eGFP* transgenic boar (Renner, Braun-Reichhart et al. 2013, Kemter, Cohrs et al. 2017).

Blood glucose levels of diabetic *INS*^{C94Y} and *INS*^{C94Y}/*INS-eGFP* breeding sows were kept by daily insulin treatment in the range of 100-150 mg/dL when non-pregnant and for the first three weeks after insemination. When pregnancy was confirmed by ultrasound analysis at embryonic day E21/E22, daily insulin treatment was adapted within one week for maintaining a fasting blood glucose level at 300 mg/dL. Blood glucose concentrations were measured every day and animals were treated with a combination of long-acting and short-acting insulin (Lantus[®] and Novorapid[®]).

2. Materials

2.1. Chemicals

| | |
|---|-----------------------|
| Agarose UltraPure™ | Invitrogen, Karlsruhe |
| Bromophenol Blue | Roth, Karlsruhe |
| Ethanol | Roth, Karlsruhe |
| Glucosteril [®] 50% Glucose solution | B. Braun, Melsungen |
| HCl (Hydrochloric acid) | Roth, Karlsruhe |

| | |
|---|-------------------------------|
| MgCl (Magnesium chloride) | Fluka Chemie, Schweiz |
| NaCl (Sodium chloride) | Sigma-Aldrich, St. Louis |
| KCl (potassium chloride) | Sigma-Aldrich, St. Louis |
| Na ₂ HPO ₄ *2H ₂ O (sodium hydrogen Phosphate) | Sigma-Aldrich, St. Louis |
| MgSO ₄ (Magnesium sulfate) | Sigma-Aldrich, St. Louis |
| CaCl ₂ *2H ₂ O (Calcium chloride) | Sigma-Aldrich, St. Louis |
| KH ₂ PO ₄ (Potassium dihydrogen phosphate) | Sigma-Aldrich, St. Louis |
| Hepes | Sigma-Aldrich, St. Louis |
| NaHCO ₃ (sodium hydrogen carbonate) | Sigma-Aldrich, St. Louis |
| MgCl ₂ *6H ₂ O (magnesium chloride hexahydrate) | Sigma-Aldrich, St. Louis |
| Glucose | Sigma-Aldrich, St. Louis |
| RBS [®] 50x (83462-1L) | Merck, Darmstadt |
| Aprotinin (A3428) | US-Biological Life Science |
| Paraformaldehyde | VWR, Darmstad |
| BSA (Bovine Serum Albumin) | Sigma-Aldrich, St. Louis |
| Agarose low-melting | Roth, Karlsruhe |
| Paraformaldehyde (#86148) | Sigma-Aldrich, St. Louis |

2.2. Perifusion materials

| | |
|---|----------------------------------|
| Dow Corning High-Vacuum silicone grease (Z273554-1EA) | Sigma-Aldrich, St. Louis |
| Chamber platform (P-5) | Warner Instruments, Holliston |
| Cell culture chamber (RC-20H) | Warner Instruments, Holliston |
| Glass cover slip (CS-15-R) | Warner Instruments, Holliston |
| Polyethylene Tubing (PE-160/10) | Warner Instruments, Holliston |
| 2 stop tubing with connectors (PERI-TUBSET) | Biorep Technologies, Miami |

| | |
|---|-------------------------------|
| Tubing (PERI-TUB-040) | Biorep Technologies, Miami |
| PERI-NOZZLE | Biorep Technologies, Miami |
| Periclips | Biorep Technologies, Miami |
| Y connectors with 200 series barb (Peri – FITTING -3) | Biorep Technologies, Miami |

2.3. Consumables

| | |
|---|---|
| Cell culture dish | Corning Inc., Somerville |
| Cell culture plates | Corning Inc., Somerville |
| Aiguilles injection | B. Braun, Melsungen |
| Cotton tipped applicators | D&D Medical Equipment |
| Steril surgical blades (BB522) | B. Braun, Melsungen |
| Adhesive tape | Tesa, Beiersdorf |
| CBAS [®] Heparin Coated Clear PU Cath 7Fr | B. Braun, Melsungen |
| Combitips [®] plus (2.5 mL, 10 mL) | Eppendorf, Hamburg |
| Cover slips (24x40 mm) | Corning Inc., Somerville |
| Discofix [®] 3-way stop-cock with connection line (10 cm) | B. Braun, Melsungen |
| Disposable syringes (2, 5, 10, 20 mL) | Henry Schein [®] Vet GmbH, Hamburg |
| Neolus [®] hypodermic needles (30 G) | B. Braun, Melsungen |
| Falcon [®] centrifuge tubes (15, 50 mL) | Biologix, Shandong |
| FreeStyle Precision [®] glucose stripes | FreeStyle, Abbott |
| Hypodermic needles (18 G, 20 G) | B. Braun, Melsungen |
| Monovette [®] blood collection system (Plasma, EDTA, 9 mL) | Sarstedt, Nümbrecht |
| Original Perfusor [®] Line (50 cm) | B. Braun, Melsungen |
| Original Perfusor [®] syringes (50 mL) | B. Braun, Melsungen |
| Parafilm [®] M | American Can Company, USA |

| | |
|--|------------------------|
| PCR reaction tubes (0.2 mL) | Applied Biosystems |
| Pipette tips with filter | Eppendorf, Hamburg |
| SafeGrip [®] latex gloves | SLG, Munich |
| Scalpel blade sterile No.36 | B. Braun, Melsungen |
| Sempermed [®] supreme latex OP gloves | Sempermed, USA |
| Star Frost [®] microscope slides 3-way-stopcock Variostop [®] | Engelbrecht, Edermünde |
| Surgicryl suture | B. Braun, Melsungen |
| Uni-Link embedding cassettes | EngelBrecht, Edermünde |

2.4. Devices

| | |
|--|---|
| Biorep Perifusion System (Peri 4.2) | Biorep Technologies, Miami |
| Vibratome (VT1200S) | Leica, Wetzlar |
| Tecan Reader | Tecan [™] , Männergdorf |
| ART-Micra D-8 tissue-homogenizer AU 480 analyzer | ART, Müllheim |
| FreeStyle Precision [®] neo glucometer | FreeStyle, Abbott |
| HM 315 microtome | Microm, Walldorf |
| inoLab [®] pH meter 7110 | WTW [™] Fisher Scientific, Schwerte |
| Incubator 60 °C | Thermo Scientific, Waltham |
| Mastercycler [®] gradient | Eppendorf, Hamburg |
| Microwave | B. Braun, Melsungen |
| Multichannel pipette mLine [®] (300 µl) Multipipette [®] plus | Eppendorf, Hamburg |
| Pipettes (1000 µl, 200 µl, 100 µl, 10 µl, 2 µl) | Gilson Inc., USA |
| Power Pac 300 gel electrophoresis unit | Bio-Rad, Berkeley |
| Tecan infinite M200Pro ELISA reader | Tecan [™] , Männergdorf |
| Thermomixer 5436 | Thermo Scientific, Waltham |
| Plates shaker | Roth, Karlsruhe |

| | |
|--------------------------------------|-------------------------------|
| AU480 auto analyzer | Beckman-Coulter |
| Elisa Reader (680) | Bio-Rad, Berkeley |
| Tissue processor EpreDia™ Excelsior™ | Thermo Scientific, Waltham |
| Axio Scan.Z1 slide scanner | Zeiss, Jena, Germany |

2.5. Drugs

| | |
|-----------------------------------|----------------------------------|
| Cloprostenol (Estrumate-Schwein®) | Intervet, Unterschleißheim |
| Ketamine 10% (Ursotamin®) | Serumwerke Bernburg, Bernburg |
| Azaperone (Stresnil®) | Jansen Pharmaceutical, Beerse |
| Fentanyl (Fentadon®) | Dechra, Northwich |
| Insulin (Novorapid®) | Novo Nordisk, Bagsværd |
| Insulin (Lantus®) | Sanofi, Paris |

2.6. Kits

| | |
|---|----------------------------------|
| Cisbio HTRF® insulin assay | Cisbio Bioassays S.A.S., Codolet |
| Mercodia Insulin ultra sensitive ELISA | Mercodia, Uppsala |
| Nexttec™ Genomic DNA Isolation Kit from Tissue and Cells | Nexttec GmbH, Leverkusen |

2.7. Software

| | |
|-------------------------------|--|
| Graph Pad Prism® version 5.02 | GraphPad Software Inc., USA |
| QuPath | © Copyright 2019-2024, QuPath docs authors. Revision 6ba1235b |
| Perseus statistical analysis | Copyright © Max-Planck-Institute of Biochemistry |

2.8. Buffers and solutions

2.8.1. Solutions for perfusion system

Krebs

| | Chemical | MW | 1x final concentration [mM] | g/L (4-fold) |
|---|--|--------|-----------------------------|-----------------------|
| Solution 1A: 4x | NaCl | 58.44 | 137 | 32.0 |
| | KCl | 74.56 | 5.36 | 1.6 |
| | Na ₂ HPO ₄ *2 H ₂ O | 177.99 | 0.34 | 0.2 |
| | MgSO ₄ | 120.38 | 0.81 | 0.4 |
| | CaCl ₂ * 2 H ₂ O | 147 | 1.26 | 0.7 |
| | KH ₂ PO ₄ | 136 | 0.44 | 0.2 |
| | | | | H₂O |
| Solution 1B (60mM K+): 4x | NaCl | 58.44 | 82.8 | 19.35 |
| | KCl | 74.56 | 59.56 | 17.8 |
| | Na ₂ HPO ₄ *2 H ₂ O | 177.99 | 0.34 | 0.24 |
| | MgSO ₄ | 120.38 | 0.81 | 0.4 |
| | CaCl ₂ * 2 H ₂ O | 147 | 1.26 | 0.7 |
| | KH ₂ PO ₄ | 136 | 0.44 | 0.2 |
| | | | | H₂O |
| Solution 2: Hepes Bicarbonate (4x) | Hepes | 238.31 | 10 | 9.5 |
| | NaHCO ₃ | 84.01 | 4.17 | 1.4 |
| | | | H₂O | to 1L |

For 1x solution 1A+2: combine ¼ solution 1A + ¼ solution 2 + ½ ddH₂O

For 1x solution 1B+2: combine ¼ solution 1B + ¼ solution 2 + ½ ddH₂O (this solution is used for the KCl stimulus).

ECS

| Chemical | MW | 1x final concentration [mM] | g/L (4-fold) |
|--|--------|-----------------------------|--------------|
| NaCl | 58.44 | 125 | 31.25 |
| KCl | 74.55 | 2.5 | 2.5 |
| NaH ₂ PO ₄ *H ₂ O | 119.98 | 1.25 | 1.25 |
| MgCl ₂ *H ₂ O | 203.3 | 1 | 1 |

| | | | |
|--------------------------|--------|----|--------------|
| CaCl₂ | 110.98 | 2 | 2 |
| NaHCO₃ | 84.007 | 26 | 26 |
| Hepes | 238.31 | 10 | 10 |
| Glucose | 180.16 | 3 | 3 |
| ddH₂O | | | to 1L |
| Set to pH 7.4 | | | |

2.8.2. Fixatives and other solutions

4% PFA

| Reactive | To 1 L |
|--------------------|-----------------|
| Paraformaldehyde | 40 g |
| 10 x PBS | 100 mL |
| ddH ₂ O | Add until 0.9 L |
| 5 M NaOH | 100 µL |
| Adjust pH | |
| ddH ₂ O | Add until 1L |

Dissolve at 50°C in water bath (shaking occasionally); cool down when everything is dissolved, and the pH is adjusted at 7.35-7.4. After it the PFA was filtered and stored at 4%.

10x PBS

| Reactive | MW g/mol | g/ L |
|----------------------------------|-----------------|--------------|
| NaCl | 55.44 | 79.5 |
| Na ₂ HPO ₄ | 141.96 | 11.5 |
| KCl | 74.55 | 2.0 |
| KH ₂ PO ₄ | 136.08 | 2.0 |
| ddH ₂ O | | 950 mL |
| Adjust pH 7.35-7.4 | | |
| ddH ₂ O | | Add until 1L |

2.8.3. Buffer for PCR

dNTP-mix

2 mM dATP, dCTP, dGTP, dTTP

Mixed in distilled water

Aliquoted and stored at -20 °C

TAE buffer (50×)

242 g 2 M Tris

100 mL 0.5 M EDTA (pH 8.0)

57 mL glacial acetic acid

1000 mL distilled water

Filtrated and autoclaved for storage

Before usage diluted to single concentration

3. Methods

The schematic Figure 1 shows the methods and strategy applied in this thesis work. All animal experiments were carried out in compliance with the German Animal Welfare Act and Directive 2010/63/EU on the protection of animals used for scientific purposes and approved by the appropriate local authority (Regierung von Oberbayern). Parent pigs had free access to tap water. Non-diabetic breeding pigs were fed twice per day, whereas diabetic pigs were fed once per day timely coordinated with daily glucose measurement and insulin treatment. Animals were kept in groups if feasible. Enrichment materials such as toys were always available.

3.1. Reproduction management of the sows

Healthy (WT) (n=5) and INS^{C94Y} (MIDY) transgenic sows (n=6) aged 9 ± 0.84 months were artificially inseminated with semen from the same healthy boar. Pregnancy was confirmed by ultrasonography 21 days after insemination. Starting at pregnancy day 113, pregnant sows were monitored for signs of birth. Birth was hormonally induced at E115 if not occurring spontaneously by a single intramuscular injection of cloprostenol (Estrumate[®], 0.175 mg per animal). Farrowing took place between 24 to 36 hours after birth induction.

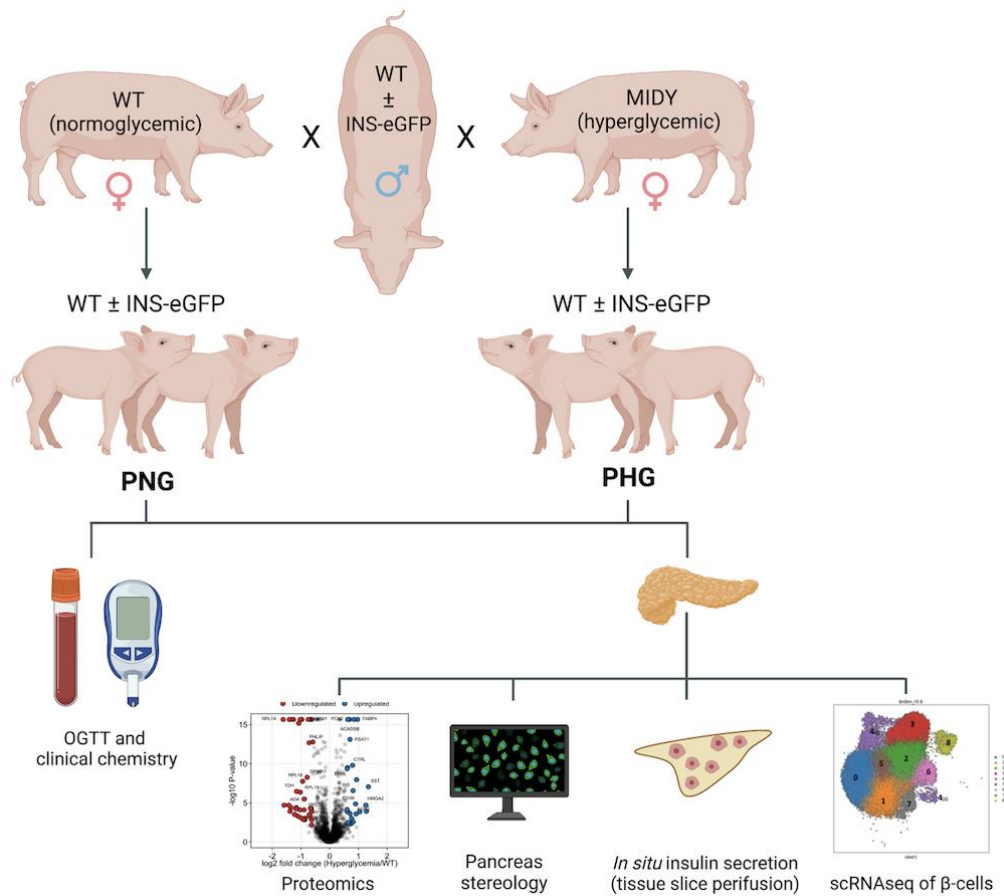


Figure 1: Methods used in this work. The normo- and hyperglycaemic sows were mated with the same healthy boar and analysis are conducted on healthy piglets from healthy mothers (PNG) and hyperglycaemic mothers (PHG).

3.2. Oral glucose tolerance test (OGTT) of new-born piglets

OGTT was performed in neonatal piglets (PNG: n= 39, and PHG: n= 13). Shortly after birth before first milk intake, piglets were separated from the mother, weighed, and then placed in a rescue deck with a red heating lamp. After a recovery period

of 30 min after birth, OGTT was performed by application of a glucose bolus [4 mL per kg body weight (BW) of a 50% glucose solution (B. Braun)] via a gastric tube. This procedure is suitable in piglets that are not yet able to digest a meal, taking advantage of the suckling reflex. Before glucose application at time point (TP) 0, and then at TP 15, 30, 45, 60, 90 and 120 minutes after oral glucose application, blood glucose concentration was measured by ear vein puncture using a glucometer (FreeStyle-Freedom Lite). Moreover, 1mL EDTA blood samples were collected from the jugular vein at TP 0, 30, 60 and 120 minutes, immediately put on wet ice, centrifuged at 2800 rpm for 20 minutes at 4°C, aliquoted and stored at -80°C.

3.3. Blood sampling from the sows

The piglets' clinical analysis has to be compared to the sows' clinical analysis to exclude the possibility of detecting maternal parameters in the bloodstream of newborn piglets. Therefore, blood samples were taken also from the sows from the ear vein during the delivery (healthy: n= 4, and *INS*^{C94Y}: n=4). While giving birth, the sows lie on their side, and we took advantage of this moment to collect blood from the ear vein, using a tourniquet, and to obtain samples of EDTA, serum, and Li-Hep for backup storage.

3.4. Clinical-chemical analysis of blood samples

Table 1: Clinical-chemical parameters

| | Biomarker |
|--------------------------------|------------------|
| Carbohydrate metabolism | Insulin |
| | Glucose |
| | Lactate |
| | LDL |
| | ALT |
| Lipid metabolism | Cholesterol |
| | HDL |
| | LDL |
| | Lipase |

| | |
|---------------------|---------------|
| | NEFA |
| | Triglycerids |
| | Bilirubin |
| | Total Protein |
| Electrolytes | Na |
| | Cl |

Clinical-chemical parameters (Table 1) were determined from EDTA plasma both of TP0 of new-born piglets (PNG: n= 47, and PHG: n=14) and of samples of the mothers during the delivery using an AU480 auto analyser (Beckman-Coulter) and adapted reagent kits from Beckman-Coulter, Randox or Wako Chemicals. Optical density was measured with a photometric lamp. Clinical-chemical analyses except for insulin were performed by Dr. Birgit Rathkolb, Helmholtz Munich.

3.5. Ultrasensitive Insulin-ELISA immunoassay (Merco[®])

The measurement and evaluation of plasma insulin concentration of the OGTT was performed with the insulin-ELISA immunoassay (Merco[®]). This solid-phase immunoassay is based on the sandwich technique in which two monoclonal antibodies are directed against two different antigens located on the insulin molecule. During incubation, the insulin contained in the sample reacts with a peroxidase-conjugated anti-insulin antibody and a well-bound anti-insulin antibody. A manual wash step, in which unbound antibodies are removed, is performed with 300 μ L of wash solution. The conjugate bond is detected with TMB (tetramethylbenzidine) the reaction is stopped by adding an acid solution that provides a colorimetric scale that is read using a spectroscope. The reading is made at 450 nm using the Elisa Reader (Model 680 Bio-Rad). Each sample was pipetted in duplicate, and the background was subtracted. The final data was obtained with the mean of the 4PL Plot calculation.

3.6. Identification of piglets' genotype using polymerase chain reaction (PCR)

Tail punches were obtained and stored at -20 °C. Genomic DNA was isolated using the “nexttecTM Genomic DNA Isolation Kit from Tissue and Cells” (nexttec

GmbH, Leverkusen) according to the manufacturer's instructions. Briefly, samples were cut in small pieces and incubated with an appropriate lysis buffer. Samples were incubated 1 h to overnight at 60°C in a thermomixer. Lysates were then purified using nexttec™ clean columns to elute purified DNA.

Next, genotyping was performed by polymerase chain reaction (PCR). The specific primers used are listed in Table 2.

Table 2: primer sequence for the PCR reaction

| | | Sequence |
|---|---------------|----------------------------------|
| <i>INS</i> ^{C94Y} transgene | C94Y_21_f | 5'-CTC TGCAGCTCATGTGGATCAG-3' |
| | neokanF | 5'-GAC AAT AGC AGG CAT GCT G -3' |
| <i>INS</i> -eGFP transgene | INS-GFP_2_for | 5'-TCGTTAAGACTCTAATGACCTC-3' |
| | INS-GFP_5_rev | 5'-ATGAACTTCAGGGTCAGCTTGCC-3' |
| Neomycin resistance cassette (<i>neo</i>) | neo_1_for | 5'-ACAACAGACAATCGGCTGCTCTG-3' |
| | neo_2_rev | 5'-TGCTCTTCGTCCAGATCATCCTG-3' |

Beside the construct specific genotyping PCR, an additional PCR for amplification of a part of the neomycin resistance cassette which is present in both transgene expression cassettes was performed.

PCR components were mixed on ice to a final volume of 20 µL in 0.2-mL reaction tubes. Genomic DNA from WT pigs served as negative control and from *INS*^{C94Y}/*INS*-eGFP dual transgenic pigs were used as positive control and distilled water was used as a non-template control. Details from master mix ingredients and PCR conditions are listed in Table 3:

Table 3: Master mix components per PCR reaction

| Master Mix components | <i>INS</i> ^{C94Y} µL | <i>INS</i> -eGFP µL | neo µL |
|-----------------------|-------------------------------|---------------------|--------|
| H ₂ O | 13 | 7.65 | 7.65 |
| dNTP | 2 | 1 | 1 |
| 10X Coral | 2 | 2 | 2 |
| MgCl ₂ | 1 | 4 | 4 |
| Q-Sol | / | 1.25 | 1.25 |
| Primer (f) (10µM) | 0.4 | 2 | 2 |
| Primer (r) (10µM) | 0.4 | 1 | 1 |
| HotStar-Taq | 0.2 | 0.1 | 0.1 |

19 µl of the master mix were put in the 0.2 µL reaction tubes, and 1 µl of template or control were added. Details of PCR reaction conditions are listed in Table 4 & 5.

Table 4: PCR reaction conditions for *INSC94Y*

| | | | |
|------------------|------|--------|------|
| Denaturation | 95°C | 5 min | |
| Denaturation | 94°C | 30 sec | 35 x |
| Annealing | 58°C | 30 sec | |
| Elongation | 72°C | 30 sec | |
| Final Elongation | 72°C | 5 min | |
| Termination | 4°C | 5 min | |

Table 5: PCR reaction conditions for *INSeGFP* and *neo*

| | | | |
|------------------|------|--------------|------|
| Denaturation | 94°C | 5 min | |
| Denaturation | 94°C | 30 sec | 35 x |
| Annealing | 60°C | 30 sec | |
| Elongation | 72°C | 1 min 20 sec | |
| Final Elongation | 72°C | 10 min | |
| Termination | 4°C | 5 min | |

An agarose gel electrophoresis was run to visualize the final PCR products. Therefore, a 1.5% agarose gel was prepared by heating 1 x TAE buffer with 1 g/100 mL universal agarose in the microwave. After cooling down to about 55 °C, the gel was decanted into an electrophoresis chamber (OWL Inc., USA) for polymerization. Samples were mixed with 2.5 µL 10× DNA loading buffer and pipetted individually into the slot chambers of the gel. Six µL of Gene Ruler™ 100 bp DNA molecular weight marker (MBI Fermentas) was included for the determination of DNA fragment sizes. An electric field with a voltage of 130 V was applied for 30 minutes. After separation DNA samples were visualized under ultraviolet (UV) light.

3.7. Necropsy

After the body weight measurement, PHG and PNG piglets undergone necropsy at an age of three days, or when flow cytometry for scRNAseq study or *in situ* tissue slice perfusion was performed, also at day 1 or 2 after birth. They were first anaesthetized with ketamine 10% (20 mg/kg BW) and azaperone (2 mg/kg BW), for analgesic use 0.5 ml fentanyl. Once the piglet was properly sedated, 9 ml EDTA,

Li-Heparin and a 9 ml serum blood samples were taken from the left jugular vein. Afterwards, euthanasia took place. Euthanasia and blood sampling were performed by veterinarians. Heparin and EDTA vials were placed on ice and serum at RT for 20 minutes. They were then centrifugated at 2800 rpm for 20 minutes at 4°C. The supernatant was collected in 1.5-mL tubes and placed in -80°C. Organs were dissected and weighed to the nearest mg. Tissue samples were collected as described previously (Albl, Haesner et al. 2016) and routinely fixed in 4% PBS-buffered paraformaldehyde or modified oyoy solution for 2 days prior paraffin embedding or frozen immediately on dry ice and stored at -80 °C for molecular profiling.

3.8. Sampling of the pancreas

The pancreas was processed as first organ immediately after the necropsy. First the part attached to the spleen was recognized and it was separated removing the mesenterium, using surgical scissors (right before the splenic artery). To have a clearer view, the intestine was put on the right side, in this way the part attached to the left kidney is visible and it can be separated concentrically from the peritoneum, following the natural way, it can be removed from the intestine and the stomach. Make sure not to injure the left adrenal gland which is in between the back and the pancreas. Once most of the left part has been removed, the intestine was put on the other side and the pancreas could be removed from the rest of the stomach and the duodenal part became therefore well visible. After removal of the rest of the pancreas from the intestine, the last part is the link to the duodenal duct, and it was carefully separated with the point of the scissors. After the pancreas was completely removed from the intestine, it was cleaned from connective tissue, fat and lymph nodes and it was weighed.

3.8.1.1. Processing of the pancreas

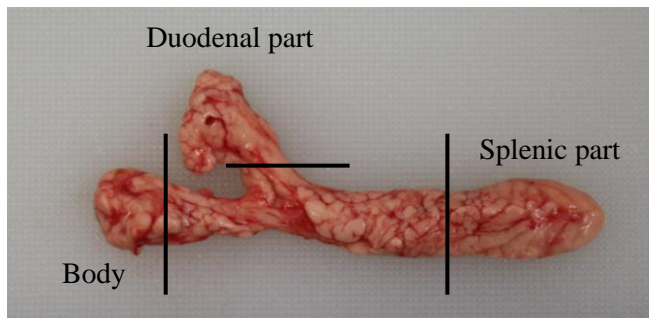


Figure 2: Piglet's pancreas anatomy. The splenic part is the part closest to the spleen, which corresponds to the 'tail' of the human pancreas anatomy. While the duodenal part of the porcine pancreas corresponds to the 'head' of the human pancreas.

After recognizing the different parts of the pancreas (Fig. 2), the sampling was performed according to the following procedure: Cut a small piece of pancreas from the splenic part and the duodenal part and put them directly in the cassettes for Methacarn. Afterwards, cut a piece from the duodenal splenic part and cut it into smaller pieces, and execute

the frozen shock on dry ice and put them in the 2-mL tubes. Put the rest of the pancreas in a separated falcon with PFA and complete the cut afterwards under chemical flow. After 2 hours in PFA on ice, the process of the pancreas can start. Under the flow: the pancreas is cut in parallel lamellae to obtain random systematic samples. The piglet pancreas' length is around 7 cm, start from the splenic part and with a scalpel obtain pieces 0.5 cm long and alternate between the cassette for the paraffin embedding and for the sucrose gradient embedding.

The cassettes with the organs are placed in a container filled up with fresh 4% PFA and they rest on a shaker on ice for 48 hours. The ice was constantly checked and replaced in case of thawing, to guarantee the constant temperature.

3.8.2. Sampling of the other organs

After the preparation of the pancreas, all the other organs for the establishment of a Biobank were processed. The organs taken during the autopsy are listed in the Table 6. All the organs were cut in small pieces, shock-frozen on dry ice and put in 2-mL tubes. Big pieces of the organs are put in PFA and Methacarn. The brain is cut in half and the entire left lobe is put in the 4%PFA and the right half of the hypothalamus is native fixed in tissue Tek.

Table 6: organ list collected during the dissection

| Organ System | Organ/ Tissue | Site | PFA | Methacarn | native -80° |
|---------------------------------|-------------------|-------------------------|-----|-----------|----------------|
| Hepatobiliary and Pancreatic | Pancreas | Spleen part | + | + | + |
| | | Duodenal part | + | + | + |
| | Liver | Left lobe | + | + | + |
| Endocrine | Adrenal gland | / | + | + | + |
| | Thyroid Gland | / | + | + | + |
| Cardiovascular | Heart | Left Ventricle | + | + | + |
| | | Left Atrium | + | + | + |
| | | Random | + | + | - |
| Respiratory | Lungs | Left | + | + | + |
| Nervous | Brain | Left part | + | - | - |
| | | Hypothalamus (right) | - | - | + |
| Urinary | Kidney | Cortex | + | + | + |
| | | Medulla | + | + | + |
| Immune and hematopoietic | Thymus | / | + | + | + |
| | Spleen | / | + | + | + |
| Musculoskeletal | Muscle | Longissimus | + | + | + |
| | | Bicep | + | + | + |
| | | Soleus | + | + | + |
| Integument | Skin | / | + | + | + |
| | Adipose tissue | Subcutaneous | + | + | + |
| | | Visceral | + | + | + |
| Fluids | Serum | / | + | + | + |
| | Plasma | EDTA | + | + | + |
| | | Li-Heparin | + | + | + |
| | Urine | / | + | + | + |

3.9. Immunofluorescence staining and stereological quantification of endocrine cell volume ratio

3.9.1. Processing of fixated tissue

After 48 hours on the shaker, the cassettes with the fixated tissue were routinely processed in a carousel tissue processor (Thermo Scientific EpreDia™ Excelsior™). Following paraffin embedding with the TBS 88 Paraffin Embedding System, 3 µm thick slides from 4% PFA-fixed paraffin embedded tissues from different part of the pancreas were cut with a HM 315 microtome, mounted on glass slides and stored at 37 °C until immunofluorescence staining.

3.9.2. Immunofluorescence (IF) staining

Paraffin sections were deparaffinized and rehydrated through a descending alcohol row according to Table 7.

Table 7: Deparaffinization and rehydration of paraffin sections

| | | |
|-------------------|---------------|-----------|
| Deparaffinization | Xylene | 2× 20 min |
| Rehydration | Ethanol 100 % | 2× 5 min |
| | Ethanol 96 % | 2× 5 min |
| | Ethanol 70 % | 5 min |
| Washing | aq. dest. | 2× 1 min |

The antigen-retrieval was performed using Tris EDTA buffer/ 0.05% Tween pH 9.0, boiled at the max temperature in the microwave and 19 minutes of sub-boiling (320 watt). After the permeabilization in PBS/ 0.1% Triton X100 for 10 minutes, the slides were washed 3 times in PBS for 5 minutes and the blocking was performed using 5% donkey serum (in PBS/Tween 0.05%) for 1h at RT. Afterwards, the sections were incubated with the primary Abs overnight at 4°C. The day after, after 10 minutes (2x5 minutes) washing in PBS/Tween 20 0.1%, they were incubated with the secondary Abs for 1h at RT in the dark. Slides were washed with PBS/Tween 20 0.1% and stained with DAPI for 10 minutes at RT. Finally, they were incubated with the Vector True View (Autofluorescence Quenching Kit #SP-8400) for 5 minutes to reduce the auto-fluorescence and mounted with

Mounting Vectashield Vibrance (#M-1700) after 10 minutes (2x5 minutes) washing in PBS.

Table 8: Abs list for the proliferation markers staining

| Target | 1 st Ab | 2 nd Ab |
|----------|--|---|
| Insulin | 1:2000 mouse IgG2 -anti-insulin (#66198-1-Ig, proteintech) | 1 :1000 Alexa Fluor plus 488-conjug. AffiniPure donkey-anti-mouse IgG (H+L) (#A32766, Invitrogen) |
| Glucagon | 1:3000 guinea pig-anti-Glucagon (#M182, TAKARA) | 1:500 AF647 donkey-anti-guinea pig IgG (H+L) (#706-605-148, Jackson ImmunoResearch) |

3.9.3. Image acquisition and digital image analysis

Whole tissue sections were scanned by an Axio Scan.Z1 slide scanner (Zeiss, Jena, Germany) using a 20x/0.8NA Plan-Apochromat (a 0.55 mm) objective at the Core Facility Pathology & Tissue Analytics at the Helmholtz Center Munich.

The assessment of biomarkers by digital image analysis was conducted using the open-source software QuPath. First, pixel classifiers for detection of tissue and islets were trained using a training image. After the recognition of the tissue area and three types of islets classifiers (depending on the strength of the fluorescence signals), the tissue area and islets were automatically identified based on detection and machine learning. After the tissue and the islets recognition, the “endocrine and exocrine tissue” settings were automatically generated, and all the detections were put in hierarchy. Then, object classifiers were applied for specific detection of α cells and β cells. These object classifiers were obtained by intense training using training images and at least 500 positive and negative events for each object classifier. Various details, including the entire tissue section information, exocrine and endocrine areas, the number of islets per section, and the total count of α cells and β cells, and combinations thereof, were obtained. The analysis and pixel classifier identification for the islets was done considering different part of several images (ROI) for creating the training picture and the identification was done considering the big islets as well as the single cells.

For tissue detection, the Pixel classification → Create thresholder command was utilized. After applying the fill hole's function, the tissue was manually inspected for artefacts. Subsequently, the proper islets pixel classifier was downloaded → consider object > then 12 cm² and split → annotation → fill holes. Also in this case, the islets were manually adjusted where necessary. After the hierarchy, the cell detection was performed based on the DAPI, first it was set on islets and then on the exocrine tissue. The cells were recognized as areas of staining above the background level, applying optimized nucleus threshold, segmentation parameters (Median filter radius and Sigma), and cell expansion. The cell detection was optimized for each slide to have the best match for the identification of the cellular nucleus. The main parameter setting was the following, although it was changed several times for the no-fitting slides: 0.344; 6; Median filter: 0.5; Sigma: 0.9; Minimum object size: 8; Maximum object size: 200; background: 150; cell size: 2.45 um. Finally, smoothed features were incorporated to derive new measurements considering the cell features within a 25µm range. For endocrine cell detection, different classifier was created for the best fitting match of the different hormones. The main object classifier used for the hormonal staining, were obtained using a training image with several ROI. To adjust the classifier where it was not fitting, other slides with the same or similar intensity of fluorescence, were considered in the previous training analysis, using the “point” options to distinguish first the positive cells and the ignore cells and then, these points were saved and used together to improve the object classifier. Cell mean intensity thresholds. Finally, after the identification of the best object classifier for each slide, a composite classifier was created and applied, after that, the distance to annotation 2D was established. Annotation measurements were exported, providing information on islet size, cell composition, and the number of positive cells.

3.10. *In situ* dynamic glucose stimulation insulin secretion (GSIS) on pancreatic tissue slices

Dynamic glucose stimulation insulin secretion was assessed *in situ* on living porcine pancreatic tissue slices of newborn PHG or PNG at an age of 2 to 3 days,

with a modified protocol adapted from that developed by Speier et al (Marciniak, Cohrs et al. 2014).

3.10.1. Pancreas processing and vibratome slices

Immediately after euthanasia and exsanguination, 37 °C warm 1.75% low-melting agarose (#39346-81-1, Carl Roth) supplemented with 25 KIU/mL (kallikrein inactivator unit per ml) aprotinin (#A2300-05, US Biological Life Science) were applied into the splenic pancreas lobe by exogenous G27 needle injection. After hardening of agarose on wet ice, small pieces of approx. 1-1.5 mm³ of the splenic lobe were cut and embedded in 2.5% low-melting agarose. Subsequently, 150 µm thick vibratome tissue slices were obtained using the vibratome settings thickness 150 µm, amplitude 1.0, and feed 0.1 mm/sec (Leica VT1200S).

Before beginning the vibratome procedure, it's crucial to ensure the razor blade is securely inserted into the cutting unit to prevent any unexpected movements that could pose a risk of injury. Once the blade is properly in place, the vibratome can be switched on using the switch located at the right rear end of the unit. This action prompts the vibratome to move to its initial position. Next, the calibration unit should be attached to the vibratome, with the cable connected to the unit at the left rear end. Following the flashing buttons on the control unit, the calibration process involves pressing the "Down" button to initiate movement of the cutting unit forward and downward. Subsequently, the flashing "Run/Stop" key is pressed to commence vibration. Once numbers appear on the display, adjustments should be made until the left number reads "0", indicating optimal calibration. This adjustment process involves loosening and tightening screws as necessary. Upon successful calibration, the calibration unit can be removed, and the white tray attached to the vibratome. Carefully insert the black tray afterward. Tissue pieces should then be prepared in a 6 cm cell culture dish, cutting cuboids with a scalpel and detaching agarose from the dish edges. Individual agarose blocks can be removed and placed onto the black sample plate, followed by trimming with the scalpel to leave a narrow edge around the tissue piece (Figure 3). To ensure smooth slicing, the sample plate is held against the razor blade, and a thin layer of glue is applied to the plate before placing the agarose blocks onto the surface. Additional glue can be applied to the edges of the blocks for better adhesion. After a brief

waiting period, the sample plate is placed in the black tub and filled with 3 mM ECS. Simultaneously, a 6 cm cell culture dish is filled with 6 mL KRBH buffer for slice acquisition. Slicing is initiated by moving the sample table upwards until the razor blade is fully immersed in the buffer, setting the start and end positions accordingly. Continuous slicing between these positions is facilitated by activating the "AUTO/MAN" and "SINGLE/CONT" buttons. Adjustments to cutting parameters can be made as necessary before slicing commences. The process can be paused or resumed using the "Pause" button, with slicing completed by pressing "Run/Stop". After discarding the initial slices, subsequent slices are transferred into the 6cm cell culture dish with KRBH buffer until the desired number is achieved. Additional dishes may be prepared if more than 40 slices are required.

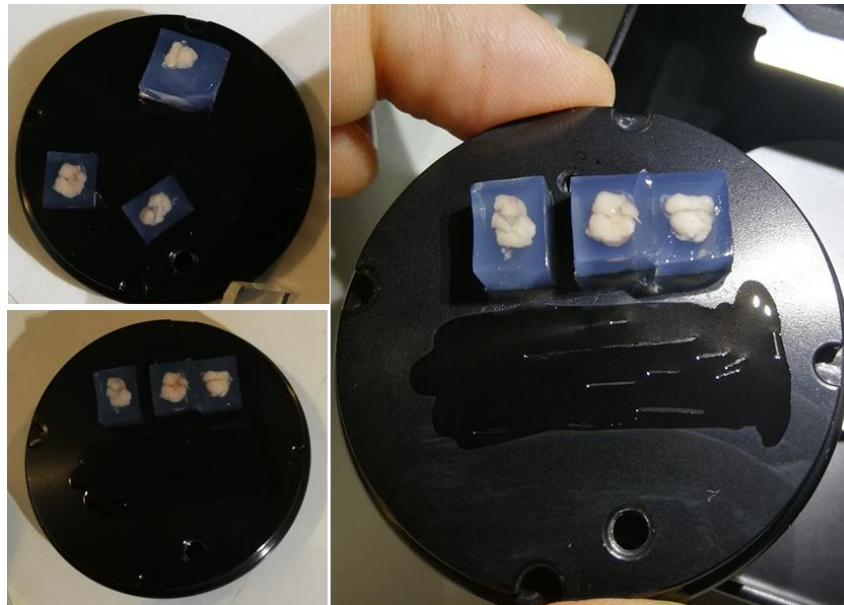


Figure 3: Pancreas assessment for vibratome cutting. The pancreas is perfused with a 1.75% agarose solution and aprotinin. It is cut in small pieces (1-2 cm), and it is immersed in a 2.5% agarose solution that solidified after few minutes. Small squares are cut and they are glue on the magnetic disc for the vibratome cutting.

3.10.2. Samples equilibration and perfusion experiment

After an equilibration and resting time of the slices for 2 hours on an orbital shaker at room temperature (RT) in Krebs-Ringer buffer (KRB) (137 mM NaCl, 5.36 mM KCl, 0.34 mM Na₂HPO₄, 0.81 mM MgSO₄, 4.17 mM NaHCO₃, 1.26 mM CaCl₂,

0.44 mM KH_2PO_4 , 10 mM HEPES, 0.1% BSA, pH 7.3) supplemented with 3 mM glucose and aprotinin (25 KIU/ mL), 2-3 slices were placed each into a closed perfusion chamber (#64-0223 and #64-0281 [P-5], Warner Instruments) and connected to a perfusion system with automated tray handling (#PERI4-02-230-FA, Biorep Technologies). For the preparation of the perfusion system, the cassettes are clipped onto the pump, and unnecessary channels are blocked with dead-end tubings to prevent air from entering the system. The column holder can be disassembled if necessary, and connectors are used to attach the perfusion tubings to the output channels. The solutions are then placed into the tube/flask holder unit, matching the protocol requirements, and the tubings are inserted into the buffers to ensure they are properly filled. Unused channels are clamped, and the system is primed to remove air and fill the tubings with solution. Vacuum grease is applied to the bottom of the perfusion chamber, and a coverslip is placed on top, ensuring the chamber walls remain dry. Slices are then inserted into the chamber, and excess buffer is removed before sealing the chamber with another coverslip and locking ring. To connect the perfusion chambers to the system, they are transferred one by one and connected to the inflow and outflow tubings. The protocol is started, and the system is monitored to ensure proper filling of the chambers without air bubbles.

In fact, before the start of the experiment, pre-priming and priming of all tubes is always carried out; this procedure is important for two reasons:

1. It eliminates all air bubbles that could affect the flow of solutions, which must be homogeneous and arrive simultaneously in all samples to allow real monitoring of all solutions minute by minute.
2. The solution used for pre-priming and priming is a Krebs salt solution (pH 7-7.4) containing BSA (Bovine Serum Albumin - Sigma-). Albumin is a protein that is 'sticky' for plastic and is responsible for saturating all tube sites to which cytokines might bind.

The other components of this saline solution are calcium chloride, magnesium chloride, potassium chloride, sodium chloride and HEPES (all products are from Sigma).

The entire system is maintained at a constant temperature of 37°C except for the mechanical arm, which houses the plate, which is maintained at a temperature of 4°C and the eluate is collected in 96-well plates that are changed manually.

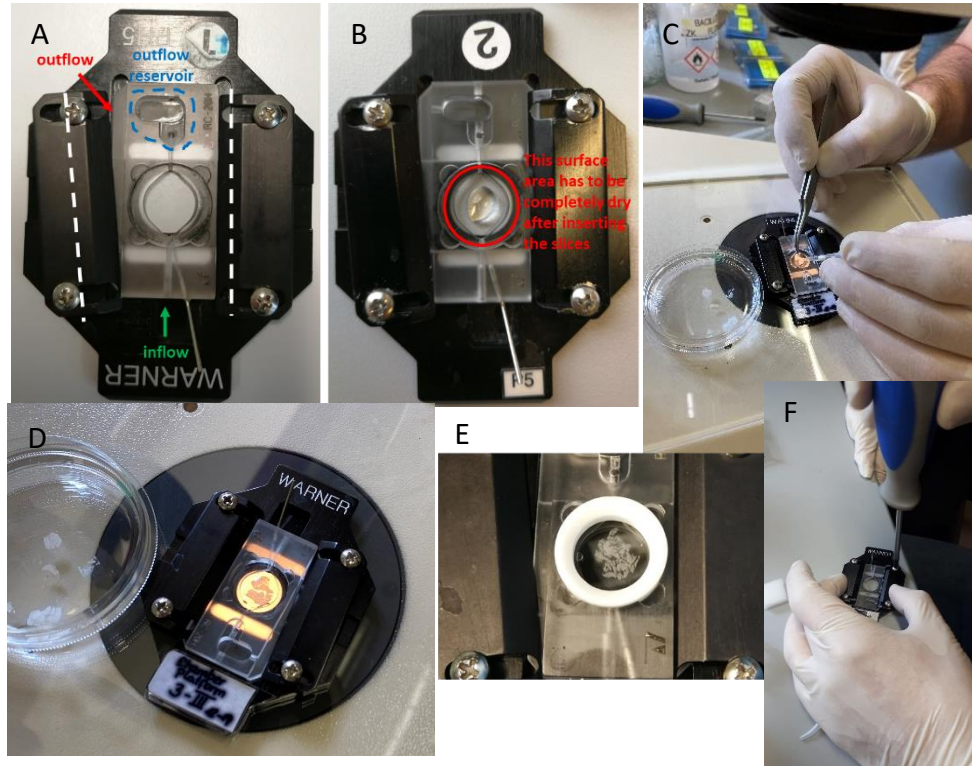


Figure 4: Preparation and mounting of the chambers using the pancreatic tissue slices. A: different compartment of the chamber. B: glass where to place the tissue slices. The wet part must be only the glass, the surrounding must be dry to avoid leakage problems. C: placement of the slides on the glass. D-E: the slides are nicely spread on the glass surface, and they are closed using another glass. F: closing of the entire chamber.

Tissue slices were perfused at a flow rate of 100 $\mu\text{L}/\text{minute}$, and samples were collected in 96-well plates with a 120-second interval. Slices were flushed for 60 minutes with 3 mM glucose KRB containing aprotinin (25 KIU/mL) to wash out accumulated hormones and enzymes from the tissue. Then, slices were perfused with KRB buffer with 3 mM glucose for 10 minutes, followed by 30 minutes in 16.7 mM glucose, 30 minutes with 3 mM glucose, 20 minutes with 16.7 mM and 60 mM KCL, and, after that, 10 minutes in 3 mM glucose. All solutions were supplemented with aprotinin (25 KIU/ mL). After perfusion, tissue slices were gently removed from the chambers and transferred to 500 μl glacial acid EtOH. All

samples were frozen at -20°C until assayed for insulin content using an ultra-sensitive insulin HTRF assay (#62IN2PEG, CISBIO/Perkin Elmer).

3.10.3. HTRF assay for determination of insulin of tissue slice GSIS

HTRF (Homogeneous Time Resolved Fluorescence) is a no-wash technology. It combines standard FRET technology with time-resolved measurement of fluorescence, eliminating short-lived background fluorescence. For a sandwich assay, two antibodies that recognize a protein of interest are used, with one antibody coupled to a donor, and the other with the acceptor. If the 2 antibodies recognize the analyte, the donor will emit fluorescence upon excitation and the energy will be transferred to the nearby acceptor, giving specific acceptor fluorescence. The donor fluorescence is also measured and a ratio with the acceptor fluorescence is applied. First add your analyte or sample to your microplate, then add the detection reagents: Anti-analyte conjugated donor and acceptor conjugated antibody. Incubate 2 hours (up to overnight for some assays). The assay is then ready to be read on an HTRF compatible or certified microplate reader. The emission of light by the acceptor will be proportional to the level of interaction.

3.11. scRNA sequencing on porcine β -cells

3.11.1. Generation of scRNA-seq samples from pigs

3 PHG piglets are compared with 3 PNG piglets at day one post-natal. scRNA-seq experiments were performed in cooperation with the scRNA-seq unit at the Institute of Diabetes and Regeneration Research (head: Prof. Heiko Lickert) at the Helmholtz Center Munich.

3.11.2. Flow cytometry

Pancreas of piglets harbouring the *INS*-eGFP transgene were cut in small pieces and collagenase digested as described elsewhere (Kemter, Muller et al. 2021). For flow cytometry, isolates were further digested with TrypLE (#12605, Life Technologies) to obtain a single-cell suspension, that was finally resuspended in 1-2 mL flow cytometry buffer (2% FCS, 2 mM EDTA in PBS), and passed through 40- μm cell strainer caps of FACS tubes. GFP positive cells were sorted using FACS-Aria III

(FACSDiva software v.6.1.3, BD Bioscience) with a 100- μ m nozzle. For all experiments, single cells were gated according to their FSC-A (front scatter area) and SSC-A (side scatter area). Singlets were gated dependent on the FSC-W (front scatter width) and FSC-H (front scatter height), and dead cells were excluded using 7-AAD (#00-6993-50, eBioscience).

3.11.3. Single-cell sequencing

The cell suspensions were immediately used for single-cell RNA-seq library preparation with a target recovery of 10,000 cells. Libraries were prepared using the Chromium Single Cell 3' Reagent Kits v3.1 (10X Genomics, PN-1000121) according to the manufacturer's instructions. Libraries were pooled and sequenced according to 10X Genomics' recommendations on an Illumina NovaSeq6000 system with a target read depth of 50,000 reads/cell.

3.11.4. Improved genome annotation for *Sus scrofa*

As for *Sus scrofa* the gene annotation was incomplete for certain genes of interest, Beiki et al. (Beiki 2019) generated an annotation for the pig genome by the integration of poly(A) selected single-molecule long-read isoform sequencing (Iso-seq) and Illumina (short read) RNA sequencing (RNA-seq). A new annotation was created by combining the latest Ensembl annotation (version 101) and the transcripts generated by Beiki et al. The data provided in the gtf from Beiki et al. (iso-seq annotation) from <https://github.com/hamidbeiki/Porcine-PacBio> was downloaded and annotated with the transcripts with gffcompare (Pertea and Pertea 2020) using the annotation from Ensembl version 101 as reference. In the next step, "pseudogene" and "processed_pseudogene" biotypes genes were removed from the Ensembl annotation and the associated same strand transcripts from the iso-seq annotation were added to the Ensembl annotation. Furthermore, the gene bodies were extended if the added transcripts required it. In case a transcript was added to a gene, the suffix -iso was added to the respective gene ID. Additionally, an "extension gene" downstream of the gene body was added, where its length was defined by the maximum possible region of 1-10kb (in 1kb steps) that does not overlap with any other same strand gene. The extension genes were named by

adding the suffix -ext'x'kb to the name of the original genes, whereby 'x' stands for the integer length of the addition from 1-10.

In the end, the final gene counts were obtained by summing the -iso and -ext'x'kb versions of each gene.

3.11.5. Pre-processing of droplet-based scRNA-seq data

Preprocessing was performed using Python 3.9 and the Scanpy package (Wolf, Angerer et al. 2018) as described below. All samples were processed separately, and filtering thresholds were chosen individually for each sample.

3.11.5.1. Data preparation

The raw data obtained from the Cell Ranger pipeline was pre-filtered by using the scanpy `pp.filter_cells` and `pp.filter_genes` function, to remove cells with less than 1 count and genes detected in less than 1 cell.

3.11.5.2. Ambient gene detection

The R package DropletUtils (Lun, Riesenfeld et al. 2019) was used in R 4.3 for the detection of ambient genes. The p-value cutoff for ambient genes was set to 0.00065 after visual inspection.

3.11.5.3. Empty Droplets

To identify empty droplets, again the R package DropletUtils was used in R 4.3. The output obtained from DropletUtils was then combined with the barcodes available from the filtered matrix provided by the Cell Ranger pipeline. The intersection of barcodes between these two methods were then used for downstream analysis.

3.11.5.4. Quality Control

Quality control and further cell filtering was done according to published best practice guidelines (Luecken and Theis 2019). In brief, cells with very low or high number of counts were excluded, as well as cells with very low numbers of genes. In addition, cells with a high fraction of mitochondrial genes were excluded. For the exact values of the values, see Data and Code Availability and the provided notebooks.

3.11.5.5. Doublet detection

For the doublet detection a total of 5 different programs were used. In this process, each cell received a score between 0 and 5, depending on how many of the programs used identified it as a doublet. The programs used in this step were Scrublet (Wolock, Lopez et al. 2019) and DoubletDetection in python and scDbfFinder (Germain, Lun et al. 2021), scds (Bais and Kostka 2020) and DoubletFinder (McGinnis, Murrow et al. 2019) in R. At this step, identified putative doublets were not removed.

3.11.5.6. Concatenation and normalization

The samples were then concatenated and only genes that were present in all samples were kept. The concatenated object was normalized in order to account for differences in sequencing depth using the scran package in R (Lun, Bach et al. 2016). Subsequently, the values were log-transformed ($\log(\text{expr} + 1)$).

3.11.5.7. Integration

Samples were integrated using scvi-tools (Gayoso, Lopez et al. 2022). First, the top 4000 highly variable genes (HVGs) were identified using Scanpy, using `flavor="seurat"` and the individual samples as batches. Potential ambient genes (see "Ambient gene detection") were excluded from the HVGs. Next, a scvi model was trained on the filtered HVGs with the following options: `batch_key = "sample"`, `layer = "raw_counts"`, 20 latent dimensions and 256 hidden layers, gene-batch as dispersion, `zinb as gene_likelihood` and a normal latent_distribution.

3.11.5.8. Single-cell manifolds and visualization

In order to obtain a Uniform Manifold Approximation and Projection (UMAP) (Becht, McInnes et al. 2018), a neighbourhood graph of the individual cells was computed using the `pp.neighbors` function in the implementation of scanpy, with the parameters `n_neighbors=25`, `n_pcs = 20` and `metric='correlation'`. Then the UMAP was calculated with Scanpy using the default parameters and `min_dist=0.2`.

3.11.5.9. Doublet Removal

To exclude potential doublets from further analysis, high-resolution leiden clustering (Becht, McInnes et al. 2018), as implemented in Scanpy, was performed

(resolution = 2), and the resulting clusters where more than 70 percent of the cells were identified as doublets by at least one method, and more than 30 percent were identified as doublets by at least 2 methods were excluded from the further analysis. Next, from all remaining cells the cells identified as doublets by 3 or more methods were excluded as well. Afterwards, the UMAP was recalculated using the scanpy standard parameters.

3.11.5.10. Clustering and Cell Type annotation

Clustree (Zappia and Oshlack 2018) was used in R to visualize and compare different leiden clustering resolutions. A resolution of 1.3 was chosen for the annotation. Cycling cells were identified scoring genes associated with the S and G2M phase of the cell cycle respectively using the Scanpy implementation (Satija, Farrell et al. 2015). Cell types were annotated based on known marker genes (see supplementary table) which were scored using the scanpy function `tl.score_genes`. The clusters were then labeled based on the marker gene score.

3.11.5.11. Differential gene expression between offspring of healthy and diabetic mom

Differential gene expression between the samples deriving from the offspring of a healthy mother were compared to the samples deriving from the offspring of a diabetic mother using Delegate which is a wrapper for edgeR.

3.12. Holistic proteomic analysis by LC/MS-MS

The analysis was processed by Lafuga laboratory, from Bachuki Shashikadze and Dr. Thomas Froelich.

3.12.1. Sample processing and LC/MS-MS

Fresh frozen (FF) tissue samples (pancreas spleen and duodenum side) were pulverized using cryoPREP Automated Dry Pulverizer from Covaris. Proteins were extracted using 8 M urea/50 mM ammonium bicarbonate buffer with the aid of ultrasonication. Protein concentration was determined using the Thermo Pierce 660 nm assay and 50 µg lysate was digested with Lys-C/trypsin.

For proteome analysis a Q Exactive HF-X mass spectrometer equipped with an UltiMate 3000 nano-LC system (Thermo Scientific) was used. Peptides were transferred to a PepMap 100 C18 trap column (100 µm×2 cm, 5 µM particles,

Thermo Fisher Scientific) and separated on an analytical column (PepMap RSLC C18, 75 μm ×50 cm, 2 μm particles, Thermo Fisher Scientific) at 250 nL/min with an 80-min gradient of 5-20% of solvent B followed by a 9-min increase to 40%. Solvent A consisted of 0.1% formic acid in water and solvent B of 0.1% formic acid in acetonitrile. After gradient, the column was washed with 85% solvent B in 9-min, followed by 10-min re-equilibration with 3% solvent B. Spectra were acquired using one survey scan at a resolution of 60000 from 350 to 1600 m/z followed by MS/MS scans of the 15 most intense peaks at a resolution of 15,000.

3.12.2. Data analysis

The analysis was processed by Lafuga laboratory, from Bachuki Shashikadze and Dr. Thomas Fröhlich.

For protein identification (FDR < 1%) and label-free quantification, MaxQuant (v. 1.6.1.0) (Tyanova, Temu et al. 2016) and the NCBI RefSeq Sus scrofa database (v. 3-13-2018) was used. Reverse peptides, common contaminants and identifications only by site were excluded from further analyses. Proteins having at least two peptides detected in at least three replicates of each condition were tested for differential abundance using the MSEmpire algorithm (Ammar, Gruber et al. 2019). To handle missing values, imputation was performed using the DEP package. Proteins with a Benjamini–Hochberg (BH)-corrected P-value <0.05 and a fold-change ≥ 1.5 were regarded as significant. Data visualization was performed with the tidyverse package collection in R (Tabelow, Clayden et al. 2011). Heatmaps were built with distance method “Euclidean” and column dendrogram method “average” using the Complexheatmap R package (Gu, Eils et al. 2016). Principal component analysis was performed using covariance matrix in R. Pre-ranked gene set enrichment analysis (GSEA) was performed using STRING (Szklarczyk, Morris et al. 2017). Signed (based on fold-change direction) and log-transformed p-values were used as ranking metrics and FDR stringency was set to 5%. For the redundancy minimization significant Gene Ontology (GO) biological processes were grouped into similar ontological terms using REVIGO (Supek, Bosnjak et al. 2011) at an allowed similarity of 0.7.

3.13. Statistical analysis

All data are presented as means \pm standard error of the mean (SEM). Glucose and insulin levels during OGTT were evaluated by ANOVA (Linear Mixed Models; SAS 8.2) taking the fixed effects of Group (diabetic vs. healthy mother), Sow (nested within Group), Gender (of the piglet), Time (relative to glucose administration), the interactions Group*Gender, Group*Time, and Group*Gender*Time as well as the random effect of the individual piglet into account. p values < 0.05 were considered significant.

Statistical differences regarding clinical-chemical parameters were evaluated by analysis of variance (General Linear Models; SAS 8.2) taking the fixed effects of Group (PHG vs PNG), Gender (females and males) and the interaction Group*Gender into account. Body weight, absolute and relative organ weights were statistically evaluated by analysis of variance (PROC GLM; SAS 8.2) taking the fixed effect of Group (PHG vs PNG) into account. Differences between two groups regarding quantitative-stereological analyses, expression levels and areas under the glucose/insulin curve were evaluated by Mann-Whitney-U test in combination with an exact test procedure (SPSS 21.0). Area under the curve (AUC) for insulin and glucose were calculated using Graph Pad Prism® software (version 5.02). P values less than 0.05 were considered to be significant.

scRNAseq data genes of the volcano plot were considered significant passing thresholds of 0.5 and 13.0.

Stereological statistical analysis was conducted using the T. test: two-tailed distribution; two-sample equal variance (homoscedastic). P values less than 0.05 were significant.

IV. RESULTS

1. First observation during the pregnancy and immediately after the birth

1.1. General aspects

This study aimed to investigate the effect of maternal diabetes in non-diabetic offspring with the focus on glucose metabolism and β -cell function. For this purpose, as a translational model for human research, we used a non-obese genetically diabetic (*INS*^{C94Y} transgenic) pig model characterized by severe hyperglycaemia (Renner, Braun-Reichhart et al. 2013). The pre-gestational diabetes in this model therefore also covers the impact of intrauterine hyperglycaemia in first trimester where organogenesis take place. In this study, the serum clinical parameters of OGTT from newborn WT piglets born to hyperglycaemic mothers (PHG) were compared to the profiles of WT controls born to normoglycemic mothers (PNG). In addition, beside *in situ* study of glucose stimulated insulin response on insulin secretion of live pancreatic tissue slices, holistic scRNAseq studies on β -cells and proteomic analysis of pancreas complemented to understand the pathophysiology of the impact of maternal hyperglycaemia on β -cell health in neonatal offspring.

1.2. Pregnancy rate between healthy vs hyperglycaemic sows

Pregnancy rate during mating, for cycling healthy sows, had an average of 56%, while *INS*^{C94Y} animals showed an average of the 33% compared to the total amount of inseminated sows (Table 9). These results show the first average conception rate which is less (-59%) in *INS*^{C94Y} mothers compared to the control group.

Table 9: Pregnancy rate

| CONDITION | N. INSEMINATED | N. CONCEIVED | CONCEPTION RATE |
|-----------|----------------|--------------|-----------------|
| DIABETIC | 33 | 11 | 33% |
| HEALTHY | 18 | 10 | 56% |

1.3. Hyperglycaemia caused reduced litter size, increases the number of stillborn and occasionally malformations in offspring

Litter size from non-diabetic mother ranged from 8 to 14 piglets (mean 11.6), whereas *INS^{C94Y}* sows gave birth between 7 to 12 piglets (mean 8.4). In contrast to 1 stillborn piglet (1.7% of all PNG born) in the PNG group, 6 piglets of the PHG group died pre- or perinatal (14.3% of PHG born), thereof one was mummified. Malformations were observed in 7 piglets of the PHG group and in none of the PNG group (Table 10). In further analysis, *INS^{C94Y}* transgenic piglets were excluded and restricted to non- *INS^{C94Y}* transgenic piglets in the PHG group.

Table 10: PHG piglets' born from diabetic mothers exhibiting malformations

| Piglet Genotype | Piglet gender | Malformation and/or pathological signs | Destiny of the piglet |
|--|----------------------|--|--|
| WT | male | Several distinct malformations all over the body (specially nose and legs not completely formed) | Euthanized day 0 |
| <i>INS^{C94Y}</i> / <i>INS</i> -eGFP | female | One of the ears missing | Dissection 3 months old |
| <i>INS</i> -eGFP | male | Hints legs problems | Dissection 3 days |
| <i>INS</i> -eGFP | male | Frontal legs problems | Dissection 3 days |
| WT | female | Cataract both eyes | Euthanized day 2 |
| WT | male | one kidney was missing | Euthanized day 2 |
| <i>INS^{C94Y}</i> | female | No anus present | Euthanized day 0 |
| <i>Healthy</i> (n=9) | Mix | Restrictive cardiomyopathy | Euthanized respecting the autopsy schedule |

1.4. Pre-gestational diabetes led to reduced birth weight in offspring

Monitoring of birth weight, clinical and clinical-chemical analysis, and OGTT were performed in offspring of 5 litters each from non-diabetic and from diabetic sows.

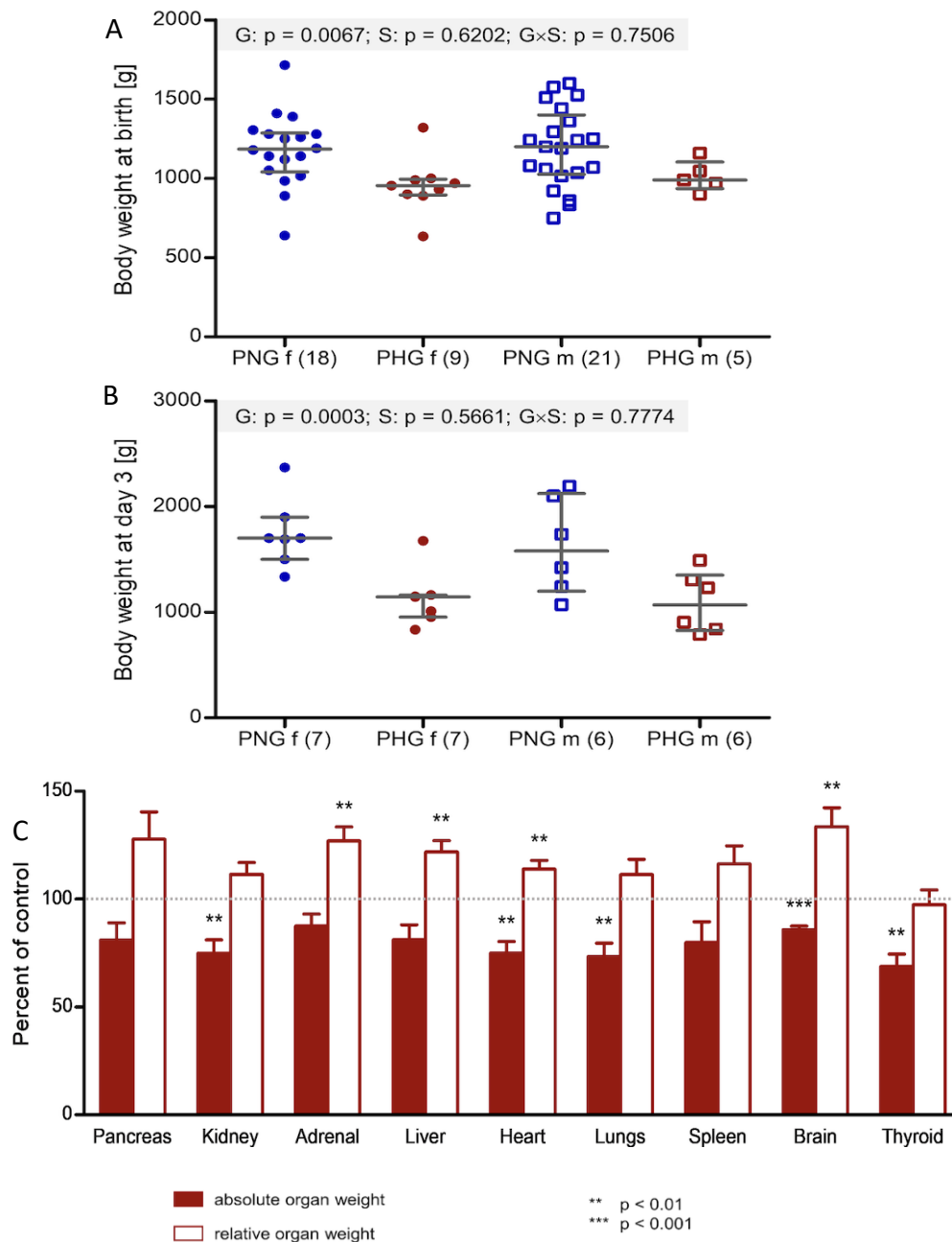


Figure 5: A: body weight at birth (g). the results show that PHG group (red) has a lower body weight at birth compared to PNG group (blue). A gender effect is not visible. B: body weight 3 days after the birth. PHG group has low body weight compared to PNG group. C: Organs weight absolute (red) and relative to the body weight (clear). The relative diagrams show that the organs weight is higher in the PHG group compared to PNG.

Birth weights were distinctly decreased in new-borns of the PHG group compared to the PNG group (Fig. 5a), without showing a gender effect (Group $p=0.0067$; Sex $p=0.6202$; Group \times Sex $p=0.7506$). This was still evident looking at 3-day old piglets (Group $p=0.0003$; Sex $p=0.5661$; Group \times Sex $p=0.7774$) (Fig. 5b).

Moreover, in PHG 3 days old piglets, the absolute weight of the organs was smaller compared to the age-matched PNG piglets (Table 11; Fig. 5c).

Table 11: percentage of the absolute and relative organs weight of the PHG piglets compared to PNG group

| Organ | Relative % (related to 100) | Difference in % (relative) | Absolute % (related to 100) | Difference in % (absolute) |
|----------------|--|---------------------------------------|--|---------------------------------------|
| Pancreas | 129 | +29% | 82 | -18% |
| Liver | 118 | +18% | 81 | -19% |
| Brain | 121 | +21% | 88 | -12% |
| Kidneys | 111 | +11% | 78 | -22% |
| Heart | 115 | +15% | 79 | -21% |
| Spleen | 127 | +27% | 90 | -10% |
| Lungs | 110 | +10% | 76 | -24% |
| Adrenal Glands | 127 | +27% | 90 | -10% |
| Thyroid Gland | 96 | -4% | 69 | -31% |

2. Phenotypic characterization of the glucose metabolism in PHG piglets

2.1. Piglets born from diabetic mothers exhibited hyperglycaemia, hyperinsulinemia and altered glucose and insulin metabolism with gender effect upon OGTT

Basal blood glucose and insulin concentrations were distinctly higher in new-born piglets 30 min after birth of the PHG group compared to the PNG group (Fig. 6a, 6c). Of note, a gender effect was observed. Compared to sex-matched offspring of normoglycemic mothers which did not show a gender effect on basal glucose levels, male piglets for diabetic mother exhibited 2.4-fold higher glucose levels whereas these of females were 1.8-fold higher (PHG males n=5, Glc 113.2 ± 15.6 mg/dl; females n=9, Glc 81.5 ± 15.6 mg/dl vs. PNG males n=26, Glc 46.7 ± 21.3 mg/dl; females n=22, Glc 45.3 ± 22.6 mg/dl, $p < 0.0001$) (Fig 6a). Further, at TP 120 the glucose level in PHG males was still 2.3-fold higher (Fig. 6a), as well as PHG females presented a 2-fold higher glucose level compared to PNG female offspring (PHG males n=5, Glc 296 ± 49.7 mg/dl; females n=9, Glc 221.4 ± 41.3 mg/dl vs. PNG males n=26, Glc 130.6 ± 67 mg/dl; females n=22, Glc 116.5 ± 50.3 mg/dl, $p < 0.0001$). The area under the curve (AUC) diagram (Fig.6b) confirmed the higher glucose secretion of the PHG offspring compared to the PNG, with a gender effect present only in the PHG group, where PHG males have a 1.6-fold higher glucose secretion, compared to the PNG group and the PHG females has a 1.4-fold higher glucose secretion compared to the sex-matched group (PHG males, AUC Glc 24240 ± 5253 mg/dl; females, AUC Glc 20739 ± 2426 mg/dl vs. PNG males, AUC Glc 15248 ± 5011 mg/dl; females, AUC Glc 14359 ± 4072 mg/dl; $p < 0.0001$).

The insulin graph (Fig. 6c) shows that at birth, PHG offspring had higher basal insulin levels than PNG offspring, where males PHG show a 9-fold higher insulin secretion compared to the control males group and the PHG females with a 5-fold insulin secretion compared to the PNG females (PHG males n=5, Ins 4.493 ± 2.377 mU/L; females n=9, Ins 3.273 ± 1.941 mU/L vs. PNG males n=26, Ins 0.497 ± 0.461 mU/L; females n=22, Ins 0.642 ± 0.915 mU/L, $p = 0.0267$). Of note, a gender effect of insulin levels during the whole OGTT was observed in offspring of diabetic mothers. The Matsuda index (Fig. 6e), that indicates the insulin sensibility of the whole organism, is lower in the PHG group compared to the PNG, without showing

a clear gender effect. Moreover, the HOMA-IR that is used as an index to indicate the insulin resistance, was higher in the PHG group (Fig. 6f).

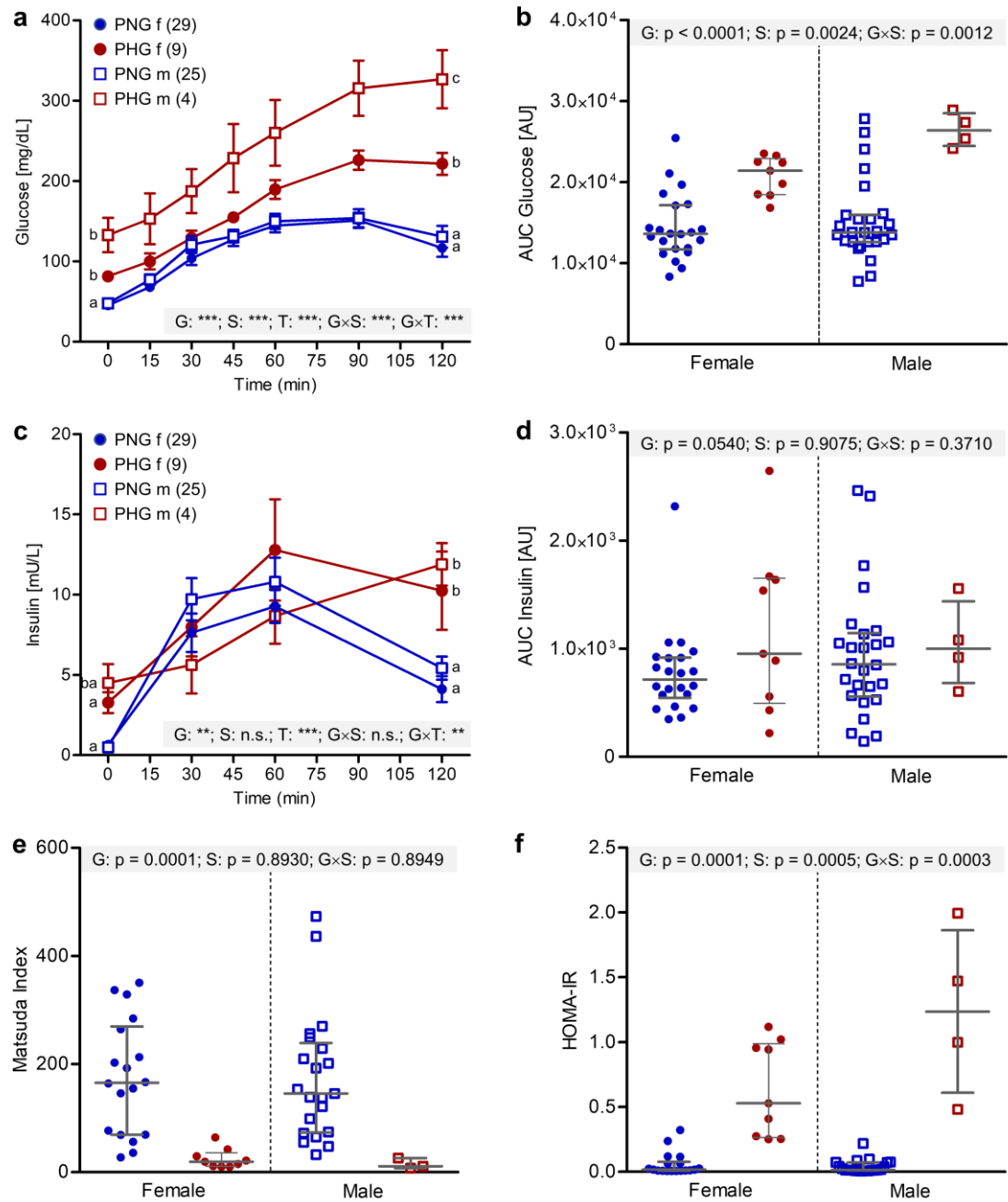


Figure 6: **a.** Blood glucose level (BGC) during the time in PNG females (blue-dots line), PNG males (blue-square line), PHG females (red-dots line) and PHG males (red-square line); **b.** glucose AUC (area under the curve); **c.** plasma insulin level; **d.** AUC insulin; **e.** Matsuda index; **f.** HOMA-IR.

2.2. Clinical-Chemical Parameters

Further biomarkers, related to the glucose metabolism, were analysed using the plasma samples at TP0. 18 parameters were considering for the analysis: albumin (1.4-fold higher secretion PHG vs PNG females - $p=0.0042$; PHG males 1.5-fold secretion compared to PNG males - $p=0.0122$), total protein, triglycerides (2-fold higher secretion PHG vs PNG females - $p<0.0001$; PHG males 1.9-fold secretion compared to PNG males - $p<0.0001$), lactate (1.7-fold higher secretion PHG vs PNG females; PHG males 2.4-fold secretion compared to PNG males - $p=0.0001$ females and males), urea (PHG females 1.4-fold higher than PNG females; PHG males 1.5-fold higher than PNG males - $p=0.0001$ females and males), uric acid (PHG females 1.7-fold higher than PNG females - $p=0.0135$; PHG males 1.6-fold higher than PNG males - $p=0.4885$), lipase (PHG females 1.4-fold higher than PNG females - $p=0.0330$; PHG males 1.7-fold higher than PNG males - $p=0.0157$) and bilirubin 2, show a significant differentiation between the PHG and PNG offspring (Table 12). The piglets' biomarkers were compared to the mother's ones during the delivery (Table 13). Looking at the matched biomarkers in the sows' bloodstream, none of them was significantly altered.

Table 12: Clinical-chemical parameters in blood serum of neonatal piglets developed in mothers with normal (PNG) or high (PHG) blood glucose levels.

SE= Standard Error.

| Parameter [unit] | PNG (17 f, 20 m) | | | PHG (10 f, 4 m) | | | Analysis of variance | | |
|---------------------|---------------------|-------|------|--------------------|--------|-------|----------------------|--------|--------|
| | Sex | mean | SE | Sex | mean | SE | Group | Sex | G×S |
| TG | f | 7.98 | 0.41 | f | 17.21 | 1.84 | <0.0001 | n.s. | n.s. |
| | m | 8.29 | 0.48 | m | 16.47 | 0.45 | | | |
| Chol | f | 27.60 | 5.63 | f | 30.08 | 2.86 | n.s. | n.s. | n.s. |
| | m | 39.18 | 1.67 | m | 26.05 | 3.29 | | | |
| Lact | f | 3.05 | 0.35 | f | 6.74 | 0.78 | <0.0001 | 0.0588 | 0.0163 |
| | m | 3.38 | 0.24 | m | 9.41 | 1.79 | | | |
| HDLchol | f | 12.22 | 1.35 | f | 14.92 | 2.00 | n.s. | n.s. | n.s. |
| | m | 14.21 | 0.69 | m | 11.95 | 1.67 | | | |
| Gluc | f | 54.99 | 4.45 | f | 119.95 | 18.83 | <0.0001 | n.s. | n.s. |

| | | | | | | | | | |
|------------|---|--------|--------|---|--------|-------|---------|--------|------|
| | m | 50.68 | 5.48 | m | 134.40 | 17.71 | | | |
| Lipase | f | 8.78 | 0.81 | f | 12.87 | 1.51 | <0.0001 | n.s. | n.s. |
| | m | 8.88 | 0.61 | m | 14.57 | 1.31 | | | |
| TG_HDLchol | f | 0.713 | 0.055 | f | 1.313 | 0.201 | <0.0001 | n.s. | n.s. |
| | m | 0.652 | 0.082 | m | 1.459 | 0.192 | | | |
| TG_Gluc | f | 0.164 | 0.015 | f | 0.150 | 0.010 | n.s. | n.s. | n.s. |
| | m | 0.180 | 0.013 | m | 0.130 | 0.020 | | | |
| Crea | f | 1.247 | 0.102 | f | 1.330 | 0.240 | n.s. | n.s. | n.s. |
| | m | 1.312 | 0.067 | m | 1.257 | 0.252 | | | |
| Urea | f | 22.96 | 0.49 | f | 31.96 | 1.96 | <0.0001 | n.s. | n.s. |
| | m | 22.57 | 0.79 | m | 34.42 | 5.01 | | | |
| Albumin | f | 0.634 | 0.056 | f | 0.975 | 0.075 | <0.0001 | n.s. | n.s. |
| | m | 0.682 | 0.023 | m | 0.995 | 0.167 | | | |
| Tprot | f | 1.728 | 0.071 | f | 2.138 | 0.143 | 0.0006 | n.s. | n.s. |
| | m | 1.695 | 0.063 | m | 2.100 | 0.139 | | | |
| LDH | f | 334.89 | 129.76 | f | 525.60 | 94.27 | n.s. | n.s. | n.s. |
| | m | 500.36 | 23.73 | m | 356.57 | 70.93 | | | |
| AST | f | 38.30 | 9.95 | f | 55.52 | 11.45 | n.s. | 0.0384 | n.s. |
| | m | 53.49 | 4.79 | m | 24.72 | 7.40 | | | |
| Bilirubin | f | 0.097 | 0.068 | f | 0.191 | 0.025 | n.s. | n.s. | n.s. |
| | m | 0.177 | 0.006 | m | 0.172 | 0.053 | | | |
| Uric acid | f | 0.218 | 0.015 | f | 0.414 | 0.087 | 0.0015 | n.s. | n.s. |
| | m | 0.247 | 0.012 | m | 0.340 | 0.054 | | | |
| Na | f | 123.49 | 1.82 | f | 118.21 | 2.20 | n.s. | n.s. | n.s. |
| | m | 121.98 | 2.07 | m | 123.52 | 2.52 | | | |
| Cl | f | 84.19 | 0.98 | f | 78.96 | 1.77 | 0.0679 | n.s. | n.s. |
| | m | 82.03 | 1.37 | m | 80.50 | 1.93 | | | |

Table 13: Clinical-chemical parameters in blood serum of sows during the delivery.

| Parameter [unit] | Healthy (n= 4) | | <i>INS^{C94Y}</i> (n= 4) | | Analysis of variance Group |
|---------------------|-------------------|--------|-------------------------------------|--------|----------------------------------|
| | mean | SE | mean | SE | |
| TG | 27.625 | 7.313 | 37.225 | 7.313 | n.s. |
| Chol | 30.675 | 3.096 | 40.875 | 3.096 | n.s. |
| Lact | 2.3225 | 0.771 | 2.320 | 0.771 | n.s. |
| HDLchol | 16.725 | 0.849 | 21.025 | 0.849 | 0.0117 |
| Gluc | 99.325 | 23.3 | 422.425 | 23.3 | <0.0001 |
| Lipase | 4.2 | 2.460 | 8.625 | 2.460 | n.s. |
| Bili - D | 0.1525 | 0.047 | 0.0625 | 0.047 | n.s. |
| Bili - T | 0.4525 | 0.1335 | 0.2275 | 0.1335 | n.s. |
| Crea | 3.355 | 0.152 | 2.2575 | 0.152 | 0.0022 |
| Urea | 33.175 | 4.645 | 26.675 | 4.645 | n.s. |
| Albumin | 4.0275 | 0.124 | 3.4675 | 0.124 | 0.0188 |
| Tprot | 7.1275 | 0,224 | 7.2775 | 0.224 | n.s. |
| LDH | 965.325 | 349 | 596.375 | 349 | n.s. |
| AST | 93.9 | 27.78 | 39.775 | 27.78 | n.s. |
| ALT | 42.725 | 6.834 | 38.425 | 6.834 | n.s. |

2.3. Dynamic GSIS assay with pancreatic tissue slices showed an impaired insulin secretion in PHG offspring

In dynamic glucose stimulation insulin secretin (d-GSIS), the pancreatic slices were stimulated with high glucose (16.7mM) and high glucose and KCl (16.7mM +KCl) and an insulin response is evident in all the 4 groups. A minimum number of 4 piglets (PNG f=4; PHG f=4; PNG m=4; PHG m=5) from at least 3 different litters were considered in the analysis for each group, in order to estimate the reproducibility of the assay. At basal level (3 mM Glucose) (Fig.7a, 7c), the PNG

group starts from a low insulin secretion (PNG males = 0.0209 ± 0.0127 ng/ml; PNG females = 0.0092 ± 0.006 ng/ml), while 16.7mM Glucose stimulated insulin secretion was 0.027 ± 0.03 in the female group and 0.065 ± 0.035 in males (average secretion \pm SD), demonstrate that, when expose to a higher amount of glucose, a physiological insulin release, where the first and the second waves of the insulin granules are high recognizable. Whereas the PHG groups were not able to orchestrate an adequate insulin response. In fact, at the basal (3mM glucose) concentration, PHG group (both female and male), started from a higher insulin level compared to the PNG group; PHG females showed a 5.9-fold higher insulin secretion vs PNG females; PHG males 3.12-fold higher insulin secretion vs PNG males (PHG males = Ins baseline 0.0655 ± 0.0414 ng/ml; PHG females = Ins baseline 0.055 ± 0.046 ng/ml) (Fig.7a, 7c).

The stimulation index (SI) (Fig.7b, 7d) between basal and the highest pick reached during the high glucose stimulus is 4.426 ± 1.36 in the PNG female group and 1.674 ± 0.44 in the PNG males, while, in the PHG group it is 0.483 ± 0.64 for the females and 0.192 ± 0.21 for males.

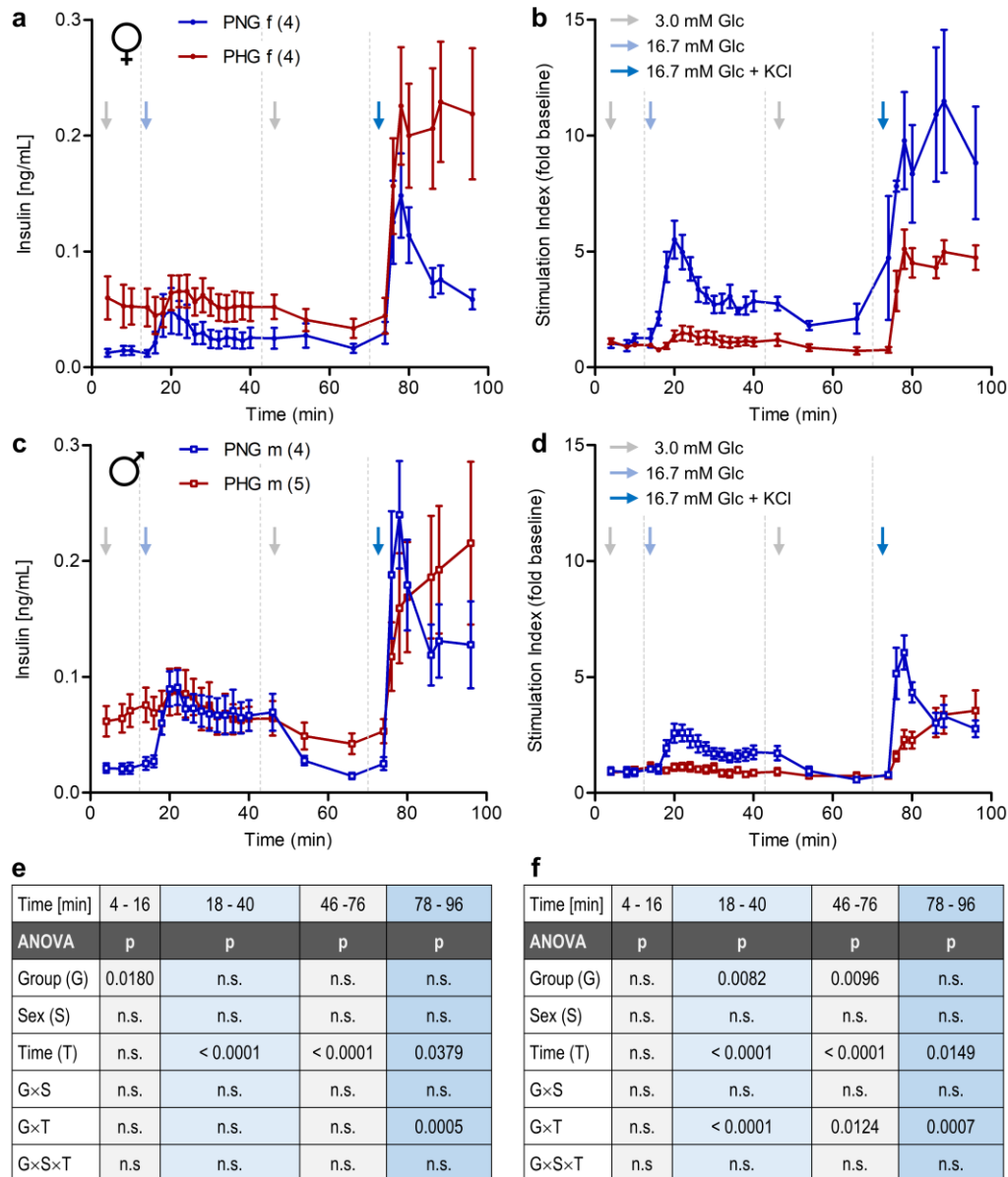


Figure 7: *In situ* GSIS on pancreatic tissue slices. A: absolute values in the females group where PHG (red) show impaired insulin secretion compared to the PNG (blue). B: stimulation index (on the basal) of the females group. C: absolute values in the males with the PHG impaired insulin secretion. D: stimulation index of the males. E: anova analysis of the absolute values analysed per group, sex and time. F: Anova analysis of the stimulation index values.

3. Omics studies for the insight characterization of the β -cells

3.1. Holistic proteomics revealed alterations in both exocrine and endocrine compartment of the pancreas in PHG

Further investigations utilizing proteomic analysis of the offspring's pancreas unveiled distinct patterns within the offspring born to diabetic mothers. In the pancreas (spleen side) a total of 32,393 peptides could be identified and mapped to 3,714 proteins (false-discovery rate $< 1\%$).

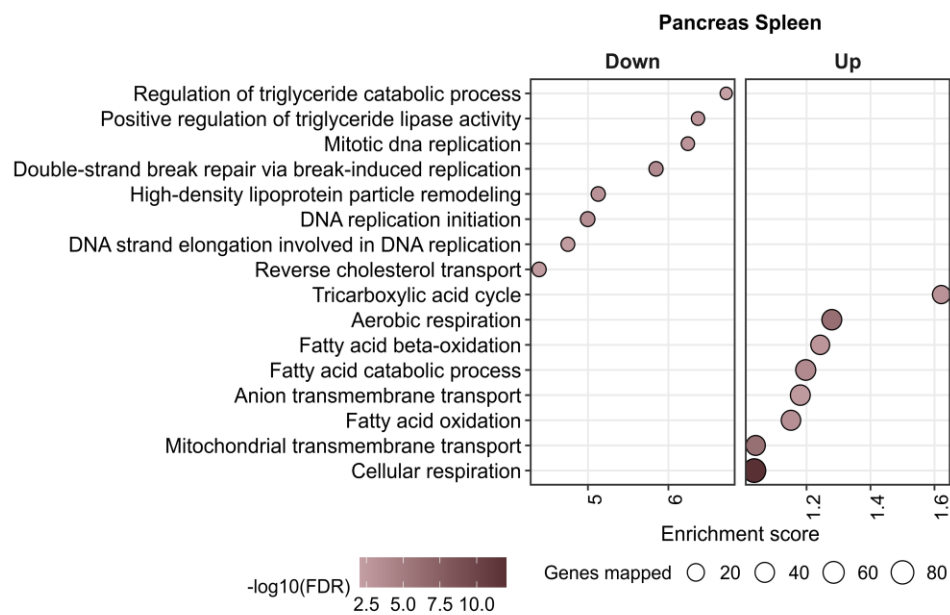


Figure 8: Pre-ranked enrichment analysis using STRING with gene sets according to gene ontology (GO) biological process databases. Significantly enriched GO terms ($FDR < 0.05$) were summarized with REVIGO by grouping semantically similar ontology terms. The size of the bubble indicates the corresponding number of quantified proteins (referred to as genes mapped in the figure) associated with the term and the color the significance of enrichment. Fold enrichment represents the magnitude of over-representation.

Insulin was significantly elevated in the PHG (+75% increase). Principal component analysis which is a dimensionality reduction technique and is used to project multidimensional omics data in the lower dimensional space, revealed the clustering based on hyperglycaemic status (Fig. 9a). Volcano plot shows the magnitude of change and the significance for each protein (Fig. 9b).

Quantitative analysis revealed 26 proteins that were changed in abundance. 13 proteins were increased in abundance while 13 proteins were decreased. Hierarchical clustering of the Z-score normalized intensities for each protein that were differentially abundant shows intensity profile of each protein in all samples.

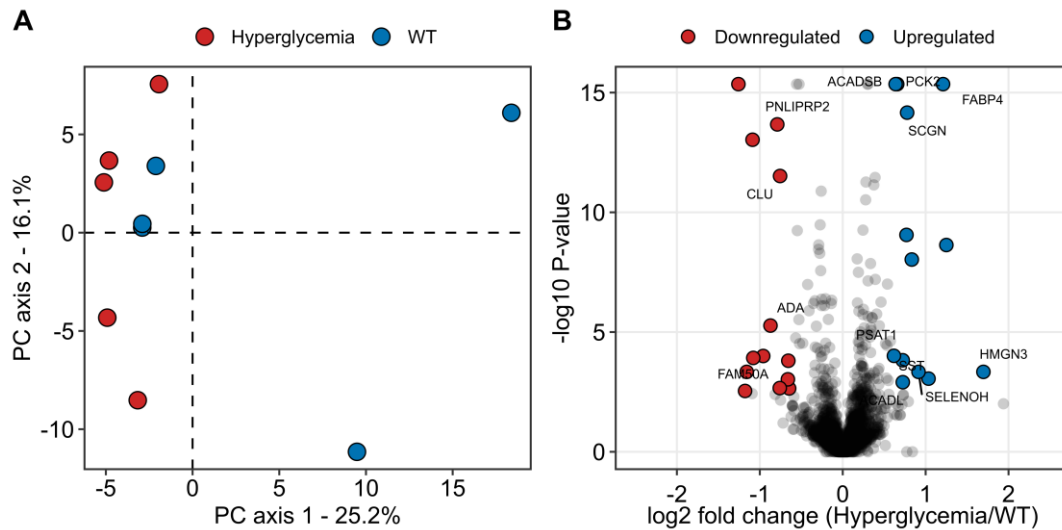


Figure 10: Quantitative proteome analysis of duodenum side pancreas tissue from hyperglycemia exposed and WT piglets. A: Principal component analysis of proteomics data. B: Volcano plot of log₂ fold changes. Red and blue dots indicate differentially abundant proteins. (PHG n=5; PNG n=5; gender = females)

3.2. Findings of scRNAseq on β -cells

To understand more selectively how the β -cell profile of the PHG group differs

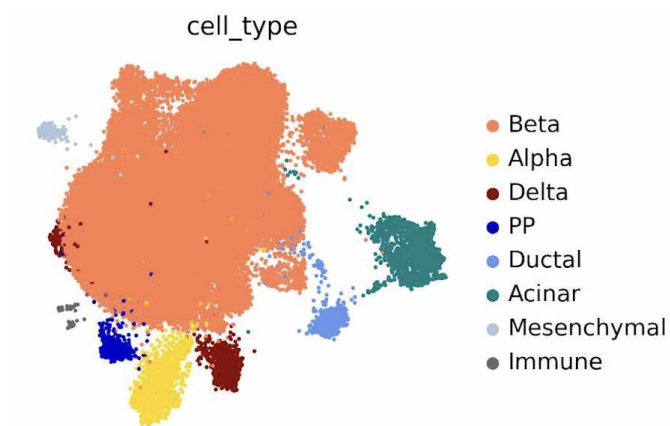


Figure 11: Distribution of cell type. 2 dimensions overlaid show that the cells are well separated.

from the PNG group and so how it changes across the intrauterine glucotoxic environment, we analysed the transcriptome profile of 6 samples (PNG: n=3; PHG: n=3). Through the gene-based cluster analysis, the cell subsets and the conditions were screened and overlaid in 2 dimensions (Figs. 11 and

12) and their proportion in each sample and the cell type, was displayed using the bar diagrams.

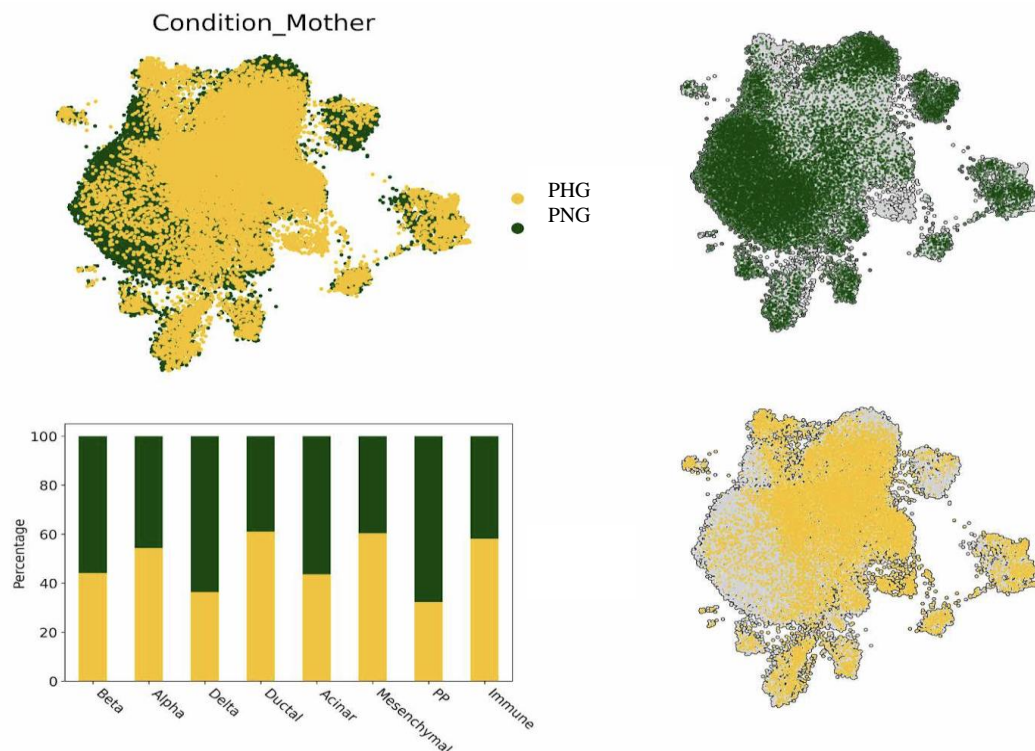


Figure 12: Distribution based on PHG and PNG group that shows a good separation between the two group and the cells type % in the group.

These data display first the good separation and quality of the samples based on the cell type (collectively, the data show high density of β -cells in each sample) and the

conditions (Fig. 11) and, furthermore, in the PHG piglets the abundance of β -cells is visibly decreased compared to the PNG in the bar diagram (Fig. 12).

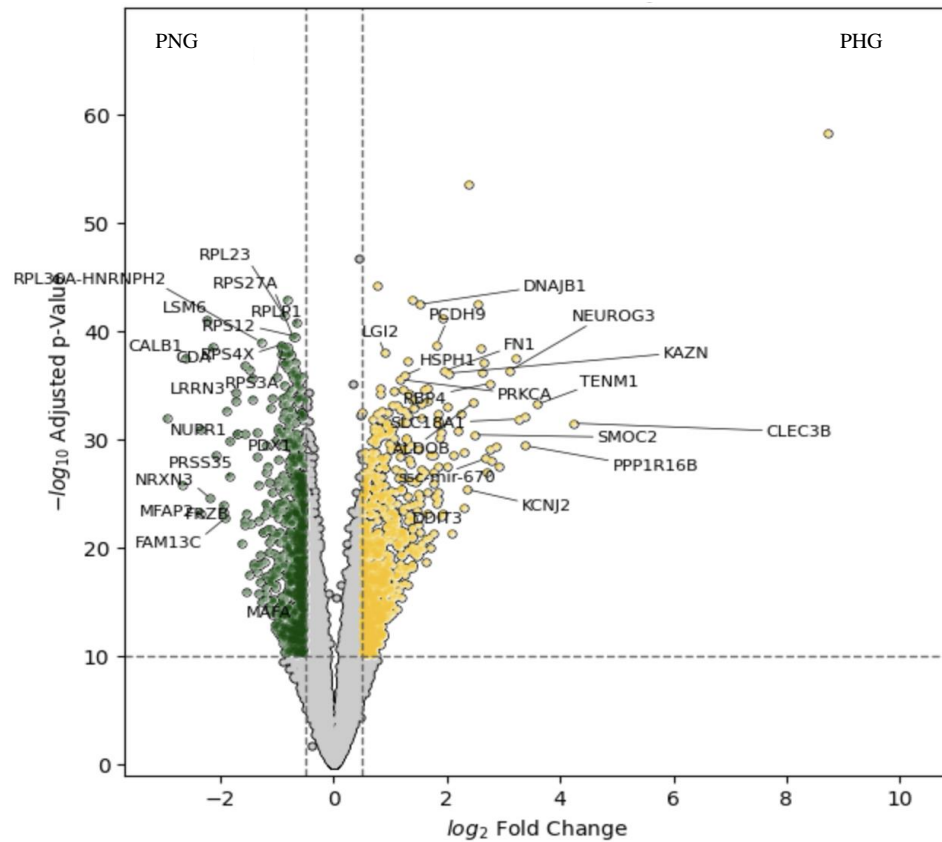


Figure 13: Volcano plot showing the upregulated and downregulated genes expressed in PHG vs. PNG. 824 genes upregulated and 781 downregulated in PHG β -cells compared to PNG. Data genes of the volcano plot were considered significant passing thresholds of 0.5 and 13.0.

We further focused on the β -cells and on the differential expressed genes in the PHG group compared to the PNG, and the volcano plot displays 824 genes upregulated and 781 downregulated in PHG β -cells compared to PNG (Figure 13).

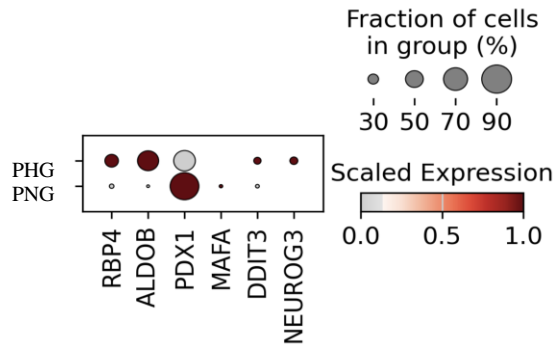


Figure 14: Dot-Plot visualization, key genes shared with human for the assessment of expression pattern.

We checked 6 key genes shared with humans for the assessment of the expression patterns of known immaturity (*RBP4* and *NEUROG3*), maturity (*MAFA*), insulin transcription (*PDX1*), ER stress (*DDIT3*), cell dysfunction (*ALDOB*) for a first evaluation of our assumption (Fig. 14).

The data show different expression between PHG and PNG and, moreover, these patterns are complementary, when consider the opposite activity of cell maturation markers (*MAFA* and *RBP4*) and immature markers (*NEUROG3*), supported by the higher amount of expressed misfunctioned cell (*ALDOB*) in the PHG group that cause an increased ER stress (*DDIT3*) in these cells.

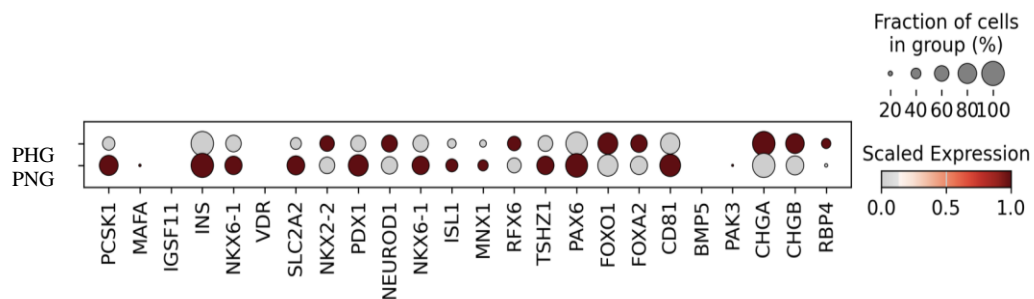


Figure 15: Dot-Plot visualization, β -cell signature markers. Groups listed on y-axes and known genes listed along the x-axis. Dot size reflects percentage of cells in a cluster expression each gene; dot colour reflects expression level (as indicated in the legend). Expression of known β -cell signature markers across the two groups. Several genes listed are associated with the cell immaturity (as FOXO1 and 2 or Neurod1) are upregulated in PHG group.

To better understand the molecular mechanism that underly the β -cell dysfunction between the 2 groups, we analyzed the expression of genes that are known to be involved and being specific in β -cells development. Six gene groups resulted from

this analysis: β -cell signature markers (Fig. 15), β -cell growth factors (Fig. 16), genes involved in insulin synthesis (Fig. 17), genes involved in insulin secretion (Fig. 18), ER stress genes (Fig. 19), and genes involved in apoptosis (Fig. 20).

Interesting, the first group, which represent the genes most involved in the β -cell characterization, showed that the genes involved in the cell differentiation, that are usually upregulated in the progenitors, were downregulated in the PNG group, while were upregulated in the PHG group (Fig. 15).

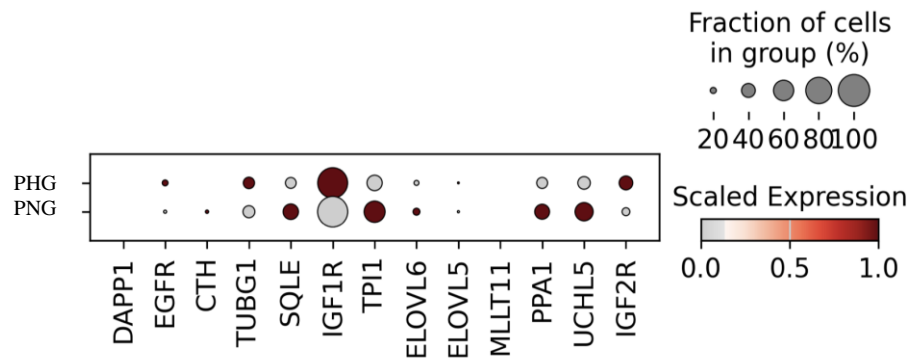


Figure 16: Dot-Plot visualization, Expression of known β -cell growth factors. Groups listed on y-axis and known genes listed along the x-axis. Dot size reflects percentage of cells in a cluster expression each gene; dot color reflects expression level (as indicated in the legend).

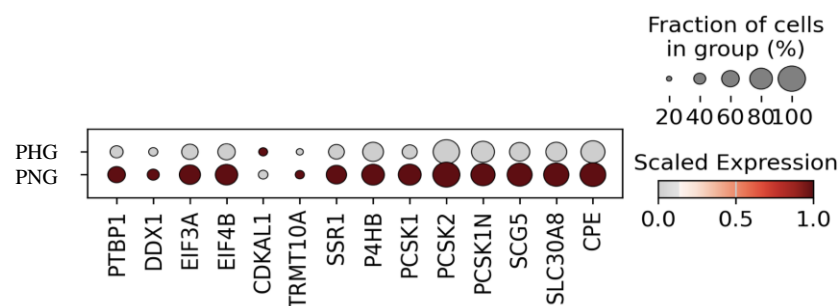


Figure 17: Dot-Plot visualization, insulin synthesis genes. All the genes detected are downregulated in the PHG group, indicating a reduced insulin synthesis.

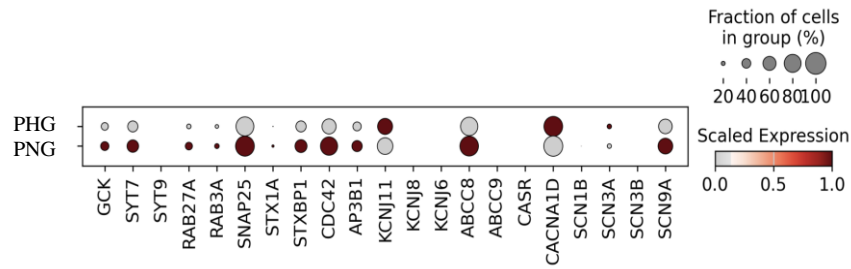


Figure 18: Dot-Plot visualization, insulin secretion genes. This group shows the genes involved in the formation of insulin granules and most of them are downregulated in the PHG group.

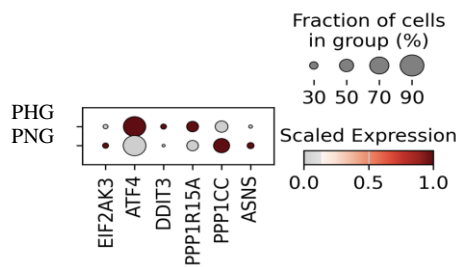


Figure 19: Dot-Plot visualization, genes considered markers of ER stress are mostly upregulated in the PHG group.

These results also reflect the evidence that, in the PHG group, the β -cell growth factor genes are downregulated, although the *EGFR* (essential for proper foetal development and growth of pancreatic islets) and *IGF1R* and *IGF2R* were upregulated (known to be apoptosis protectors for the β -cells) (Fig. 16). The genes related to the insulin (granules, synthesis, and secretion) are nearly all

downregulated in the PHG group compared to the PNG (Fig. 17-18), while the ER stress genes are mostly upregulated (Fig. 19). The genes involved in apoptosis seem to be not expressed differently between the 2 groups (Fig. 20).

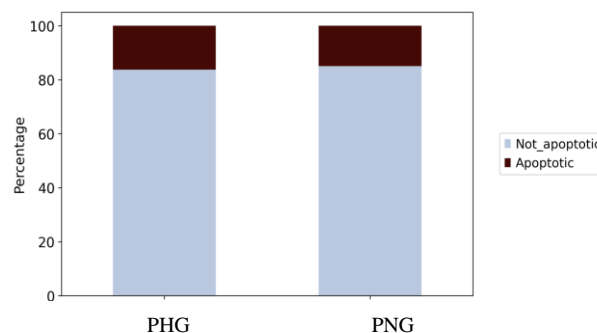


Figure 20: Bar diagrams show the percentage of the number of apoptotic and not-apoptotic cells in the PNG vs. PHG. The results show no differences in the number of apoptotic cells.

4. Immunofluorescence analysis for the validation of the alterations of the β -cells

Morphometric analyses were conducted, using QuPath software, to monitoring the cauterization of the endocrine cells (INS+ and GCG+ cells). Analysis was performed in 3-day-old piglets (PNG f: n= 8; PHG f: n= 6; PNG m: n = 7; and PHG m: n= 3) looking at the splenic part of the pancreas. Moreover, the clausterization was performed looking at 3 sizes (clusters: 1-5 endocrine cells; >10-50 endocrine cells; >50 endocrine cells), based on the % of the number of the endocrine cells that compose the cluster, on the total number of islets (Table 14; Fig. 21).

Smaller clusters (1-5 endocrine cells) were increased in the PNG group (PNG f = 84.98 ± 2.22 ; PNG m = 85.42 ± 3.10), without showing a gender effect, compared to the PHG group (PHG f = 79.90 ± 2.28 ; PHG m = 79.11 ± 2.97).

Medium size clusters (>10-50 endocrine cells) and bigger clusters (>50 endocrine cells) were increased in the PHG group compared to the PNG (Fig. 22).

Medium size clusters were significantly bigger in the PHG group (both females and males) (PNG f = 7.3 ± 1.4 ; PNG m = 6.5 ± 2 ; PHG f = 10.1 ± 1.4 ; PHG m = 10.8 ± 1.74) compared to the PNG, without showing a gender effect (Fig. 22).

Biggest clusters (>50 endocrine cells) were increased in the PHG group, both females and males. Moreover, PHG males have the biggest clusters (>50) compared to the sex-matched clusters and compared to the group-matched PHG females (PNG f = 0.8 ± 4.7 ; PNG m = 0.87 ± 0.54 ; PHG f = 1.21 ± 0.72 ; PHG m = 1.66 ± 0.76).

Table 14: Endocrine clusters splenic part (T. test: two-tailed distribution; two-sample equal variance (homoscedastic))

| | | 1-10 endocrine cells | >10-50 endocrine cells | > 50 endocrine cells |
|--------|---------|----------------------------|------------------------------|----------------------------|
| PNG f | Average | 84.98 | 7.30 | 0.82 |
| | SD | 2.22 | 1.43 | 0.47 |
| PHG f | Average | 79.90 | 10.11 | 1.22 |
| | SD | 2.28 | 1.44 | 0.72 |
| t.test | | 0.00 | 0.00 | 0.22 |
| PNG m | Average | 85.42 | 6.51 | 0.88 |
| | SD | 3.10 | 2.00 | 0.55 |
| PHG m | Average | 79.11 | 10.84 | 1.67 |
| | SD | 2.97 | 1.74 | 0.76 |
| t.test | | 0.01 | 0.01 | 0.06 |

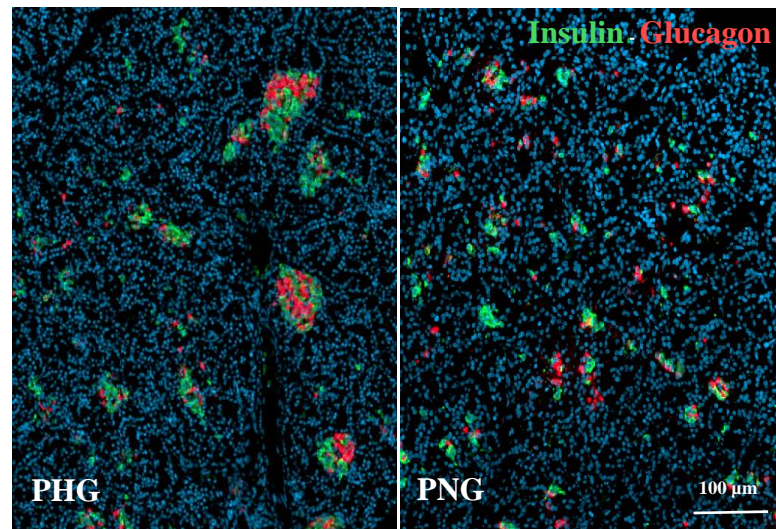


Figure 21: Representative image of 2-hormonal staining on pancreatic paraffin slides in the PNG vs. PHG. In the PHG group the endocrine cells are more clustered compared to the PNG.

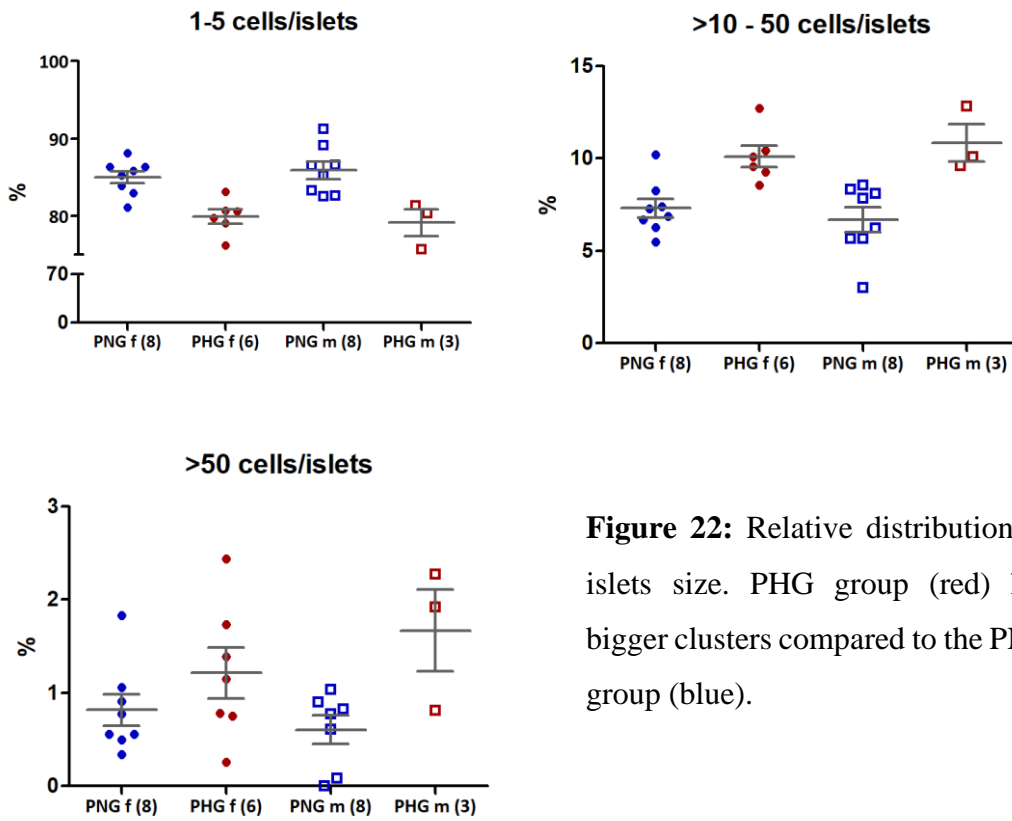


Figure 22: Relative distribution of islets size. PHG group (red) has bigger clusters compared to the PNG group (blue).

V. DISCUSSION

Maternal hyperglycaemia during pregnancy, whether through pre-existing diabetes or gestational diabetes, significantly impacts offspring health. This hyperglycaemic intrauterine environment leads to short-term complications like perinatal death, congenital malformations, and macrosomia. Additionally, it increases the risk of long-term issues such as T2DM, obesity, cardiac anomalies, and neurological impairments in adulthood (Bloom, Belfort et al. 2016, Lowe, Scholtens et al. 2019).

However, comprehending the intricate molecular mechanisms underlying these effects remains challenging in human studies due to ethical limitations. The reliance on retrospective clinical observations or accessible biological samples only scratches the surface, leaving a gap in understanding the direct impact on pancreatic β -cells *in situ*.

While murine models have been predominant in research due to practical advantages, their anatomical and physiological disparities from humans limit their translational relevance (Kleinert, Clemmensen et al. 2018, Ludwig, Wolf et al. 2020).

In contrast, pigs emerge as a promising model for diabetes research due to their anatomical and physiological similarities with humans. The resemblance in pancreas structure, GLUT expression, and islet organization underscores the potential of pigs as a more representative model compared to mice. Pigs display greater parallels in pancreatic islet development, genetic regulation, and intra-islet signalling, making them a more reliable model for understanding human pancreatic function and the impact of maternal diabetes on offspring health (Renner, Dobenecker et al. 2016, Bakhti, Bottcher et al. 2019).

In this study, we use our MIDY porcine model as translational model for human research, for the *in situ* study of the effect of severe maternal diabetes on the β -cell health of the offspring.

A total of n=21 healthy piglets born from *INS*^{C94Y} mothers were produced by breeding over a period of 2 and half year. The non-diabetic genotype was confirmed by a PCR analysis of DNA isolated from individual tail biopsies. In the analysis,

the *INS^{C94Y}* piglets born from *INS^{C94Y}* mothers were excluded, to exclusively see the effect of the intrauterine environment without a genetic component.

1. The MIDY *INS^{C94Y}* pig model as adequate model for the study of maternal diabetes' effect on the offspring

1.1. Pregnancy rate and malformations in offspring

The first evidence of the maternal diabetes consequences was evident looking at the fertility complications. Our results showed that *INS^{C94Y}* mothers had a less pregnancy rate compared to the control group, and this is evident in human as well. In women, in fact, diabetes is considered a reproductive disorder (Satpathy, Fleming et al. 2008, Thong, Codner et al. 2020).

The productive dysfunction caused by diabetes is a side effect not proper study. Nevertheless, the spectrum of reproductive health problems in diabetes encompasses delayed puberty, menstrual abnormalities, low fertility, adverse pregnancy outcomes and early menopause (Codner, Merino et al. 2012).

One of the reasons that women with T1DM have more problems as amenorrhoea and infertility is due to hypogonadism. This is the main reason why insulin treatment cannot solve this reproductive problem.

The reasons why this happens are largely studied, first studies were focusing at the potential delayed in ovulation, suggesting a longer follicular phase (Steel, Johnstone et al. 1984), but this was quickly abandoned.

More recently, it was involved the sexual dysfunction, with a less sexual desire and increased sexual distress (Caruso, Rugolo et al. 2006).

In sows, it was largely demonstrated that stress factors can influence the pregnancy rate (Lucy and Safranski 2017).

One of the pregnancy outcomes largely demonstrated of maternal diabetes are malformations in offspring. In our work, maternal diabetes caused malformations in offspring in different organs.

These results are evident is human as well as other animals. Our results showed that maternal diabetes can cause defects in the craniofacial features, as one of the piglets was presenting several malformations like missing the nose, several malformations occurred in the legs in at least 3 piglets, renal defects (in one piglet, a kidney was

missing) and gastrointestinal defects. The same categories were present in the human (Sheffield, Butler-Koster et al. 2002, Wu, Liu et al. 2020, Kokhanov 2022).

1.2. Low body weight at birth

Unlike pigs, human neonates have a higher fat mass at birth, indicating species-specific differences in metabolic development (Litten-Brown, Corson et al. 2010), suggesting a different distribution in adipose tissue.

Although it is well studied that babies born from maternal diabetes show macrosomia, several studies delineate a link between the excess foetal insulin secretion in utero and childhood impaired glucose tolerance, independent of macrosomia (Silverman, Metzger et al. 1995). Additionally, research on pre-pubertal children suggests that elevated maternal glucose during gestation correlates with poor insulin sensitivity and increased β -cell responsiveness in offspring, irrespective of their adiposity (Bush, Chandler-Laney et al. 2011).

We are aware that, in this study, PHG group has a lower body weight at birth and in 3-day-old piglets, compared to the PNG, suggesting a under development of the adipose tissue, although in human, one of the most evidence in the short-term effects in children, is macrosomia. Anyway, different studies in small human cohorts (Leng, Hay et al. 2016, Chen, Xiao et al. 2021, Meek, Corcoy et al. 2021) display the possibility for women with diabetes during pregnancy, to give birth to small for the gestation age (SGA) kids, but most of them focused on the mother's height and BMI and the insulin intake during the pregnancy and the studies focused on the children are controversial (Mahizir, Briffa et al. 2016).

Although we did not observe increased foetal body fat mass or overgrowth in this study, but clear evidence of SGA, the relative weight of most of the organs taken in analysis, was increased compared to the PNG group, specifically, the liver and heart weights in PHG offspring. This aligns with the macrosomia observed in human neonates born to diabetic mothers.

Moreover, increased adrenal gland volume is a marker of impaired metabolic state and it is associated with higher level of triglycerides, hypertension, and impaired glucose metabolism, in particular, this is associated to DM in a cohort study (Askani, Rospleszcz et al. 2022).

Anyway, it is difficult to assess the macrosomia observed in humans into pigs. The variation in birth weight (BW) within the same litter can be attributed to inherent factors. Pigs, being polytomous species, often engage in competition for maternal glucose supply among (Fowden, Forhead et al. 1997). While foetal glucose levels are mainly influenced by maternal nutritional status, in pigs, factors like the relative placental mass of each fete and litter size can impact foetal glucose consumption and concentrations (Comline, Fowden et al. 1979, Fowden, Forhead et al. 1997). Moreover, differences in placental morphology between humans and pigs can affect nutrient transport efficiency and thereby foetal growth. Unlike the highly permeable haemochorial placenta in humans, pigs possess a less permeable epitheliochorial placenta. For instance, the transport of NEFAs (non-esterified fatty acids) is restricted in pig placentas compared to human placentas (Litten-Brown, Corson et al. 2010).

1.3. Clinical chemical parameters of offspring born in diabetic mothers

Even if we did not see macrosomia at birth, we can assume important changing in the lipid metabolism, looking at the blood chemical parameters at birth.

On note, most of the blood analysis conducted in babies, referred at GDM mothers and not severe diabetic mothers, which make difficult the exact comparison between the human studies and our work (Shao, Lan et al. 2022). Although lipid profiles in neonates born to diabetic mothers were not extensively studied, our results suggest significant changes in triglycerides, HDL, and total protein levels between the two groups, reflecting potential differences in the lipid metabolism. Most of these parameters seem to be persistent in kids born from GDM mothers between 3 and 9 years old, where they show still high triglycerides/HDL cholesterol ratio (Yang, Leng et al. 2021). On not, high triglycerides in human and in pigs are sign of liver disease, diabetes, and overweight and obesity (Franks, Hanson et al. 2007, Juonala, Viikari et al. 2008, Keely, Malcolm et al. 2008, Burns, Letuchy et al. 2009), as most of the digestion of the TG is brought by pancreatic lipase in the upper part of the intestinal lumen (Lauridsen 2020).

Furthermore, we examined lactate and lactate dehydrogenase (LDH) metabolism, which are directly related to glucose metabolism, as long as glucose is the major source of lactate and lactate is the major substrate for endogenous glucose production (Adeva-Andany, Lopez-Ojen et al. 2014). Although not significantly

different were exhibited in the LDH levels, PHG piglets showed a significantly higher lactate level post oral glucose challenge compared to controls, indicating enhanced non-oxidative glycolysis (Thorburn, Gumbiner et al. 1990, Del Prato, Bonadonna et al. 1993).

This aligns with studies showing altered glucose metabolism in diabetic patients and highlights potential early metabolic adaptations in offspring exposed to maternal hyperglycaemia.

Further studies indicate that in pregnancies complicated by diabetes, maternal hyperglycaemia could lead to excessive lactate production in the placenta, as we see in our results. Studies in chronic catheterized sows and foetal piglets indicate that lactate concentrations are increased in the foetal circulation compared to the maternal circulation (Pere 1995, Pere 2001), which is also true for humans (Gilfillan, Tserng et al. 1985, Bell, Brown et al. 1989). During pregnancies complicated by diabetes, elevated maternal blood glucose levels can potentially lead to increased lactate production in the placenta. For instance, studies involving *in vitro* perfusion of human placentas from uncomplicated pregnancies, with gradually rising glucose concentrations, suggest a proportional increase in placental lactate production (Hauguel, Desmaizieres et al. 1986). However, this relationship is not confirmed in perfusion studies involving placentas from women with gestational diabetes mellitus (GDM) (Osmond, Nolan et al. 2000). Conversely, another study found a 23% increase in lactate concentration in the umbilical vein in pregnancies affected by GDM (Taricco, Radaelli et al. 2009).

2. Intrauterine glucotoxic environment impaired insulin sensitivity in new-born healthy piglets.

In our study, offspring born to INS^{C94Y} mothers demonstrated insulin resistance at birth, as evidenced by elevated and impaired glucose tolerance at neonatal age. This research marks an important *in vivo* examination of metabolic changes in newborn offspring from a large animal model of severe maternal diabetes.

2.1. The PHG piglets show an impaired glucose tolerance 30 minutes after the birth

The high fasting plasma glucose levels observed in PHG offspring shortly after birth, may result from alterations in maternal glucose concentrations during gestation, which was transferred to the foetus. It is established that the foetus primarily source of energy is the maternal glucose, which reach the foetal circulation by facilitated diffusion, thanks to the maternal-placental-foetal glucose gradient (Kalhan, D'Angelo et al. 1979, Kalhan and Parimi 2000). In fact, it is well documented that there is a linear relationship between maternal and foetal glucose concentrations, which is observed in normoglycemia and hyperglycaemia (Whaley, Zuspan et al. 1966). As in human, also in pigs it was observed that the maternal glucose is used as main substrate for the development and growth (Tobin, Roux et al. 1969, Ford, Reynolds et al. 1984, Soltesz, Harris et al. 1985, Pere 1995) and elevation of maternal glucose correlates with increased foetal glucose levels in the umbilical vein (Fowden, Comline et al. 1982, Pere 2001). Recent studies conducted in pigs (Almeida and Dias 2022, Johnson, Seo et al. 2023) showed that the trophoblasts utilize glucose via the aerobic glycolytic pathway and its intermediates are vehicle in the *de novo* synthesis of amino acid and nucleotides.

This maternal-foetal gradient is maintained thanks to the action of specific glucose transporters that are highly represented in different isoforms in the placenta as well as the foetal developing β -cells. This family of transporters are the GLUT transporters family, acting independently from insulin (Illsley 2000, Baumann, Deborde et al. 2002, Ruiz-Palacios, Ruiz-Alcaraz et al. 2017), where the predominant isoform used by human, pigs and mice is GLUT-1. During the normoglycemic intrauterine environment, the glucose gradient between the mother and the foetus is mostly maintained thanks to the symmetrical distribution of GLUT-1 within the placenta that regulates the glucose distribution; moreover, despite the pig placenta being more selective than the human counterpart, the interface between the pig uterus and placenta undergoes significant folding and maturation of areolae. This process aims to maximize the exchange surface between the mother and foetus. As a result, in both humans and pigs, the concentration of glucose in the maternal blood exceeds around 40-50% of the concentration found

in the foetus, creating in both a maternal-foetal glucose gradient, recognized as the main driving force for the glucose facilitate diffusion in the foetus (Pere 2003).

On the other hand, in the hyperglycaemic environment, there is an increment of GLUT1 that leads a massive amount of glucose that arrives to the foetus (Illsley and Baumann 2020) and the maternal-foetal glucose gradient is destroyed. On note, in pigs the foetal glucose concentration was increased of the 166% during the maternal diabetes, compared the normoglycemic condition (Ramsay, Wolverton et al. 1994).

These data are in line with our findings that show that, during the OGTT, PHG group has high fast plasma glucose level at the basal point and that continues during the whole procedure. The same was observed in humans (Wang, Jokelainen et al. 2019), where the glucose curve in impaired glucose tolerance children, after the OGTT, was significantly higher looking at the peripheral blood glucose concentration.

2.2. Impaired insulin response after OGTT in PHG compared to PNG piglets

Foetal and neonatal hyperinsulinemia is evident in hyperglycaemic pregnancies, and it is correlated to the maternal hyperglycaemia (Group, Metzger et al. 2008, Metzger, Persson et al. 2010). In fact, studies conducted in mild maternal hyperglycaemia show a higher insulin response in response to a higher amount of glucose in pigs (Renner, Martins et al. 2019), as well as in rats (Kervran, Guillaume et al. 1978, Bihoreau, Ktorza et al. 1986) indicating that foetal pancreatic endocrine alterations must be present as to overcome elevated glucose levels already in mild hyperglycaemic mothers.

Several other studies support this thesis, suggesting that offspring exposed to higher levels of glucose in the womb are at risk of developing impaired glucose tolerance. However, it's less clear whether similar risks exist in environments where mothers have pre-diabetic conditions, and the specific timing of these metabolic alterations is not fully understood. Also, in human there were evidence of insulin resistance at birth, to understand whether the processes leading to metabolic syndrome and

diabetes in adults might also be present before birth (Silverman, Metzger et al. 1995, Plagemann, Harder et al. 1997, Lindsay, Dabelea et al. 2000).

Dyer (Dyer, Rosenfeld et al. 2007) conducted a study on a Hispanic cohort of newborns, a population group with a high risk of developing metabolic syndrome. They found increased insulin resistance in macrosomic babies born to mothers with gestational diabetes, compared to newborns born in normal conditions, within 24-48 hours of birth. Similarly, Catalano (Catalano, Presley et al. 2009) analysed samples collected from the umbilical vein during delivery and observed increased insulin resistance, measured by the homeostasis model of insulin resistance, in neonates of obese mothers. They also found a positive correlation between foetal adiposity and insulin resistance. These studies collectively suggest that foetal metabolic programming can be influenced by chronic exposure to even mild forms of maternal hyperglycaemia, leading to metabolic alterations apparent at birth.

On the other hand, our study reports the effect of insulin resistance in a severe glucose intrauterine environment. We report that PHG offspring secret higher amount of insulin at birth at the basal level (TP0) compared to PNG group, but it shows a delayed and lower response at high plasma glucose level during the OGTT, although the total amount of insulin secreted doesn't seem to be affected. This indicates an impaired insulin sensitivity to the glucose level, confirmed by the Matsuda index and the HOMA-IR. The same result that was observed in human in pre-diabetic or diabetic conditions (Wang, Jokelainen et al. 2019), sign of the massive amount of glucose and the severe glucotoxic prolonged environment, to which the piglets were subjected.

In vivo, the insulin secretion depends on glucose, mainly, but also from other stimuli, as amino acids, fatty acid and hormones as leptin, estrogen, GLP1 and growth hormone (GH) (reviewed in (Fu, Gilbert et al. 2013)).

To avoid any other metabolic interference that can affect the axis glucose-insulin and to detect the specific answer of the β -cells, we performed a GSIS on porcine pancreatic tissue slices using the Biorep Perifusion System. The reason to use the pancreatic tissue slices is replaced in the fact that it does not suffer to limitations related to the isolation procedure of the islets of Langerhans, which induced islets stress and eliminate the potential crosstalk with liver and the other insulin-dependent organs. Moreover, in this work, the risk is to reduce or eliminate the

effect of the hyperglycaemic intrauterine environment. The pancreatic tissue slices let the islets being intact and distributed in their natural environment, without being expose to any chemical and physical stress. This technique was developed in rodents (Panzer, Cohrs et al. 2020).

In vitro GSIS confirmed what it was shown in the OGTT, showing that PHG have a higher insulin secretion at the basal level, when the tissue slices were perfused with low glucose concentration, and this level was maintained constant during the whole experiment stimulus, but with an insulin response only during the KCl depolarization, sign of β -cell dysfunction to proper answer at the high glucose stimulus. In contrast, PNG group demonstrated a sustainable increase in insulin secretion, when stimulated with high glucose and KCl depolarization.

The stimulation index indicated that the PNG group showed a clear insulin response at the high glucose stimulus and at the KCl depolarization, but, in the PHG group, the insulin response to high glucose was severely decreased. The overall insulin secretion looked inferior, looking at the statistical analysis of the group effect, although, anyway, there is a preserved basal insulin secretion.

Also, the kinetics seemed altered in the PHG group, showing approximately 5 minutes delay in the response to high glucose, compared to the PNG, but was preserved in the KCl stimulus, indicating a functional deficit. Interesting, this is the same that was observed in diabetic human donors when compared to non-diabetic donors (Panzer, Hiller et al. 2020).

This evidence suggested that at basal level, PHG group had more insulin content compared to the PNG group, but it was not adequately responsiveness to the glucose stimuli, both *in vivo* and *in vitro*, indicating that new-born piglets born from diabetic mothers, already suffer of impaired glucose tolerance.

2.3. Sex specific effect in the PHG group due to the hyperglycaemic intrauterine environment

Moreover, a sex specific effect was evident in the PHG group but not in the PNG group looking at the glucose physiology and insulin secretion, revealing the males more affected than the females.

This finding is supported by several studies that support the physiological way of women to be more protected by the pre-diabetic syndrome (Mauvais-Jarvis 2015), such as the ability of females to facilitate glucose absorption (glucose efficacy),

compared with healthy males of the same age, to exhibit higher postprandial plasma insulin and C-peptide concentrations after a meal (Basu, Dalla Man et al. 2006), confirmed that, after islets transplant, islets from female donors showed an improved clinical outcome compare of the male donors (Marchese, Rodeghier et al. 2015). Several human studies tried to explain the correlation between the prevalence of metabolic syndrome and the gender, first looking at the DNA methylation of gene specific sex differences that are associated with altered insulin secretion in human islets, showing that most of the genes were located on the chromosome X, that include genes known to affect insulin secretion that are more affected in males and this could explain the tendency in males to secrete less insulin (Hribal, Presta et al. 2011, Hall, Volkov et al. 2014).

However, how the maternal diabetes can predispose alterations in insulin secretion in a gender way, it is still unknown (Gautier, Fetita et al. 2018).

Our data show that during OGTT, the males started from a higher glucose plasma concentration and glucose curve stays higher during the whole OGTT, compared to the females of the PHG group, making the males more affected if compared to the sex-matched PNG group. This result was confirmed by the AUC of the glucose, that showed a higher value in the male piglets.

As expected, the insulin curve of the PHG males during the OGTT showed a higher insulin basal level (at TP0) and, controversially to the PHG female's one, that looked 30 minutes delayed compared to the sex-matched PNG, the male PHG didn't look match the higher glucose blood concentration and the peak seems to be 120 min delayed compared to the males PNG.

This results were in line with the *in vivo* studies in humans (Basu, Dalla Man et al. 2006, Marchese, Rodeghier et al. 2015, Wang, Jokelainen et al. 2019), although studies in rodents of offspring born from diabetic dams, there are controversial results that demonstrate that both gender have effects, but the males seem more affected in term of insulin sensitivity and impaired glucose tolerance (Agarwal, Brar et al. 2019, Nicholas, Nagao et al. 2020, Casasnovas, Damron et al. 2021) compared to the females, and others that demonstrate how only females offspring from high-fed-diet dams show insulin resistance at neonatal and adult age (Akhaphong, Gregg et al. 2021).

It is not clear how the insulin sensitivity to glucose can be affected by the gender, but the steroid hormones seem to play a fundamental role.

First, as we have mentioned, in humans it has been shown that an increase in adrenal gland volume is a marker of altered metabolic status (Askani, Rospleszcz et al. 2022), indicating an anatomical role of the hormone secretion in humans and, in addition, the ovary-islets and testis-islets axis makes a huge contribution to explaining this sex-specific effect.

In our findings, in fact, males seemed more affected than females *in vivo*, showing an impaired insulin secretion, this can be due to a loss of testosterone secreted that influences the β -cell sensitivity. The way how maternal diabetes can influence the sexual hormone synthesis in neonatal age is still unclear, but there are evidences in humans where a metabolic disturbed environment can provoke a loss of testosterone synthesis (Wittert and Grossmann 2022, Yeap and Wittert 2022), resulting in a positive feedback mechanism.

To the best of our knowledge, there is no evidence of how the glucotoxic environment may affect estrogen synthesis, but in our results, as seen in humans, females appear to be more responsive than males, demonstrating the protective role of estrogen in insulin sensitivity.

This is confirmed by perfusion GSIS, where, in the absence of pathways that may interfere with insulin synthesis, there are no differences in the PHG of males and females.

3. Omics studies for the molecular characterization of the β -cells

To explore how chronic exposure to hyperglycaemic intrauterine environment affect transcriptomes and proteomes of the β -cells, a multi-omics analysis was performed. Here we speculate how the excess of maternal glucose that fuel in the placenta, impacts various pathways involved in the maturation, proliferation, and function of pancreatic β -cells, leading to the β -cells exhaustion, and potentially developing T2DM.

In this work we assessed whole pancreas proteomic studies focusing on the hormones secreted from the islets of Langerhans, in collaboration with Lafuga laboratory at the Gene Centre (processed and analysed by Bachuki Sashikadze and Dr. Thomas Fröhlich)

In the splenic part of the pancreas insulin abundance was increased; this is in line with our OGTT results, where, at TP0, PHG offspring had a higher amount of basal insulin secretion compared to the PNG, as well as the GSIS results. This can be a consequence for the massive amount of glucose that fuel to the β -cell of the offspring, forcing in an initial massive amount of insulin release.

Looking at the duodenal part (which corresponds to the head in the human pancreas), insulin does not seem to be one of the proteins increased in the PHG group, and this can be due to the less presence of β -cells in the islets of Langerhans in the duodenal part, which is also present in human and rodents (Wang, Misawa et al. 2013).

To better understand how the β -cell profile changed in response to intrauterine glucotoxicity, we analysed the transcriptome profiles of PHG piglets compared to controls.

It is known that, in the context of constant glucotoxicity, such as exposure to maternal hyperglycaemia during pregnancy, β -cell functionality declines primarily due to apoptosis mechanisms and loss of differentiation. Moreover, recent research suggest that β -cell dedifferentiation plays a significant role in early to mid-stage diabetes development, rather than an increase in β -cell death.

Specifically, glucose upregulates *MAFA*, a transcriptional activator crucial for insulin gene expression, affecting β -cell function, development, and potentially diabetes onset.

Genetic and phenotypic analyses in pigs reveal similarities in the expression of critical genes like *MAFA* and *PDX1* between pigs and humans, particularly in pancreatic development, highlighting the potential of pigs as an alternative model for investigating human pancreatic islet development and function (Kim, Whitener et al. 2020, Tritschler, Thomas et al. 2022).

For these reasons, we first analysed the differences in gene expression of these two transcripts. Interesting, these genes seem to be downregulated here, as it is evident in diabetic conditions.

In fact, studies that used omics techniques to elucidate the transition from pre-diabetic to diabetic conditions, revealed a downregulation of β -cell-enriched genes, particularly insulin, mediated by alterations in key transcription factors like PDX1 and MAFA. This downregulation is associated with oxidative stress and ER stress, among other mechanisms and can lead to islet dysfunction, affecting calcium fluxes, metabolism, and insulin secretion (Guo, Dai et al. 2013, Fu, Cui et al. 2017).

Moreover, studies using murine models have confirmed the loss of β -cell identity in chronic hyperglycaemia (Brereton, Rohm et al. 2016). Additionally, diabetic mice and rats with partial pancreatectomy exhibit β -cell dedifferentiation, evidenced by decreased expression of differentiation markers such as insulin, PDX1, and MAFA. Upregulation of pancreatic progenitor-associated transcription factors in β -cells following partial pancreatectomy suggests a dedifferentiated state (Talchai, Xuan et al. 2012).

Glucotoxicity also affects the expression of genes involved in maintaining β -cell phenotype, contributing further to β -cell dedifferentiation.

FOXO1 has emerged as a potential transcription factor linking metabolic stress to β -cell dedifferentiation in T2DM (Talchai, Xuan et al. 2012). Under oxidative stress, FOXO1 stimulates the expression of genes like *NEUROD1* (which is upregulated in our findings) and *MAFA*. Transgenic mouse models indicate FOXO1's role in compensatory mechanisms during insulin resistance, enhancing β -cell proliferation, function, and antioxidant gene expression. Deletion of *Foxo1* in β -cells leads to β -cell dedifferentiation, accompanied by upregulation of progenitor and pluripotency markers. In our data, *FOXO1* is upregulated, which is a sign of the cell distress in this condition (Talchai, Xuan et al. 2012). Additionally, in transgenic mouse models, FOXO1 has been implicated in compensatory mechanisms in β -cells during insulin resistance by enhancing β -cell mass, function, and the expression of antioxidant genes (Zhang, Kim et al. 2016). Intriguingly, the deletion of *Foxo1* specifically in β -cells led to β -cell dedifferentiation in aging male mice and multiparous female mice, accompanied by the upregulation of markers associated with progenitor and pluripotency states (Talchai, Xuan et al. 2012).

Of note, another gene largely characterized as typically expressed in progenitors' cells and upregulated in various diabetic animals in the β -cells, is *NeuroG3*

(Talchai, Xuan et al. 2012, Wang, York et al. 2014), which was upregulated in our findings. A characteristic of *NeuroG3*, is that it was upregulated in expanded rodent islets *in vitro* (Lin, Cheng et al. 2020).

ALDOB, considered as a marker of β -cell dysfunction, was among the most upregulated genes in the PHG group. This gene is negatively associated with insulin secretion in humans (Gerst, Jaghutriz et al. 2018). It encodes a glycolytic enzyme and is normally silenced in mature β -cells; its upregulation is associated with diabetes (Haythorne, Rohm et al. 2019).

Another gene taken under consideration in our analysis as a sign of mature β -cells is *Rbp4*, which was shown to inhibit GSIS in rats (Artner, Hang et al. 2010). This gene codes for a protein RBP4 which is the principal carrier of retinol in the plasma and elevated levels of this protein are evident in T2DM, but reduced levels are detected in T1DM (Pullakhandam, Palika et al. 2012). In our studies *Rbp4* looks upregulated.

Other studies display that several transcription factors expressed in progenitor cells at the embryonic stage are upregulated in diabetic animal models during β -cell dedifferentiation, indicating trans-differentiation potential. Major causes of β -cell dedifferentiation highlighted in recent studies include ROS production and ER stress. For instance, several genes involved in the ER stress of the β -cell, as *DDIT3*, were upregulated in the PHG group. In fact, *DDIT3* is considered a target gene for revealing the hypoxia status (Bensellam, Jonas et al. 2018) and pro-apoptotic condition in the β -cells (Schroder and Kaufman 2005, Lai, Teodoro et al. 2007, Karunakaran, Kim et al. 2012, Schwarz and Blower 2016).

Notably, in our finding's genes associated with β -cell differentiation were downregulated in the PHG group, while progenitor characteristic genes were upregulated, indicating a shift towards a less differentiated state. Additionally, β -cell growth factor genes were downregulated in the PHG group, while genes known to protect against apoptosis were upregulated.

On note, gene encoding receptors, such as EGFR, IGF1R, and IGF2R, were upregulated in the PHG group. Specifically, epidermal growth factor receptor (EGFR) signaling is essential for proper fetal development and growth of pancreatic

islets, in fact, his loss lead to the diabetes in adulthood in mice (Miettinen, Ustinov et al. 2006).

Another interesting finding in this section is that IGF2 and IGF1 receptor (IGF1R and IGF2R) were upregulated. These receptors are involved in the GLP1 pathway, and this is a common developmental pathway between human and pigs, but not in mice (and this is, for instance, one of the reasons why pigs might offer a more representative model for certain aspects of human processes compared to mice).

GLP1 increases its activity by augmenting IGF1R expression and by stimulating insulin secretion; this mechanism is required for GLP-1–induced protection against apoptosis (Miettinen, Ustinov et al. 2006).

Moreover, insulin like growth factor 1 (*IGF1*) mRNA concentrations were increased in foetal tissue by maternal diabetes (34%) (Ramsay, Wolverson et al. 1994).

Also, in our finding's genes related to insulin production and secretion were mostly downregulated in the PHG group, while ER stress genes were predominantly upregulated (as *DDIT3*). Interestingly, there was no significant difference in the representation of cell death genes between the two groups. These findings highlight the complex molecular changes underlying β -cell dysfunction in response to intrauterine glucotoxicity, shedding light on potential mechanisms involved in the development of diabetes.

VI. CONCLUSION

As conclusion, in a healthy and normoglycemic condition the maternal-foetal glucose gradient is maintained thanks to the action of the maternal metabolism and several glucose transporters at the placental and foetal level. The amount of glucose that fuel to the β -cell of the foetus is adequate and the foetal insulin transcription factors are not stimulated and the insulin secretion is nearly absent (Pere 2003).

In hyperglycaemic intrauterine conditions, the maternal-foetal gradient is destroyed and the glucose pass freely through the placenta and it stimulates the foetal β -cells (Pere 2003).

This is the first work that studies in a deep molecular way, what happens in the foetal β -cell when exposed in a glucotoxic condition in the intrauterine life, in a big animal model.

For this reason, the information that we have about this topic are lacking and the most of molecular information we have, are about the β -cell in glucotoxic environment (as in diabetic conditions).

It is known that, when the glucose arrives at the β -cell, the insulin transcription factors are activated (Poitout, Hagman et al. 2006). This is also true in a state of hyperglycaemia, where the massive and initial amount of glucose stimulates the insulin production and secretion. In a constant and massive hyperglycaemic condition, the expression of GLUT transporter increase on the β -cell, leading to a massive absorption of glucose in the cells (Fu, Gilbert et al. 2013). The amount of insulin starts increasing and it stimulates, through a positive feedback mechanism, the overexpression of the IRs that re-uptake the insulin secreted and start leading to the cell dysfunction (Petersen and Shulman 2018).

This is called the “activation phase” or the “phase I” in the study of the development of diabetes, when there is the massive insulin production and secretion. This phase is probably the reason why in our findings, we see a higher amount of insulin in the proteomic and in the *in vivo* and *in vitro* GSIS, in the PHG group. In this phase, the dedifferentiation factors are still not active.

If this phase persists, the cell slips in the second phase, which is called the “compensation phase”. Once the cell enters this phase, we are in the “pre-diabetic” condition.

During this phase, the cells start to activate protective mechanisms to avoid the apoptosis. For this reason, they start activating the dedifferentiation factors that lead

to a downregulation of the insulin transcription factors and cause the insulin secretion dysfunction and the impaired insulin secretion to the glucose stimulus. Substantially, the huge amount of insulin secretion causes the ER stress in the cells that provokes the activation of the UPR in the cell (Papa 2012).

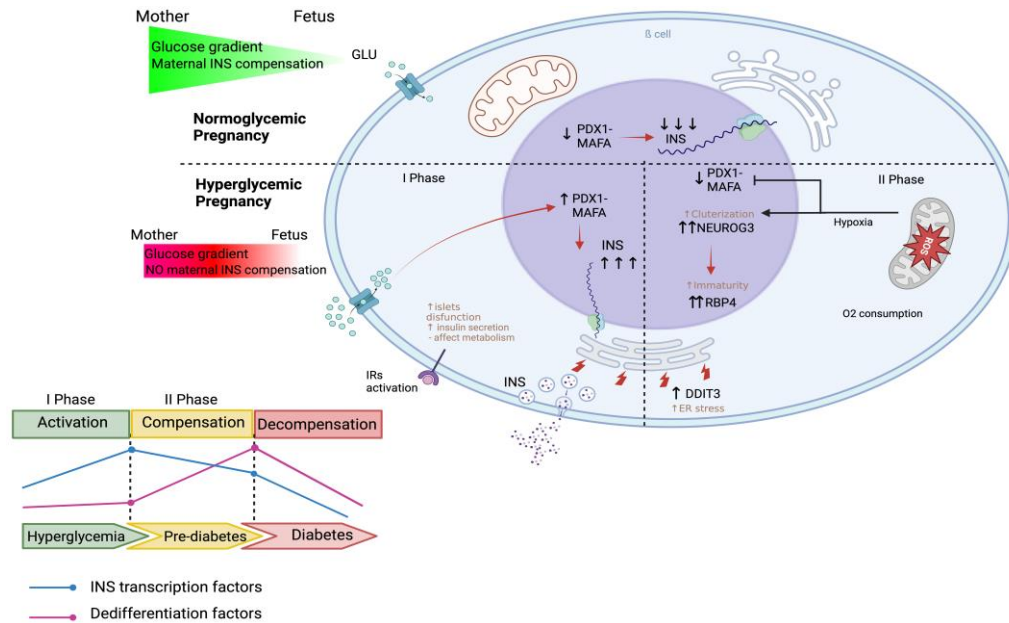


Figure 23: Schematic representation underlying mechanism of offspring β -cell dedifferentiation when exposed to maternal diabetes. In the normoglycemic conditions (upper part) the mother-fetus gradient is not disrupted and the insulin production in the fetal β -cells is nearly absent. In the hyperglycemic intrauterine conditions (lower part), the fetal β -cells start undergoing a series of metabolic events that induce the insulin over-expression and the initiating of adaptive event such as the dedifferentiation.

We are aware that most of the molecular studies are conducted in rodents, for this reason, most of the references used are referred to mice. This is an incentive to focus studies on animals that are metabolic more like humans.

These transcription factors upregulate the expression of antioxidant genes but also pro-apoptotic genes such as Ddit3, which contributes to β -cell death after prolonged ER stress (Schroder and Kaufman 2005, Lai, Teodoro et al. 2007, Karunakaran, Kim et al. 2012, Schwarz and Blower 2016). Further studies need to clarify the crosstalk between the ER and mitochondria (Khin, Lee et al. 2021), although it can be assumed that hypoxia and inflammation in the loss of adaptive UPR under chronic hyperglycaemia. Under chronic hyperglycaemia, the acceleration of

mitochondrial metabolism and the stimulation of ATP consuming cellular processes, increases β -cell O_2 consumption. It is known, in fact, that ROS are produced in different subcellular location (e.g., mitochondria, peroxisomes, and ER) during cellular metabolism (Guo, Dai et al. 2013).

Thus, high ROS level, produced from the ER stress, accelerate the β -cells dedifferentiation and a loss of function. In fact, in immortalised β -cells exposed to high glucose to mimic the glucotoxicity, show an increased ROS production but a decreased insulin secretion via MAFA downregulation (Guo, Dai et al. 2013, Fu, Cui et al. 2017), as it is confirmed in our results, showing that MAFA and PDX1 are downregulated because of the dedifferentiation protective mechanism. This is probably the reason why, although we can detect the presence of insulin at the basal level in the GSIS, there is not furthermore production, and its secretion seem disrupted.

Throughout the dedifferentiation, obviously, several transcription factors typically expressed in progenitor cells at the embryonic stage and repressed in adult β -cells were upregulated in β -cells of various diabetic animal models (Talchai, Xuan et al. 2012, Wang, York et al. 2014). Specifically, *in vitro* studies of mice and rats' islets, NeuroG3 was detected in higher expression level in expanded islets clusters, suggesting that it is required for islets expansion and propagation (Lin, Cheng et al. 2020). This can be the explanation why we display bigger clusters in our data in the PHG group compared with the PNG.

VII. SUMMARY

This study delves into the ramifications of maternal hyperglycaemia on offspring health, particularly focusing on the well-being of pancreatic β -cells. It is well-established that maternal hyperglycaemia during pregnancy significantly impacts offspring health, yet the precise molecular mechanisms at play remain elusive, especially in human studies. While murine models have been extensively utilized, their translational relevance to humans is somewhat limited. This prompted our exploration of pigs as a more promising model due to their closer anatomical and physiological resemblance to humans, particularly in terms of pancreas structure and gene expression.

In our investigation, we aimed to uncover the immediate metabolic shifts observed in offspring born to mothers with severe diabetes (*INS^{C94Y}*).

Our first results showed that maternal diabetes poses significant risks to both reproductive health and offspring development. *INS^{C94Y}* sows' observations were associated with reduced fertility and adverse pregnancy outcomes, including birth defects. In fact, babies born to diabetic mothers may exhibit various birth defects affecting organs like the craniofacial features, limbs, kidneys, heart, and gastrointestinal system. While human neonates often display macrosomia, our results show that PHG piglets may have low birth weight but show relative organ hypertrophy. Nevertheless, our results demonstrate that maternal diabetes also influenced offspring lipid metabolism and lactate metabolism, looking at the clinical chemical parameters.

We found that such offspring exhibit compromised glucose tolerance and insulin response right from birth. Our experiments unveiled a compromised ability of the offspring to handle glucose, as evidenced by elevated plasma glucose levels shortly after birth. This phenomenon likely stems from alterations in maternal glucose concentrations during gestation, which subsequently affect the maternal-foetal glucose gradient. Despite elevated insulin levels at birth, offspring displayed a reduced response to insulin secretion during the OGTT. This suggests impaired insulin secretion, a phenomenon well-documented in humans as well. Interestingly, male offspring appeared to be more susceptible to metabolic alterations, exhibiting higher glucose levels during the oral glucose tolerance test and delayed insulin response compared to females.

By analyzing whole pancreas proteomics, the study identified initial increases in insulin levels in the splenic part of the pancreas, consistent with elevated insulin levels observed during glucose tolerance tests. However, insulin levels in the duodenal part remained relatively unchanged, possibly due to fewer β -cells in this region.

This study investigated how exposure to high maternal glucose levels during pregnancy affects the transcriptomes of pancreatic β -cells. Our research suggests that chronic hyperglycemia impacts various pathways crucial for β -cell maturation and function, ultimately resulting in β -cell exhaustion and dedifferentiation.

Chronic hyperglycemia induced declines in β -cell functionality primarily through apoptosis mechanisms and loss of differentiation. Key transcription factors like MAFA, crucial for insulin gene expression, were affected, potentially contributing to diabetes onset.

Comparisons with existing literature highlight similar patterns observed in both pigs and humans, particularly in pancreatic development and gene expression changes associated with β -cell dysfunction. Downregulation of genes associated with β -cell differentiation and upregulation of progenitor characteristic genes suggest a shift towards a less differentiated state in response to hyperglycemia. Additionally, upregulation of genes involved in ER stress indicates a potential role in β -cell dysfunction, consistent with findings from other studies.

Moreover, changes in growth factor receptors such as EGFR, IGF1R, and IGF2R, potentially influencing fetal pancreatic development, align with existing literature. Notably, upregulation of IGF1 and IGF2 receptors, integral to the GLP-1 pathway's protective role against apoptosis, is consistent with previous research.

VIII. ZUSAMMENFASSUNG

Auswirkung des mütterlichen Diabetes auf die Gesundheit der β -Zellen in den Nachkommen - eine Studie an Nachkommen von diabetischen MIDY-Schweinen

Diese Studie befasst sich mit den Auswirkungen der mütterlichen Hyperglykämie auf die Gesundheit der Nachkommen, insbesondere auf das Wohlergehen der β -Zellen der Bauchspeicheldrüse. Es ist bekannt, dass eine mütterliche Hyperglykämie während der Schwangerschaft die Gesundheit der Nachkommen erheblich beeinträchtigt, doch die genauen molekularen Mechanismen, die dabei eine Rolle spielen, sind nach wie vor schwer zu ergründen, insbesondere in Studien am Menschen. Mäusemodelle werden zwar ausgiebig genutzt, doch ihre Relevanz für den Menschen ist eher begrenzt. Dies veranlasste uns, Schweine als vielversprechenderes Modell zu verwenden, da sie anatomisch und physiologisch dem Menschen ähnlicher sind, insbesondere in Bezug auf die Pankreasstruktur und die Genexpression in den Langerhans'schen Inseln.

Ziel unserer Untersuchungen war es, den Einfluss von maternalem Diabetes auf den Stoffwechsel der Nachkommen in der perinatalen Periode, insbesondere die Auswirkungen auf die β Zellen aufzudecken.

Unsere Ergebnisse zeigten, dass mütterlicher Diabetes sowohl für die reproduktive Gesundheit der Mütter als auch für die Entwicklung der Nachkommen erhebliche Risiken birgt. Die Beobachtungen an den diabetischen *INS^{C94Y}*-Sauen wurden mit einer verminderten Fruchtbarkeit und ungünstigen Schwangerschaftsergebnissen, einschließlich Geburtsschäden, in Verbindung gebracht. So wiesen Nachkommen, die von diabetischen Müttern geboren werden, verschiedene Missbildungen auf, die verschiedene Gewebe und Organe wie den Schädel, die Gliedmaßen, die Nieren, das Herz und das Magen-Darm-System betrafen. Während menschliche Neugeborene häufig Makrosomie aufweisen, zeigten unsere Ergebnisse, dass PHG-Ferkel ein niedriges Geburtsgewicht hatten, aber relativ erhöhte Organgewichte aufwiesen.

Unsere Ergebnisse zeigen jedoch, dass der mütterliche Diabetes auch den Fettstoffwechsel und den Laktatstoffwechsel der Nachkommen beeinflusst, wenn man die klinisch-chemischen Parameter betrachtet.

Wir haben festgestellt, dass solche Nachkommen von Geburt an eine beeinträchtigte Glukosetoleranz und Insulinreaktion aufwiesen. Unsere Experimente haben gezeigt, dass die Fähigkeit der Nachkommen, mit Glukose umzugehen, beeinträchtigt war, was sich in erhöhten Plasmaglukosespiegeln kurz nach der Geburt widerspiegelte. Dieses Phänomen ist wahrscheinlich auf Veränderungen der mütterlichen Glukosekonzentration während der Trächtigkeit zurückzuführen, die sich anschließend auf den mütterlich-fötalen Glukosegradienten auswirken. Trotz erhöhter Insulinspiegel bei der Geburt zeigten die Nachkommen eine verminderte Reaktion auf die Insulinsekretion während des OGTT. Dies lässt auf eine gestörte Insulinsekretion schließen, ein Phänomen, das auch beim Menschen gut dokumentiert ist. Interessanterweise schienen männliche Nachkommen anfälliger für Stoffwechselveränderungen zu sein, da sie während des oralen Glukosetoleranztests höhere Glukosespiegel und eine verzögerte Insulinreaktion im Vergleich zu weiblichen Nachkommen aufwiesen.

Durch die Analyse der Proteomik der gesamten Bauchspeicheldrüse wurde in der Studie ein anfänglicher Anstieg des Insulinspiegels in der Milz Teil der Bauchspeicheldrüse festgestellt, der mit den bei Glukosetoleranztests beobachteten, erhöhten Insulinspiegeln übereinstimmt. Der Insulinspiegel im Zwölffingerdarm blieb jedoch relativ unverändert, was möglicherweise auf eine geringere Anzahl von β -Zellen in dieser Region zurückzuführen ist.

In dieser Studie wurde untersucht, wie sich die Exposition gegenüber hohen mütterlichen Glukosespiegeln während der Schwangerschaft auf das Transkriptom der β -Zellen des Pankreas auswirkt. Unsere Forschungsergebnisse deuten darauf hin, dass eine chronische Hyperglykämie verschiedene Signalwege beeinflusst, die für die Reifung und Funktion der β -Zellen entscheidend sind, was letztlich zu einer Erschöpfung und Dedifferenzierung der β -Zellen führt.

Chronische Hyperglykämie führt zu einer Verschlechterung der β -Zell-Funktionalität vor allem durch Apoptose-Mechanismen und Verlust der Differenzierung. Wichtige Transkriptionsfaktoren wie MAFA, die für die Insulin-Genexpression entscheidend sind, waren betroffen, was möglicherweise zur Entstehung von Diabetes beiträgt.

Vergleiche mit der bestehenden Literatur zeigen ähnliche Muster, die sowohl bei Schweinen als auch bei Menschen beobachtet werden, insbesondere bei der Entwicklung der Bauchspeicheldrüse und den Veränderungen der Genexpression,

die mit der Dysfunktion der β -Zellen einhergehen. Die Herabregulierung von Genen, die mit der β -Zell-Differenzierung in Verbindung stehen, und die Hochregulierung von charakteristischen Genen der Vorläuferzellen deuten auf eine Verschiebung zu einem weniger differenzierten Zustand als Reaktion auf eine Hyperglykämie hin.

Darüber hinaus deutet die Hochregulierung von Genen, die am ER-Stress beteiligt sind, auf eine mögliche Rolle bei der Dysfunktion der β -Zellen hin, was mit den Ergebnissen anderer Studien übereinstimmt.

Darüber hinaus stimmen die Veränderungen der Wachstumsfaktorrezeptoren wie EGFR, IGF1R und IGF2R, die möglicherweise die fetale Pankreasentwicklung beeinflussen, mit der vorhandenen Literatur überein. Insbesondere die Hochregulierung der IGF1- und IGF2-Rezeptoren, die für die schützende Rolle des GLP-1-Stoffwechsels vor Apoptose wesentlich sind, steht im Einklang mit früheren Forschungsergebnissen.

IX. REFERENCE LIST

Adeva-Andany, M., M. Lopez-Ojen, R. Funcasta-Calderon, E. Ameneiros-Rodriguez, C. Donapetry-Garcia, M. Vila-Altesor and J. Rodriguez-Seijas (2014). "Comprehensive review on lactate metabolism in human health." Mitochondrion **17**: 76-100.

Agarwal, P., N. Brar, T. S. Morriseau, S. M. Kereliuk, M. A. Fonseca, L. K. Cole, A. Jha, B. Xiang, K. L. Hunt, N. Seshadri, G. M. Hatch, C. A. Doucette and V. W. Dolinsky (2019). "Gestational Diabetes Adversely Affects Pancreatic Islet Architecture and Function in the Male Rat Offspring." Endocrinology **160**(8): 1907-1925.

Agarwal, P., T. S. Morriseau, S. M. Kereliuk, C. A. Doucette, B. A. Wicklow and V. W. Dolinsky (2018). "Maternal obesity, diabetes during pregnancy and epigenetic mechanisms that influence the developmental origins of cardiometabolic disease in the offspring." Crit Rev Clin Lab Sci **55**(2): 71-101.

Ahn, Y. B., G. Xu, L. Marselli, E. Toschi, A. Sharma, S. Bonner-Weir, D. C. Sgroi and G. C. Weir (2007). "Changes in gene expression in beta cells after islet isolation and transplantation using laser-capture microdissection." Diabetologia **50**(2): 334-342.

Akhaphong, B., B. Gregg, D. Kumusoglu, S. Jo, K. Singer, J. Scheys, J. DelProposto, C. Lumeng, E. Bernal-Mizrachi and E. U. Alejandro (2021). "Maternal High-Fat Diet During Pre-Conception and Gestation Predisposes Adult Female Offspring to Metabolic Dysfunction in Mice." Front Endocrinol (Lausanne) **12**: 780300.

Albl, B., S. Haesner, C. Braun-Reichhart, E. Streckel, S. Renner, F. Seeliger, E. Wolf, R. Wanke and A. Blutke (2016). "Tissue Sampling Guides for Porcine Biomedical Models." Toxicol Pathol **44**(3): 414-420.

Alcazar, O., A. Alvarez, C. Ricordi, E. Linetsky and P. Buchwald (2020). "The

Effect of Recovery Warm-up Time Following Cold Storage on the Dynamic Glucose-stimulated Insulin Secretion of Isolated Human Islets." Cell Transplant **29**: 963689720908278.

Allan, C. A. (2014). "Sex steroids and glucose metabolism." Asian J Androl **16**(2): 232-238.

Almeida, F. and A. Dias (2022). "Pregnancy in pigs: the journey of an early life." Domest Anim Endocrinol **78**: 106656.

Ammar, C., M. Gruber, G. Csaba and R. Zimmer (2019). "MS-EmpiRe Utilizes Peptide-level Noise Distributions for Ultra-sensitive Detection of Differentially Expressed Proteins." Mol Cell Proteomics **18**(9): 1880-1892.

Arrojo e Drigo, R., Y. Ali, J. Diez, D. K. Srinivasan, P. O. Berggren and B. O. Boehm (2015). "New insights into the architecture of the islet of Langerhans: a focused cross-species assessment." Diabetologia **58**(10): 2218-2228.

Artner, I., Y. Hang, M. Mazur, T. Yamamoto, M. Guo, J. Lindner, M. A. Magnuson and R. Stein (2010). "MafA and MafB regulate genes critical to beta-cells in a unique temporal manner." Diabetes **59**(10): 2530-2539.

Askani, E., S. Rospleszcz, R. Lorbeer, C. Kulka, R. von Kruchten, K. Muller-Peltzer, D. Hasic, E. Kellner, M. Reisert, W. Rathmann, A. Peters, C. L. Schlett, F. Bamberg and C. Storz (2022). "Association of MRI-based adrenal gland volume and impaired glucose metabolism in a population-based cohort study." Diabetes Metab Res Rev **38**(5): e3528.

Bais, A. S. and D. Kostka (2020). "scds: computational annotation of doublets in single-cell RNA sequencing data." Bioinformatics **36**(4): 1150-1158.

Bakhti, M., A. Bottcher and H. Lickert (2019). "Modelling the endocrine pancreas in health and disease." Nat Rev Endocrinol **15**(3): 155-171.

Barker, D. J. (1997). "Maternal nutrition, fetal nutrition, and disease in later life." Nutrition **13**(9): 807-813.

Barua, S. and M. A. Junaid (2015). "Lifestyle, pregnancy and epigenetic effects." Epigenomics **7**(1): 85-102.

Basu, R., C. Dalla Man, M. Campioni, A. Basu, G. Klee, G. Toffolo, C. Cobelli and R. A. Rizza (2006). "Effects of age and sex on postprandial glucose metabolism: differences in glucose turnover, insulin secretion, insulin action, and hepatic insulin extraction." Diabetes **55**(7): 2001-2014.

Baumann, M. U., S. Deborde and N. P. Illsley (2002). "Placental glucose transfer and fetal growth." Endocrine **19**(1): 13-22.

Becht, E., L. McInnes, J. Healy, C. A. Dutertre, I. W. H. Kwok, L. G. Ng, F. Ginhoux and E. W. Newell (2018). "Dimensionality reduction for visualizing single-cell data using UMAP." Nat Biotechnol.

Bedell, S., J. Hutson, B. de Vrijer and G. Eastabrook (2021). "Effects of Maternal Obesity and Gestational Diabetes Mellitus on the Placenta: Current Knowledge and Targets for Therapeutic Interventions." Curr Vasc Pharmacol **19**(2): 176-192.

Beiki (2019). "Correction to: Design, Synthesis, Radiolabeling, and Biologic Evaluation of Three (18)F-FDG-Radiolabeled Targeting Peptides for the Imaging of Apoptosis, by Khoshbakht S, Beiki D, Geramifar P, et al. Cancer Biother Radiopharm 2019;34(5):271-279. DOI: 10.1089/cbr.2018.2709." Cancer Biother Radiopharm **34**(6): 417.

Bell, J. D., J. C. Brown, P. J. Sadler, D. Garvie, A. F. Macleod and C. Lowy (1989). "Maternal and cord blood plasma. Comparative analyses by ¹H NMR spectroscopy." NMR Biomed **2**(2): 61-65.

Bensellam, M., J. C. Jonas and D. R. Laybutt (2018). "Mechanisms of beta-cell

dedifferentiation in diabetes: recent findings and future research directions." J Endocrinol **236**(2): R109-R143.

Bentsi-Barnes, K., M. E. Doyle, D. Abad, F. Kandeel and I. Al-Abdullah (2011). "Detailed protocol for evaluation of dynamic perfusion of human islets to assess beta-cell function." Islets **3**(5): 284-290.

Bhagat, L., V. P. Singh, A. J. Hietaranta, S. Agrawal, M. L. Steer and A. K. Saluja (2000). "Heat shock protein 70 prevents secretagogue-induced cell injury in the pancreas by preventing intracellular trypsinogen activation." J Clin Invest **106**(1): 81-89.

Biesenbach, G., P. Grafinger, J. Zazgornik, Helmut and Stoger (2000). "Perinatal complications and three-year follow up of infants of diabetic mothers with diabetic nephropathy stage IV." Ren Fail **22**(5): 573-580.

Bihoreau, M. T., A. Ktorza, A. Kervran and L. Picon (1986). "Effect of gestational hyperglycemia on insulin secretion in vivo and in vitro by fetal rat pancreas." Am J Physiol **251**(1 Pt 1): E86-91.

Bloom, S. L., M. Belfort, G. Saade, H. Eunice Kennedy Shriver National Institute of Child and N. Human Development Maternal-Fetal Medicine Units (2016). "What we have learned about intrapartum fetal monitoring trials in the MFMU Network." Semin Perinatol **40**(5): 307-317.

Blundell, C., E. R. Tess, A. S. Schanzer, C. Coutifaris, E. J. Su, S. Parry and D. Huh (2016). "A microphysiological model of the human placental barrier." Lab Chip **16**(16): 3065-3073.

Borg, D. J., M. Weigelt, C. Wilhelm, M. Gerlach, M. Bickle, S. Speier, E. Bonifacio and A. Hommel (2014). "Mesenchymal stromal cells improve transplanted islet survival and islet function in a syngeneic mouse model." Diabetologia **57**(3): 522-531.

Bouchard, L., M. F. Hivert, S. P. Guay, J. St-Pierre, P. Perron and D. Brisson (2012). "Placental adiponectin gene DNA methylation levels are associated with mothers' blood glucose concentration." Diabetes **61**(5): 1272-1280.

Brelje, T. C., D. W. Scharp, P. E. Lacy, L. Ogren, F. Talamantes, M. Robertson, H. G. Friesen and R. L. Sorenson (1993). "Effect of homologous placental lactogens, prolactins, and growth hormones on islet B-cell division and insulin secretion in rat, mouse, and human islets: implication for placental lactogen regulation of islet function during pregnancy." Endocrinology **132**(2): 879-887.

Brereton, M. F., M. Rohm, K. Shimomura, C. Holland, S. Tornovsky-Babeay, D. Dadon, M. Iberl, M. V. Chibalina, S. Lee, B. Glaser, Y. Dor, P. Rorsman, A. Clark and F. M. Ashcroft (2016). "Hyperglycaemia induces metabolic dysfunction and glycogen accumulation in pancreatic beta-cells." Nat Commun **7**: 13496.

Brett, K. E., Z. M. Ferraro, J. Yockell-Lelievre, A. Gruslin and K. B. Adamo (2014). "Maternal-fetal nutrient transport in pregnancy pathologies: the role of the placenta." Int J Mol Sci **15**(9): 16153-16185.

Burlina, S., M. G. Dalfra and A. Lapolla (2019). "Short- and long-term consequences for offspring exposed to maternal diabetes: a review." J Matern Fetal Neonatal Med **32**(4): 687-694.

Burns, T. L., E. M. Letuchy, R. Paulos and J. Witt (2009). "Childhood predictors of the metabolic syndrome in middle-aged adults: the Muscatine study." J Pediatr **155**(3): S5 e17-26.

Bush, N. C., P. C. Chandler-Laney, D. J. Rouse, W. M. Granger, R. A. Oster and B. A. Gower (2011). "Higher maternal gestational glucose concentration is associated with lower offspring insulin sensitivity and altered beta-cell function." J Clin Endocrinol Metab **96**(5): E803-809.

Cabrera, O., D. M. Berman, N. S. Kenyon, C. Ricordi, P. O. Berggren and A. Caicedo (2006). "The unique cytoarchitecture of human pancreatic islets has

implications for islet cell function." Proc Natl Acad Sci U S A **103**(7): 2334-2339.

Cabrera, O., M. C. Jacques-Silva, D. M. Berman, A. Fachado, F. Echeverri, R. Poo, A. Khan, N. S. Kenyon, C. Ricordi, P. O. Berggren and A. Caicedo (2008). "Automated, high-throughput assays for evaluation of human pancreatic islet function." Cell Transplant **16**(10): 1039-1048.

Camaya, I., S. Donnelly and B. O'Brien (2022). "Targeting the PI3K/Akt signaling pathway in pancreatic beta-cells to enhance their survival and function: An emerging therapeutic strategy for type 1 diabetes." J Diabetes **14**(4): 247-260.

Cao, Y., Z. Zhao, R. L. Eckert and E. A. Reece (2012). "The essential role of protein kinase Cdelta in diabetes-induced neural tube defects." J Matern Fetal Neonatal Med **25**(10): 2020-2024.

Carrasco-Wong, I., A. Moller, F. R. Giachini, V. V. Lima, F. Toledo, J. Stojanova, L. Sobrevia and S. San Martin (2020). "Placental structure in gestational diabetes mellitus." Biochim Biophys Acta Mol Basis Dis **1866**(2): 165535.

Caruso, S., S. Rugolo, C. Agnello, G. Intelisano, L. Di Mari and A. Cianci (2006). "Sildenafil improves sexual functioning in premenopausal women with type 1 diabetes who are affected by sexual arousal disorder: a double-blind, crossover, placebo-controlled pilot study." Fertil Steril **85**(5): 1496-1501.

Casasnovas, J., C. L. Damron, J. Jarrell, K. S. Orr, R. N. Bone, S. Archer-Hartmann, P. Azadi and K. L. Kua (2021). "Offspring of Obese Dams Exhibit Sex-Differences in Pancreatic Heparan Sulfate Glycosaminoglycans and Islet Insulin Secretion." Front Endocrinol (Lausanne) **12**: 658439.

Casella, G., E. Soricelli, L. Castagneto-Gissey, A. Redler, N. Basso and G. Mingrone (2016). "Changes in insulin sensitivity and secretion after sleeve gastrectomy." Br J Surg **103**(3): 242-248.

Catalano, P. M., L. Presley, J. Minium and S. Hauguel-de Mouzon (2009). "Fetuses of obese mothers develop insulin resistance in utero." Diabetes Care **32**(6): 1076-1080.

Chen, J., H. Xiao, Y. Yang, Y. Tang, X. Yang, Z. Zhang, W. Lu, J. Yao, L. Huang, X. Liu and W. Zhou (2021). "Demographic and Clinical Features of Small-for-Gestational-Age Infants Born to Mothers With Gestational Diabetes Mellitus." Front Pediatr **9**: 741793.

Clausen, T. D., E. R. Mathiesen, T. Hansen, O. Pedersen, D. M. Jensen, J. Lauenborg and P. Damm (2008). "High prevalence of type 2 diabetes and pre-diabetes in adult offspring of women with gestational diabetes mellitus or type 1 diabetes: the role of intrauterine hyperglycemia." Diabetes Care **31**(2): 340-346.

Codner, E., P. M. Merino and M. Tena-Sempere (2012). "Female reproduction and type 1 diabetes: from mechanisms to clinical findings." Hum Reprod Update **18**(5): 568-585.

Comline, R. S., A. L. Fowden and M. Silver (1979). "Carbohydrate metabolism in the fetal pig during late gestation." Q J Exp Physiol Cogn Med Sci **64**(4): 277-289.

Correa, A., S. M. Gilboa, L. M. Besser, L. D. Botto, C. A. Moore, C. A. Hobbs, M. A. Cleves, T. J. Riehle-Colarusso, D. K. Waller and E. A. Reece (2008). "Diabetes mellitus and birth defects." Am J Obstet Gynecol **199**(3): 237 e231-239.

Correa, A., S. M. Gilboa, L. D. Botto, C. A. Moore, C. A. Hobbs, M. A. Cleves, T. J. Riehle-Colarusso, D. K. Waller, E. A. Reece and S. National Birth Defects Prevention (2012). "Lack of periconceptional vitamins or supplements that contain folic acid and diabetes mellitus-associated birth defects." Am J Obstet Gynecol **206**(3): 218 e211-213.

Corrigan, N., D. P. Brazil and F. McAuliffe (2009). "Fetal cardiac effects of maternal hyperglycemia during pregnancy." Birth Defects Res A Clin Mol Teratol **85**(6): 523-530.

Dabelea, D., R. L. Hanson, R. S. Lindsay, D. J. Pettitt, G. Imperatore, M. M. Gabir, J. Roumain, P. H. Bennett and W. C. Knowler (2000). "Intrauterine exposure to diabetes conveys risks for type 2 diabetes and obesity: a study of discordant sibships." Diabetes **49**(12): 2208-2211.

Dabelea, D., E. J. Mayer-Davis, A. P. Lamichhane, R. B. D'Agostino, Jr., A. D. Liese, K. S. Vehik, K. M. Narayan, P. Zeitler and R. F. Hamman (2008). "Association of intrauterine exposure to maternal diabetes and obesity with type 2 diabetes in youth: the SEARCH Case-Control Study." Diabetes Care **31**(7): 1422-1426.

Dai, C., Y. Hang, A. Shostak, G. Poffenberger, N. Hart, N. Prasad, N. Phillips, S. E. Levy, D. L. Greiner, L. D. Shultz, R. Bottino, S. K. Kim and A. C. Powers (2017). "Age-dependent human beta cell proliferation induced by glucagon-like peptide 1 and calcineurin signaling." J Clin Invest **127**(10): 3835-3844.

Damm, P., A. Houshmand-Oeregaard, L. Kelstrup, J. Lauenborg, E. R. Mathiesen and T. D. Clausen (2016). "Gestational diabetes mellitus and long-term consequences for mother and offspring: a view from Denmark." Diabetologia **59**(7): 1396-1399.

De Jesus, D. F. and R. N. Kulkarni (2014). "Epigenetic modifiers of islet function and mass." Trends Endocrinol Metab **25**(12): 628-636.

de Souza, E. G., C. C. Hara, D. L. Fagundes, A. A. de Queiroz, G. Morceli, I. M. Calderon, E. L. Franca and A. C. Honorio-Franca (2016). "Maternal-Foetal Diabetes Modifies Neonatal Fc Receptor Expression on Human Leucocytes." Scand J Immunol **84**(4): 237-244.

Dearden, L., S. G. Bouret and S. E. Ozanne (2018). "Sex and gender differences in developmental programming of metabolism." Mol Metab **15**: 8-19.

Del Prato, S., R. C. Bonadonna, E. Bonora, G. Gulli, A. Solini, M. Shank and R. A. DeFronzo (1993). "Characterization of cellular defects of insulin action in type 2

(non-insulin-dependent) diabetes mellitus." J Clin Invest **91**(2): 484-494.

Demirci, C., S. Ernst, J. C. Alvarez-Perez, T. Rosa, S. Valle, V. Shridhar, G. P. Casinelli, L. C. Alonso, R. C. Vasavada and A. Garcia-Ocana (2012). "Loss of HGF/c-Met signaling in pancreatic beta-cells leads to incomplete maternal beta-cell adaptation and gestational diabetes mellitus." Diabetes **61**(5): 1143-1152.

Desoye, G., H. H. Hofmann and P. A. Weiss (1992). "Insulin binding to trophoblast plasma membranes and placental glycogen content in well-controlled gestational diabetic women treated with diet or insulin, in well-controlled overt diabetic patients and in healthy control subjects." Diabetologia **35**(1): 45-55.

Diabetes, F. o. (2022). IDF Diabetes Atlas, 10th edn. Brussels, Belgium: International Diabetes Federation, 2021. International diabetes federation.

Dimitriadis, G. K., H. S. Randeve, S. Aftab, A. Ali, J. G. Hattersley, S. Pandey, D. K. Grammatopoulos, G. Valsamakis, G. Mastorakos, T. H. Jones and T. M. Barber (2018). "Metabolic phenotype of male obesity-related secondary hypogonadism pre-replacement and post-replacement therapy with intra-muscular testosterone undecanoate therapy." Endocrine **60**(1): 175-184.

Ding, G. L., F. F. Wang, J. Shu, S. Tian, Y. Jiang, D. Zhang, N. Wang, Q. Luo, Y. Zhang, F. Jin, P. C. Leung, J. Z. Sheng and H. F. Huang (2012). "Transgenerational glucose intolerance with Igf2/H19 epigenetic alterations in mouse islet induced by intrauterine hyperglycemia." Diabetes **61**(5): 1133-1142.

Dorner, G. and A. Plagemann (1994). "Perinatal hyperinsulinism as possible predisposing factor for diabetes mellitus, obesity and enhanced cardiovascular risk in later life." Horm Metab Res **26**(5): 213-221.

Dufrane, D. and P. Gianello (2012). "Pig islet for xenotransplantation in human: structural and physiological compatibility for human clinical application." Transplant Rev (Orlando) **26**(3): 183-188.

Dufrane, D., R. M. Goebbels, I. Fdilal, Y. Guiot and P. Gianello (2005). "Impact of porcine islet size on cellular structure and engraftment after transplantation: adult versus young pigs." Pancreas **30**(2): 138-147.

Dunn, G. A. and T. L. Bale (2009). "Maternal high-fat diet promotes body length increases and insulin insensitivity in second-generation mice." Endocrinology **150**(11): 4999-5009.

Dyer, J. S., C. R. Rosenfeld, J. Rice, M. Rice and D. S. Hardin (2007). "Insulin resistance in Hispanic large-for-gestational-age neonates at birth." J Clin Endocrinol Metab **92**(10): 3836-3843.

Eriksson, J., T. Forsen, J. Tuomilehto, C. Osmond and D. Barker (2000). "Fetal and childhood growth and hypertension in adult life." Hypertension **36**(5): 790-794.

Ezekwe, M. O. and R. J. Martin (1980). "The effects of maternal alloxan diabetes on body composition, liver enzymes and metabolism and serum metabolites and hormones of fetal pigs." Horm Metab Res **12**(4): 136-139.

Feng, Y., S. Yang, Y. Ma, X. Y. Bai and X. Chen (2015). "Role of Toll-like receptors in diabetic renal lesions in a miniature pig model." Sci Adv **1**(5): e1400183.

Fetita, L. S., E. Sobngwi, P. Serradas, F. Calvo and J. F. Gautier (2006). "Consequences of fetal exposure to maternal diabetes in offspring." J Clin Endocrinol Metab **91**(10): 3718-3724.

Fiorimanti, M. R., A. L. Cristofolini, M. J. Moreira-Espinoza, M. B. Rabaglino, C. G. Barbeito and C. I. Merkis (2022). "Placental vascularization in middle and late gestation in the pig." Reprod Fertil **3**(1): 57-66.

Ford, S. P., L. P. Reynolds and C. L. Ferrell (1984). "Blood flow, steroid secretion and nutrient uptake of the gravid uterus during the periparturient period in sows." J

Anim Sci **59**(4): 1085-1091.

Fowden, A. L., R. S. Comline and M. Silver (1982). "Pancreatic beta cell function in the fetal pig and sow." Q J Exp Physiol **67**(2): 225-233.

Fowden, A. L., A. J. Forhead, P. M. Coan and G. J. Burton (2008). "The placenta and intrauterine programming." J Neuroendocrinol **20**(4): 439-450.

Fowden, A. L., A. J. Forhead, M. Silver and A. A. MacDonald (1997). "Glucose, lactate and oxygen metabolism in the fetal pig during late gestation." Exp Physiol **82**(1): 171-182.

Franks, P. W., R. L. Hanson, W. C. Knowler, C. Moffett, G. Enos, A. M. Infante, J. Krakoff and H. C. Looker (2007). "Childhood predictors of young-onset type 2 diabetes." Diabetes **56**(12): 2964-2972.

Franks, P. W., H. C. Looker, S. Kobes, L. Touger, P. A. Tataranni, R. L. Hanson and W. C. Knowler (2006). "Gestational glucose tolerance and risk of type 2 diabetes in young Pima Indian offspring." Diabetes **55**(2): 460-465.

Friess, A. E., F. Sinowatz, R. Skolek-Winnisch and W. Trautner (1981). "The placenta of the pig. II. The ultrastructure of the areolae." Anat Embryol (Berl) **163**(1): 43-53.

Fu, J., Q. Cui, B. Yang, Y. Hou, H. Wang, Y. Xu, D. Wang, Q. Zhang and J. Pi (2017). "The impairment of glucose-stimulated insulin secretion in pancreatic beta-cells caused by prolonged glucotoxicity and lipotoxicity is associated with elevated adaptive antioxidant response." Food Chem Toxicol **100**: 161-167.

Fu, Z., E. R. Gilbert and D. Liu (2013). "Regulation of insulin synthesis and secretion and pancreatic Beta-cell dysfunction in diabetes." Curr Diabetes Rev **9**(1): 25-53.

Furukawa, S., Y. Kuroda and A. Sugiyama (2014). "A comparison of the histological structure of the placenta in experimental animals." J Toxicol Pathol **27**(1): 11-18.

Gannon, M., R. N. Kulkarni, H. M. Tse and F. Mauvais-Jarvis (2018). "Sex differences underlying pancreatic islet biology and its dysfunction." Mol Metab **15**: 82-91.

Gautier, J. F., L. S. Fetita, J. P. Riveline, F. Ibrahim, R. Porcher, C. Abi Khalil, G. Velho, S. P. Choukem, S. Hadjadj, E. Larger, R. Roussel, P. Boudou, M. Marre, E. Ravussin and F. Mauvais-Jarvis (2018). "Sex Difference In the Effect of Fetal Exposure to Maternal Diabetes on Insulin Secretion." J Endocr Soc **2**(5): 391-397.

Gayoso, A., R. Lopez, G. Xing, P. Boyeau, V. Valiollah Pour Amiri, J. Hong, K. Wu, M. Jayasuriya, E. Mehlman, M. Langevin, Y. Liu, J. Samaran, G. Misrachi, A. Nazaret, O. Clivio, C. Xu, T. Ashuach, M. Gabitto, M. Lotfollahi, V. Svensson, E. da Veiga Beltrame, V. Kleshchevnikov, C. Talavera-Lopez, L. Pachter, F. J. Theis, A. Streets, M. I. Jordan, J. Regier and N. Yosef (2022). "A Python library for probabilistic analysis of single-cell omics data." Nat Biotechnol **40**(2): 163-166.

Germain, P. L., A. Lun, C. Garcia Meixide, W. Macnair and M. D. Robinson (2021). "Doublet identification in single-cell sequencing data using scDblFinder." F1000Res **10**: 979.

Gerst, F., B. A. Jaghutriz, H. Staiger, A. M. Schulte, E. Lorza-Gil, G. Kaiser, M. Panse, S. Haug, M. Heni, M. Schutz, M. Stadion, A. Schurmann, F. Marzetta, M. Ibberson, B. Sipos, F. Fend, T. Fleming, P. P. Nawroth, A. Konigsrainer, S. Nadalin, S. Wagner, A. Peter, A. Fritsche, D. Richter, M. Solimena, H. U. Haring, S. Ullrich and R. Wagner (2018). "The Expression of Aldolase B in Islets Is Negatively Associated With Insulin Secretion in Humans." J Clin Endocrinol Metab **103**(12): 4373-4383.

Gilfillan, C. A., K. Y. Tserng and S. C. Kalhan (1985). "Alanine production by the human fetus at term gestation." Biol Neonate **47**(3): 141-147.

Graham, M. L. and H. J. Schuurman (2015). "Validity of animal models of type 1 diabetes, and strategies to enhance their utility in translational research." Eur J Pharmacol **759**: 221-230.

Grasemann, C., M. J. Devlin, P. A. Rzeczowska, R. Herrmann, B. Horsthemke, B. P. Hauffa, M. Grynopas, C. Alm, M. L. Bouxsein and M. R. Palmert (2012). "Parental diabetes: the Akita mouse as a model of the effects of maternal and paternal hyperglycemia in wildtype offspring." PLoS One **7**(11): e50210.

Greco, P., A. Vimercati, M. Scioscia, A. C. Rossi, F. Giorgino and L. Selvaggi (2003). "Timing of fetal growth acceleration in women with insulin-dependent diabetes." Fetal Diagn Ther **18**(6): 437-441.

Greene, M. F. (2001). "Diabetic embryopathy 2001: moving beyond the "diabetic milieu"." Teratology **63**(3): 116-118.

Group, H. S. C. R., B. E. Metzger, L. P. Lowe, A. R. Dyer, E. R. Trimble, U. Chaovarindr, D. R. Coustan, D. R. Hadden, D. R. McCance, M. Hod, H. D. McIntyre, J. J. Oats, B. Persson, M. S. Rogers and D. A. Sacks (2008). "Hyperglycemia and adverse pregnancy outcomes." N Engl J Med **358**(19): 1991-2002.

Grupe, K. and S. Scherneck (2023). "Mouse Models of Gestational Diabetes Mellitus and Its Subtypes: Recent Insights and Pitfalls." Int J Mol Sci **24**(6).

Grussner, R., R. Nakhleh, A. Grussner, G. Tomadze, P. Diem and D. Sutherland (1993). "Streptozotocin-induced diabetes mellitus in pigs." Horm Metab Res **25**(4): 199-203.

Gu, Z., R. Eils and M. Schlesner (2016). "Complex heatmaps reveal patterns and correlations in multidimensional genomic data." Bioinformatics **32**(18): 2847-2849.

Guo, S., C. Dai, M. Guo, B. Taylor, J. S. Harmon, M. Sander, R. P. Robertson, A. C. Powers and R. Stein (2013). "Inactivation of specific beta cell transcription factors in type 2 diabetes." J Clin Invest **123**(8): 3305-3316.

Hall, E., P. Volkov, T. Dayeh, J. L. Esguerra, S. Salo, L. Eliasson, T. Ronn, K. Bacos and C. Ling (2014). "Sex differences in the genome-wide DNA methylation pattern and impact on gene expression, microRNA levels and insulin secretion in human pancreatic islets." Genome Biol **15**(12): 522.

Hauguel, S., V. Desmazieres and J. C. Challier (1986). "Glucose uptake, utilization, and transfer by the human placenta as functions of maternal glucose concentration." Pediatr Res **20**(3): 269-273.

Hausman, G. J., T. R. Kasser and R. J. Martin (1982). "The effect of maternal diabetes and fasting on fetal adipose tissue histochemistry in the pig." J Anim Sci **55**(6): 1343-1350.

Hay, W. W., Jr. (1991). "Energy and substrate requirements of the placenta and fetus." Proc Nutr Soc **50**(2): 321-336.

Haythorne, E., M. Rohm, M. van de Bunt, M. F. Brereton, A. I. Tarasov, T. S. Blacker, G. Sachse, M. Silva Dos Santos, R. Terron Exposito, S. Davis, O. Baba, R. Fischer, M. R. Duchon, P. Rorsman, J. I. MacRae and F. M. Ashcroft (2019). "Diabetes causes marked inhibition of mitochondrial metabolism in pancreatic beta-cells." Nat Commun **10**(1): 2474.

Herbert, T. P. and D. R. Laybutt (2016). "A Reevaluation of the Role of the Unfolded Protein Response in Islet Dysfunction: Maladaptation or a Failure to Adapt?" Diabetes **65**(6): 1472-1480.

Hiden, U., A. Maier, M. Bilban, N. Ghaffari-Tabrizi, C. Wadsack, I. Lang, G. Dohr and G. Desoye (2006). "Insulin control of placental gene expression shifts from mother to foetus over the course of pregnancy." Diabetologia **49**(1): 123-131.

Hoang, D. T., H. Matsunari, M. Nagaya, H. Nagashima, J. M. Millis, P. Witkowski, V. Periwai, M. Hara and J. Jo (2014). "A conserved rule for pancreatic islet organization." PLoS One **9**(10): e110384.

Hollien, J. and J. S. Weissman (2006). "Decay of endoplasmic reticulum-localized mRNAs during the unfolded protein response." Science **313**(5783): 104-107.

Houde, A. A., J. St-Pierre, M. F. Hivert, J. P. Baillargeon, P. Perron, D. Gaudet, D. Brisson and L. Bouchard (2014). "Placental lipoprotein lipase DNA methylation levels are associated with gestational diabetes mellitus and maternal and cord blood lipid profiles." J Dev Orig Health Dis **5**(2): 132-141.

Hribal, M. L., I. Presta, T. Procopio, M. A. Marini, A. Stancakova, J. Kuusisto, F. Andreozzi, A. Hammarstedt, P. A. Jansson, N. Grarup, T. Hansen, M. Walker, N. Stefan, A. Fritsche, H. U. Haring, O. Pedersen, U. Smith, M. Laakso, G. Sesti and E. Consortium (2011). "Glucose tolerance, insulin sensitivity and insulin release in European non-diabetic carriers of a polymorphism upstream of CDKN2A and CDKN2B." Diabetologia **54**(4): 795-802.

Huang, H. H., S. Harrington and L. Stehno-Bittel (2018). "The Flaws and Future of Islet Volume Measurements." Cell Transplant **27**(7): 1017-1026.

Hulme, C. H., A. Nicolaou, S. A. Murphy, A. E. P. Heazell, J. E. Myers and M. Westwood (2019). "The effect of high glucose on lipid metabolism in the human placenta." Sci Rep **9**(1): 14114.

Illsley, N. P. (2000). "Glucose transporters in the human placenta." Placenta **21**(1): 14-22.

Illsley, N. P. and M. U. Baumann (2020). "Human placental glucose transport in fetoplacental growth and metabolism." Biochim Biophys Acta Mol Basis Dis **1866**(2): 165359.

Irving-Rodgers, H. F., F. J. Choong, K. Hummitzsch, C. R. Parish, R. J. Rodgers and C. J. Simeonovic (2014). "Pancreatic islet basement membrane loss and remodeling after mouse islet isolation and transplantation: impact for allograft rejection." Cell Transplant **23**(1): 59-72.

Johnson, G. A., H. Seo, F. W. Bazer, G. Wu, A. C. Kramer, B. A. McLendon and J. W. Cain (2023). "Metabolic pathways utilized by the porcine conceptus, uterus, and placenta." Mol Reprod Dev **90**(7): 673-683.

Jonas, J. C., A. Sharma, W. Hasenkamp, H. Ilkova, G. Patane, R. Laybutt, S. Bonner-Weir and G. C. Weir (1999). "Chronic hyperglycemia triggers loss of pancreatic beta cell differentiation in an animal model of diabetes." J Biol Chem **274**(20): 14112-14121.

Joshi, A., R. Azuma, R. Akumuo, L. Goetzl and S. E. Pinney (2020). "Gestational diabetes and maternal obesity are associated with sex-specific changes in miRNA and target gene expression in the fetus." Int J Obes (Lond) **44**(7): 1497-1507.

Jun, Y., J. Lee, S. Choi, J. H. Yang, M. Sander, S. Chung and S. H. Lee (2019). "In vivo-mimicking microfluidic perfusion culture of pancreatic islet spheroids." Sci Adv **5**(11): eaax4520.

Juonala, M., J. S. Viikari, T. Ronnemaa, J. Marniemi, A. Jula, B. M. Loo and O. T. Raitakari (2008). "Associations of dyslipidemias from childhood to adulthood with carotid intima-media thickness, elasticity, and brachial flow-mediated dilatation in adulthood: the Cardiovascular Risk in Young Finns Study." Arterioscler Thromb Vasc Biol **28**(5): 1012-1017.

Kalhan, S. and P. Parimi (2000). "Gluconeogenesis in the fetus and neonate." Semin Perinatol **24**(2): 94-106.

Kalhan, S. C., L. J. D'Angelo, S. M. Savin and P. A. Adam (1979). "Glucose production in pregnant women at term gestation. Sources of glucose for human fetus." J Clin Invest **63**(3): 388-394.

Karnik, S. K., H. Chen, G. W. McLean, J. J. Heit, X. Gu, A. Y. Zhang, M. Fontaine, M. H. Yen and S. K. Kim (2007). "Menin controls growth of pancreatic beta-cells in pregnant mice and promotes gestational diabetes mellitus." Science **318**(5851): 806-809.

Karunakaran, U., H. J. Kim, J. Y. Kim and I. K. Lee (2012). "Guards and culprits in the endoplasmic reticulum: glucolipotoxicity and beta-cell failure in type II diabetes." Exp Diabetes Res **2012**: 639762.

Kasser, T. R., R. J. Martin and C. E. Allen (1981). "Effect of gestational alloxan diabetes and fasting on fetal lipogenesis and lipid deposition in pigs." Biol Neonate **40**(3-4): 105-112.

Keely, E. J., J. C. Malcolm, S. Hadjiyannakis, I. Gaboury, G. Lough and M. L. Lawson (2008). "Prevalence of metabolic markers of insulin resistance in offspring of gestational diabetes pregnancies." Pediatr Diabetes **9**(1): 53-59.

Kelstrup, L., P. Damm, E. R. Mathiesen, T. Hansen, A. A. Vaag, O. Pedersen and T. D. Clausen (2013). "Insulin resistance and impaired pancreatic beta-cell function in adult offspring of women with diabetes in pregnancy." J Clin Endocrinol Metab **98**(9): 3793-3801.

Kemter, E., C. M. Cohrs, M. Schafer, M. Schuster, K. Steinmeyer, L. Wolf-van Buerck, A. Wolf, A. Wuensch, M. Kurome, B. Kessler, V. Zakhartchenko, M. Loehn, Y. Ivashchenko, J. Seissler, A. M. Schulte, S. Speier and E. Wolf (2017). "INS-eGFP transgenic pigs: a novel reporter system for studying maturation, growth and vascularisation of neonatal islet-like cell clusters." Diabetologia **60**(6): 1152-1156.

Kemter, E., A. Muller, M. Neukam, A. Ivanova, N. Klymiuk, S. Renner, K. Yang, J. Broichhagen, M. Kurome, V. Zakhartchenko, B. Kessler, K. P. Knoch, M. Bickle, B. Ludwig, K. Johnsson, H. Lickert, T. Kurth, E. Wolf and M. Solimena (2021). "Sequential in vivo labeling of insulin secretory granule pools in INS-SNAP transgenic pigs." Proc Natl Acad Sci U S A **118**(37).

Kervran, A., M. Guillaume and A. Jost (1978). "The endocrine pancreas of the fetus from diabetic pregnant rat." Diabetologia **15**(5): 387-393.

Khin, P. P., J. H. Lee and H. S. Jun (2021). "A Brief Review of the Mechanisms of beta-Cell Dedifferentiation in Type 2 Diabetes." Nutrients **13**(5).

Kilimnik, G., J. Jo, V. Periwal, M. C. Zielinski and M. Hara (2012). "Quantification of islet size and architecture." Islets **4**(2): 167-172.

Kim, A., K. Miller, J. Jo, G. Kilimnik, P. Wojcik and M. Hara (2009). "Islet architecture: A comparative study." Islets **1**(2): 129-136.

Kim, H., Y. Toyofuku, F. C. Lynn, E. Chak, T. Uchida, H. Mizukami, Y. Fujitani, R. Kawamori, T. Miyatsuka, Y. Kosaka, K. Yang, G. Honig, M. van der Hart, N. Kishimoto, J. Wang, S. Yagihashi, L. H. Tecott, H. Watada and M. S. German (2010). "Serotonin regulates pancreatic beta cell mass during pregnancy." Nat Med **16**(7): 804-808.

Kim, S., R. L. Whitener, H. Peiris, X. Gu, C. A. Chang, J. Y. Lam, J. Camunas-Soler, I. Park, R. J. Bevacqua, K. Tellez, S. R. Quake, J. R. T. Lakey, R. Bottino, P. J. Ross and S. K. Kim (2020). "Molecular and genetic regulation of pig pancreatic islet cell development." Development **147**(6).

King, A. J. (2012). "The use of animal models in diabetes research." Br J Pharmacol **166**(3): 877-894.

Kitamura, Y. I., T. Kitamura, J. P. Kruse, J. C. Raum, R. Stein, W. Gu and D. Accili (2005). "FoxO1 protects against pancreatic beta cell failure through NeuroD and MafA induction." Cell Metab **2**(3): 153-163.

Kitzmilller, J. L. and C. A. Combs (1996). "Diabetic nephropathy and pregnancy." Obstet Gynecol Clin North Am **23**(1): 173-203.

Kleinert, M., C. Clemmensen, S. M. Hofmann, M. C. Moore, S. Renner, S. C. Woods, P. Huypens, J. Beckers, M. H. de Angelis, A. Schurmann, M. Bakhti, M. Klingenspor, M. Heiman, A. D. Cherrington, M. Ristow, H. Lickert, E. Wolf, P. J. Havel, T. D. Muller and M. H. Tschop (2018). "Animal models of obesity and diabetes mellitus." Nat Rev Endocrinol **14**(3): 140-162.

Kliegman, R. M. and T. Gross (1985). "Perinatal problems of the obese mother and her infant." Obstet Gynecol **66**(3): 299-306.

Klymiuk, N., L. van Buerck, A. Bahr, M. Offers, B. Kessler, A. Wuensch, M. Kurome, M. Thormann, K. Lochner, H. Nagashima, N. Herbach, R. Wanke, J. Seissler and E. Wolf (2012). "Xenografted islet cell clusters from INSLEA29Y transgenic pigs rescue diabetes and prevent immune rejection in humanized mice." Diabetes **61**(6): 1527-1532.

Kokhanov, A. (2022). "Congenital Abnormalities in the Infant of a Diabetic Mother." Neoreviews **23**(5): e319-e327.

Koopmans, S. J., Z. Mroz, R. Dekker, H. Corbijn, M. Ackermans and H. Sauerwein (2006). "Association of insulin resistance with hyperglycemia in streptozotocin-diabetic pigs: effects of metformin at isoenergetic feeding in a type 2-like diabetic pig model." Metabolism **55**(7): 960-971.

Kupsco, A. and D. Schlenk (2015). "Oxidative stress, unfolded protein response, and apoptosis in developmental toxicity." Int Rev Cell Mol Biol **317**: 1-66.

Lager, S. and T. L. Powell (2012). "Regulation of nutrient transport across the placenta." J Pregnancy **2012**: 179827.

Lai, E., T. Teodoro and A. Volchuk (2007). "Endoplasmic reticulum stress: signaling the unfolded protein response." Physiology (Bethesda) **22**: 193-201.

Lampl, M. and P. Jeanty (2004). "Exposure to maternal diabetes is associated with

altered fetal growth patterns: A hypothesis regarding metabolic allocation to growth under hyperglycemic-hypoxemic conditions." Am J Hum Biol **16**(3): 237-263.

Lauridsen, C. (2020). "Effects of dietary fatty acids on gut health and function of pigs pre- and post-weaning." J Anim Sci **98**(4).

Lee, I. L., E. L. M. Barr, D. Longmore, F. Barzi, A. D. H. Brown, C. Connors, J. A. Boyle, M. Kirkwood, V. Hampton, M. Lynch, Z. X. Lu, K. O'Dea, J. Oats, H. D. McIntyre, P. Zimmet, J. E. Shaw, L. J. Maple-Brown and P. s. team (2020). "Cord blood metabolic markers are strong mediators of the effect of maternal adiposity on fetal growth in pregnancies across the glucose tolerance spectrum: the PANDORA study." Diabetologia **63**(3): 497-507.

LeMay-Nedjelski, L., J. Butcher, S. H. Ley, M. R. Asbury, A. J. Hanley, A. Kiss, S. Unger, J. K. Copeland, P. W. Wang, B. Zinman, A. Stintzi and D. L. O'Connor (2020). "Examining the relationship between maternal body size, gestational glucose tolerance status, mode of delivery and ethnicity on human milk microbiota at three months post-partum." BMC Microbiol **20**(1): 219.

Lembert, N., J. Wesche, P. Petersen, M. Doser, H. D. Becker and H. P. Ammon (2003). "Areal density measurement is a convenient method for the determination of porcine islet equivalents without counting and sizing individual islets." Cell Transplant **12**(1): 33-41.

Leng, J., J. Hay, G. Liu, J. Zhang, J. Wang, H. Liu, X. Yang and J. Liu (2016). "Small-for-gestational age and its association with maternal blood glucose, body mass index and stature: a perinatal cohort study among Chinese women." BMJ Open **6**(9): e010984.

LeRoith, D. and S. Yakar (2007). "Mechanisms of disease: metabolic effects of growth hormone and insulin-like growth factor 1." Nat Clin Pract Endocrinol Metab **3**(3): 302-310.

Lesseur, C., D. A. Armstrong, A. G. Paquette, Z. Li, J. F. Padbury and C. J. Marsit

(2014). "Maternal obesity and gestational diabetes are associated with placental leptin DNA methylation." Am J Obstet Gynecol **211**(6): 654 e651-659.

Lifson, N., C. V. Lassa and P. K. Dixit (1985). "Relation between blood flow and morphology in islet organ of rat pancreas." Am J Physiol **249**(1 Pt 1): E43-48.

Lin, J. Y., J. Cheng, Y. Q. Du, W. Pan, Z. Zhang, J. Wang, J. An, F. Yang, Y. F. Xu, H. Lin, W. T. An, J. Wang, Z. Yang, R. J. Chai, X. Y. Sha, H. L. Hu, J. P. Sun and X. Yu (2020). "In vitro expansion of pancreatic islet clusters facilitated by hormones and chemicals." Cell Discov **6**: 20.

Lindsay, R. S., D. Dabelea, J. Roumain, R. L. Hanson, P. H. Bennett and W. C. Knowler (2000). "Type 2 diabetes and low birth weight: the role of paternal inheritance in the association of low birth weight and diabetes." Diabetes **49**(3): 445-449.

Litten-Brown, J. C., A. M. Corson and L. Clarke (2010). "Porcine models for the metabolic syndrome, digestive and bone disorders: a general overview." Animal **4**(6): 899-920.

Liu, H., A. Javaheri, R. J. Godar, J. Murphy, X. Ma, N. Rohatgi, J. Mahadevan, K. Hyrc, P. Saftig, C. Marshall, M. L. McDaniel, M. S. Remedi, B. Razani, F. Urano and A. Diwan (2017). "Intermittent fasting preserves beta-cell mass in obesity-induced diabetes via the autophagy-lysosome pathway." Autophagy **13**(11): 1952-1968.

Lowe, W. L., Jr., D. M. Scholtens, A. Kuang, B. Linder, J. M. Lawrence, Y. Lebenthal, D. McCance, J. Hamilton, M. Nodzenski, O. Talbot, W. J. Brickman, P. Clayton, R. C. Ma, W. H. Tam, A. R. Dyer, P. M. Catalano, L. P. Lowe, B. E. Metzger and H. F.-u. S. C. R. Group (2019). "Hyperglycemia and Adverse Pregnancy Outcome Follow-up Study (HAPO FUS): Maternal Gestational Diabetes Mellitus and Childhood Glucose Metabolism." Diabetes Care **42**(3): 372-380.

Lucy, M. C. and T. J. Safranski (2017). "Heat stress in pregnant sows: Thermal

responses and subsequent performance of sows and their offspring." Mol Reprod Dev **84**(9): 946-956.

Ludwig, B., E. Wolf, U. Schonmann and S. Ludwig (2020). "Large Animal Models of Diabetes." Methods Mol Biol **2128**: 115-134.

Luecken, M. D. and F. J. Theis (2019). "Current best practices in single-cell RNA-seq analysis: a tutorial." Mol Syst Biol **15**(6): e8746.

Lun, A. T., K. Bach and J. C. Marioni (2016). "Pooling across cells to normalize single-cell RNA sequencing data with many zero counts." Genome Biol **17**: 75.

Lun, A. T. L., S. Riesenfeld, T. Andrews, T. P. Dao, T. Gomes, J. participants in the 1st Human Cell Atlas and J. C. Marioni (2019). "EmptyDrops: distinguishing cells from empty droplets in droplet-based single-cell RNA sequencing data." Genome Biol **20**(1): 63.

Ly, L. D., S. Xu, S. K. Choi, C. M. Ha, T. Thoudam, S. K. Cha, A. Wiederkehr, C. B. Wollheim, I. K. Lee and K. S. Park (2017). "Oxidative stress and calcium dysregulation by palmitate in type 2 diabetes." Exp Mol Med **49**(2): e291.

Ma, R. C., G. E. Tutino, K. A. Lillycrop, M. A. Hanson and W. H. Tam (2015). "Maternal diabetes, gestational diabetes and the role of epigenetics in their long term effects on offspring." Prog Biophys Mol Biol **118**(1-2): 55-68.

Mackenzie, R. W. and B. T. Elliott (2014). "Akt/PKB activation and insulin signaling: a novel insulin signaling pathway in the treatment of type 2 diabetes." Diabetes Metab Syndr Obes **7**: 55-64.

Mahizir, D., J. F. Briffa, D. H. Hryciw, G. D. Wadley, K. M. Moritz and M. E. Wlodek (2016). "Maternal obesity in females born small: Pregnancy complications and offspring disease risk." Mol Nutr Food Res **60**(1): 8-17.

Mandy, M. and M. Nyirenda (2018). "Developmental Origins of Health and Disease: the relevance to developing nations." Int Health **10**(2): 66-70.

Marchese, E., C. Rodeghier, R. S. Monson, B. McCracken, T. Shi, W. Schrock, J. Martellotto, J. Oberholzer and K. K. Danielson (2015). "Enumerating beta-Cells in Whole Human Islets: Sex Differences and Associations With Clinical Outcomes After Islet Transplantation." Diabetes Care **38**(11): e176-177.

Marciniak, A., C. M. Cohrs, V. Tsata, J. A. Chouinard, C. Selck, J. Stertmann, S. Reichelt, T. Rose, F. Eehalt, J. Weitz, M. Solimena, M. Slak Rupnik and S. Speier (2014). "Using pancreas tissue slices for in situ studies of islet of Langerhans and acinar cell biology." Nat Protoc **9**(12): 2809-2822.

Martinez-Frias, M. L. (1994). "Epidemiological analysis of outcomes of pregnancy in diabetic mothers: identification of the most characteristic and most frequent congenital anomalies." Am J Med Genet **51**(2): 108-113.

Mathew, D. J. (2020). "Glucose and Fructose Transport Across the Epitheliochorial Placenta: SLC2A and the Uterine-Placental Interface in Pigs." Endocrinology **161**(12).

Mauvais-Jarvis, F. (2015). "Sex differences in metabolic homeostasis, diabetes, and obesity." Biol Sex Differ **6**: 14.

Mauvais-Jarvis, F. (2016). "Androgen-deprivation therapy and pancreatic beta-cell dysfunction in men." J Diabetes Complications **30**(3): 389-390.

McGinnis, C. S., L. M. Murrow and Z. J. Gartner (2019). "DoubletFinder: Doublet Detection in Single-Cell RNA Sequencing Data Using Artificial Nearest Neighbors." Cell Syst **8**(4): 329-337 e324.

Meek, C. L., R. Corcoy, E. Asztalos, L. C. Kusinski, E. Lopez, D. S. Feig, H. R. Murphy and C. c. group (2021). "Which growth standards should be used to identify

large- and small-for-gestational age infants of mothers with type 1 diabetes? A pre-specified analysis of the CONCEPTT trial." BMC Pregnancy Childbirth **21**(1): 96.

Merino, B. and M. Garcia-Arevalo (2021). "Sexual hormones and diabetes: The impact of estradiol in pancreatic beta cell." Int Rev Cell Mol Biol **359**: 81-138.

Merkwitz, C., O. W. Blaschuk, A. Schulz, P. Lochhead, J. Meister, A. Ehrlich and A. M. Ricken (2013). "The ductal origin of structural and functional heterogeneity between pancreatic islets." Prog Histochem Cytochem **48**(3): 103-140.

Metzger, B. E., B. Persson, L. P. Lowe, A. R. Dyer, J. K. Cruickshank, C. Deerochanawong, H. L. Halliday, A. J. Hennis, H. Liley, P. C. Ng, D. R. Coustan, D. R. Hadden, M. Hod, J. J. Oats, E. R. Trimble and H. S. C. R. Group (2010). "Hyperglycemia and adverse pregnancy outcome study: neonatal glycemia." Pediatrics **126**(6): e1545-1552.

Mi, D., H. Fang, Y. Zhao and L. Zhong (2017). "Birth weight and type 2 diabetes: A meta-analysis." Exp Ther Med **14**(6): 5313-5320.

Miettinen, P. J., J. Ustinov, P. Ormio, R. Gao, J. Palgi, E. Hakonen, L. Juntti-Berggren, P. O. Berggren and T. Otonkoski (2006). "Downregulation of EGF receptor signaling in pancreatic islets causes diabetes due to impaired postnatal beta-cell growth." Diabetes **55**(12): 3299-3308.

Morgan, D., H. R. Oliveira-Emilio, D. Keane, A. E. Hirata, M. Santos da Rocha, S. Bordin, R. Curi, P. Newsholme and A. R. Carpinelli (2007). "Glucose, palmitate and pro-inflammatory cytokines modulate production and activity of a phagocyte-like NADPH oxidase in rat pancreatic islets and a clonal beta cell line." Diabetologia **50**(2): 359-369.

Morgan, S. C., F. Relaix, L. L. Sandell and M. R. Loeken (2008). "Oxidative stress during diabetic pregnancy disrupts cardiac neural crest migration and causes outflow tract defects." Birth Defects Res A Clin Mol Teratol **82**(6): 453-463.

Murakami, T., T. Fujita, T. Miyake, A. Ohtsuka, T. Taguchi and A. Kikuta (1993). "The insulo-acinar portal and insulo-venous drainage systems in the pancreas of the mouse, dog, monkey and certain other animals: a scanning electron microscopic study of corrosion casts." Arch Histol Cytol **56**(2): 127-147.

Murakami, T., S. Hitomi, A. Ohtsuka, T. Taguchi and T. Fujita (1997). "Pancreatic insulo-acinar portal systems in humans, rats, and some other mammals: scanning electron microscopy of vascular casts." Microsc Res Tech **37**(5-6): 478-488.

Murphy, S. L., J. Xu and K. D. Kochanek (2013). "Deaths: final data for 2010." Natl Vital Stat Rep **61**(4): 1-117.

Nagaya, M., A. Hayashi, K. Nakano, M. Honda, K. Hasegawa, K. Okamoto, S. Itazaki, H. Matsunari, M. Watanabe, K. Umeyama and H. Nagashima (2019). "Distributions of endocrine cell clusters during porcine pancreatic development." PLoS One **14**(5): e0216254.

Nasteska, D., N. H. F. Fine, F. B. Ashford, F. Cuzzo, K. Vilorio, G. Smith, A. Dahir, P. W. J. Dawson, Y. C. Lai, A. Bastidas-Ponce, M. Bakhti, G. A. Rutter, R. Fiancette, R. Nano, L. Piemonti, H. Lickert, Q. Zhou, I. Akerman and D. J. Hodson (2021). "PDX1(LOW) MAFA(LOW) beta-cells contribute to islet function and insulin release." Nat Commun **12**(1): 674.

Navarro, G., C. Allard, W. Xu and F. Mauvais-Jarvis (2015). "The role of androgens in metabolism, obesity, and diabetes in males and females." Obesity (Silver Spring) **23**(4): 713-719.

Neelankal John, A., G. Morahan and F. X. Jiang (2017). "Incomplete Re-Expression of Neuroendocrine Progenitor/Stem Cell Markers is a Key Feature of beta-Cell Dedifferentiation." J Neuroendocrinol **29**(1).

Negi, S., A. Jetha, R. Aikin, C. Hasilo, R. Sladek and S. Paraskevas (2012). "Analysis of beta-cell gene expression reveals inflammatory signaling and evidence of dedifferentiation following human islet isolation and culture." PLoS One **7**(1):

e30415.

Nicholas, L. M., M. Nagao, L. C. Kusinski, D. S. Fernandez-Twinn, L. Eliasson and S. E. Ozanne (2020). "Exposure to maternal obesity programs sex differences in pancreatic islets of the offspring in mice." Diabetologia **63**(2): 324-337.

Olmos-Ortiz, A., P. Flores-Espinosa, L. Diaz, P. Velazquez, C. Ramirez-Isarraraz and V. Zaga-Clavellina (2021). "Immunoendocrine Dysregulation during Gestational Diabetes Mellitus: The Central Role of the Placenta." Int J Mol Sci **22**(15).

Ornoy, A. (2011). "Prenatal origin of obesity and their complications: Gestational diabetes, maternal overweight and the paradoxical effects of fetal growth restriction and macrosomia." Reprod Toxicol **32**(2): 205-212.

Ornoy, A., A. Livshitz, Z. Ergaz, C. J. Stodgell and R. K. Miller (2011). "Hyperglycemia, hypoxia and their combination exert oxidative stress and changes in antioxidant gene expression: studies on cultured rat embryos." Birth Defects Res B Dev Reprod Toxicol **92**(3): 231-239.

Ornoy, A., M. A. Tsadok, P. Yaffe and S. W. Zangen (2009). "The Cohen diabetic rat as a model for fetal growth restriction: vitamins C and E reduce fetal oxidative stress but do not restore normal growth." Reprod Toxicol **28**(4): 521-529.

Ornoy, A., V. Zaken and R. Kohen (1999). "Role of reactive oxygen species (ROS) in the diabetes-induced anomalies in rat embryos in vitro: reduction in antioxidant enzymes and low-molecular-weight antioxidants (LMWA) may be the causative factor for increased anomalies." Teratology **60**(6): 376-386.

Osmond, D. T., C. J. Nolan, R. G. King, S. P. Brennecke and N. M. Gude (2000). "Effects of gestational diabetes on human placental glucose uptake, transfer, and utilisation." Diabetologia **43**(5): 576-582.

Otani, H., O. Tanaka, R. Tatewaki, H. Naora and T. Yoneyama (1991). "Diabetic environment and genetic predisposition as causes of congenital malformations in NOD mouse embryos." Diabetes **40**(10): 1245-1250.

Pani, L., M. Horal and M. R. Loeken (2002). "Polymorphic susceptibility to the molecular causes of neural tube defects during diabetic embryopathy." Diabetes **51**(9): 2871-2874.

Panzer, J. K., C. M. Cohrs and S. Speier (2020). "Using Pancreas Tissue Slices for the Study of Islet Physiology." Methods Mol Biol **2128**: 301-312.

Panzer, J. K., H. Hiller, C. M. Cohrs, J. Almaca, S. J. Enos, M. Beery, S. Cechin, D. M. Drotar, J. R. Weitz, J. Santini, M. K. Huber, M. Muhammad Fahd Qadir, R. L. Pastori, J. Dominguez-Bendala, E. A. Phelps, M. A. Atkinson, A. Pugliese, A. Caicedo, I. Kusmartseva and S. Speier (2020). "Pancreas tissue slices from organ donors enable in situ analysis of type 1 diabetes pathogenesis." JCI Insight **5**(8).

Papa, F. R. (2012). "Endoplasmic reticulum stress, pancreatic beta-cell degeneration, and diabetes." Cold Spring Harb Perspect Med **2**(9): a007666.

Park, S. Y., J. F. Gautier and S. Chon (2021). "Assessment of Insulin Secretion and Insulin Resistance in Human." Diabetes Metab J **45**(5): 641-654.

Pasek, R. C. and M. Gannon (2013). "Advancements and challenges in generating accurate animal models of gestational diabetes mellitus." Am J Physiol Endocrinol Metab **305**(11): E1327-1338.

Patel, S., A. Fraser, G. Davey Smith, R. S. Lindsay, N. Sattar, S. M. Nelson and D. A. Lawlor (2012). "Associations of gestational diabetes, existing diabetes, and glycosuria with offspring obesity and cardiometabolic outcomes." Diabetes Care **35**(1): 63-71.

Pedersen, J. (1954). "Weight and length at birth of infants of diabetic mothers."

Acta Endocrinol (Copenh) **16**(4): 330-342.

Peila, C., D. Gazzolo, E. Bertino, F. Cresi and A. Coscia (2020). "Influence of Diabetes during Pregnancy on Human Milk Composition." Nutrients **12**(1).

Pere, M. C. (1995). "Maternal and fetal blood levels of glucose, lactate, fructose, and insulin in the conscious pig." J Anim Sci **73**(10): 2994-2999.

Pere, M. C. (2001). "Effects of meal intake on materno-foetal exchanges of energetic substrates in the pig." Reprod Nutr Dev **41**(4): 285-296.

Pere, M. C. (2003). "Materno-foetal exchanges and utilisation of nutrients by the foetus: comparison between species." Reprod Nutr Dev **43**(1): 1-15.

Peters, T. M. and A. S. Brazeau (2019). "Exercise in Pregnant Women with Diabetes." Curr Diab Rep **19**(9): 80.

Petersen, M. B., S. A. Pedersen, G. Greisen, J. F. Pedersen and L. Molsted-Pedersen (1988). "Early growth delay in diabetic pregnancy: relation to psychomotor development at age 4." Br Med J (Clin Res Ed) **296**(6622): 598-600.

Petersen, M. C. and G. I. Shulman (2018). "Mechanisms of Insulin Action and Insulin Resistance." Physiol Rev **98**(4): 2133-2223.

Pettitt, D. J., K. A. Aleck, H. R. Baird, M. J. Carraher, P. H. Bennett and W. C. Knowler (1988). "Congenital susceptibility to NIDDM. Role of intrauterine environment." Diabetes **37**(5): 622-628.

Pettitt, D. J., W. C. Knowler, P. H. Bennett, K. A. Aleck and H. R. Baird (1987). "Obesity in offspring of diabetic Pima Indian women despite normal birth weight." Diabetes Care **10**(1): 76-80.

Plagemann, A., T. Harder, R. Kohlhoff, W. Rohde and G. Dorner (1997). "Glucose

tolerance and insulin secretion in children of mothers with pregestational IDDM or gestational diabetes." Diabetologia **40**(9): 1094-1100.

Plank, J. L., A. Y. Frist, A. W. LeGrone, M. A. Magnuson and P. A. Labosky (2011). "Loss of Foxd3 results in decreased beta-cell proliferation and glucose intolerance during pregnancy." Endocrinology **152**(12): 4589-4600.

Poitout, V., D. Hagman, R. Stein, I. Artner, R. P. Robertson and J. S. Harmon (2006). "Regulation of the insulin gene by glucose and fatty acids." J Nutr **136**(4): 873-876.

Powe, C. E. (2017). "Early Pregnancy Biochemical Predictors of Gestational Diabetes Mellitus." Curr Diab Rep **17**(2): 12.

Pullakhandam, R., R. Palika, S. Ghosh and G. B. Reddy (2012). "Contrasting effects of type 2 and type 1 diabetes on plasma RBP4 levels: the significance of transthyretin." IUBMB Life **64**(12): 975-982.

Rahier, J., J. Wallon, W. Gepts and J. Haot (1979). "Localization of pancreatic polypeptide cells in a limited lobe of the human neonate pancreas: remnant of the ventral primordium?" Cell Tissue Res **200**(3): 359-366.

Ramachandran, K., H. H. Huang and L. Stehno-Bittel (2015). "A Simple Method to Replace Islet Equivalents for Volume Quantification of Human Islets." Cell Transplant **24**(7): 1183-1194.

Ramsay, T. G., C. K. Wolverson and N. C. Steele (1994). "Alteration in IGF-I mRNA content of fetal swine tissues in response to maternal diabetes." Am J Physiol **267**(5 Pt 2): R1391-1396.

Reece, E. A. (2012). "Diabetes-induced birth defects: what do we know? What can we do?" Curr Diab Rep **12**(1): 24-32.

Reece, E. A., C. J. Homko, Y. K. Wu and A. Wiznitzer (1998). "The role of free radicals and membrane lipids in diabetes-induced congenital malformations." J Soc Gynecol Investig **5**(4): 178-187.

Reece, E. A., X. D. Ma, Y. K. Wu and D. Dhanasekaran (2002). "Aberrant patterns of cellular communication in diabetes-induced embryopathy. I. Membrane signalling." J Matern Fetal Neonatal Med **11**(4): 249-253.

Reece, E. A., E. Pinter, C. Z. Leranath, M. Garcia-Segura, M. K. Sanyal, J. C. Hobbins, M. J. Mahoney and F. Naftolin (1985). "Ultrastructural analysis of malformations of the embryonic neural axis induced by in vitro hyperglycemic conditions." Teratology **32**(3): 363-373.

Rees, D. A. and J. C. Alcolado (2005). "Animal models of diabetes mellitus." Diabet Med **22**(4): 359-370.

Renner, S., A. Blutke, S. Clauss, C. A. Deeg, E. Kemter, D. Merkus, R. Wanke and E. Wolf (2020). "Porcine models for studying complications and organ crosstalk in diabetes mellitus." Cell Tissue Res **380**(2): 341-378.

Renner, S., C. Braun-Reichhart, A. Blutke, N. Herbach, D. Emrich, E. Streckel, A. Wunsch, B. Kessler, M. Kurome, A. Bahr, N. Klymiuk, S. Krebs, O. Puk, H. Nagashima, J. Graw, H. Blum, R. Wanke and E. Wolf (2013). "Permanent neonatal diabetes in INS(C94Y) transgenic pigs." Diabetes **62**(5): 1505-1511.

Renner, S., B. Dobenecker, A. Blutke, S. Zols, R. Wanke, M. Ritzmann and E. Wolf (2016). "Comparative aspects of rodent and nonrodent animal models for mechanistic and translational diabetes research." Theriogenology **86**(1): 406-421.

Renner, S., A. S. Martins, E. Streckel, C. Braun-Reichhart, M. Backman, C. Prehn, N. Klymiuk, A. Bahr, A. Blutke, C. Landbrecht-Schessl, A. Wunsch, B. Kessler, M. Kurome, A. Hinrichs, S. J. Koopmans, S. Krebs, E. Kemter, B. Rathkolb, H. Nagashima, H. Blum, M. Ritzmann, R. Wanke, B. Aigner, J. Adamski, M. Hrabe de Angelis and E. Wolf (2019). "Mild maternal hyperglycemia in INS (C93S)

transgenic pigs causes impaired glucose tolerance and metabolic alterations in neonatal offspring." Dis Model Mech **12**(8).

Renner, S., A. S. Martins, E. Streckel, C. Braun-Reichhart, M. Backman, C. Prehn, N. Klymiuk, A. Bahr, A. Blutke, C. Landbrecht-Schessl, A. Wunsch, B. Kessler, M. Kurome, A. Hinrichs, S. J. Koopmans, S. Krebs, E. Kemter, B. Rathkolb, H. Nagashima, H. Blum, M. Ritzmann, R. Wanke, B. Aigner, J. Adamski, M. Hrabe de Angelis and E. Wolf (2019). "Mild maternal hyperglycemia in INS(C93S) transgenic pigs causes impaired glucose tolerance and metabolic alterations in neonatal offspring." Dis Model Mech **12**(8).

Reusens, B. and C. Remale (2001). "Intergenerational effect of an adverse intrauterine environment on perturbation of glucose metabolism." Twin Res **4**(5): 406-411.

Robertson, R. P., J. Harmon, P. O. Tran, Y. Tanaka and H. Takahashi (2003). "Glucose toxicity in beta-cells: type 2 diabetes, good radicals gone bad, and the glutathione connection." Diabetes **52**(3): 581-587.

Ruchat, S. M., A. A. Houde, G. Voisin, J. St-Pierre, P. Perron, J. P. Baillargeon, D. Gaudet, M. F. Hivert, D. Brisson and L. Bouchard (2013). "Gestational diabetes mellitus epigenetically affects genes predominantly involved in metabolic diseases." Epigenetics **8**(9): 935-943.

Ruiz-Palacios, M., A. J. Ruiz-Alcaraz, M. Sanchez-Campillo and E. Larque (2017). "Role of Insulin in Placental Transport of Nutrients in Gestational Diabetes Mellitus." Ann Nutr Metab **70**(1): 16-25.

Saito, K., N. Iwama and T. Takahashi (1978). "Morphometrical analysis on topographical difference in size distribution, number and volume of islets in the human pancreas." Tohoku J Exp Med **124**(2): 177-186.

Salbaum, J. M. and C. Kappen (2011). "Diabetic embryopathy: a role for the epigenome?" Birth Defects Res A Clin Mol Teratol **91**(8): 770-780.

Satija, R., J. A. Farrell, D. Gennert, A. F. Schier and A. Regev (2015). "Spatial reconstruction of single-cell gene expression data." Nat Biotechnol **33**(5): 495-502.

Satpathy, H. K., A. Fleming, D. Frey, M. Barsoom, C. Satpathy and J. Khandalavala (2008). "Maternal obesity and pregnancy." Postgrad Med **120**(3): E01-09.

Scholl, T. O., M. Sowers, X. Chen and C. Lenders (2001). "Maternal glucose concentration influences fetal growth, gestation, and pregnancy complications." Am J Epidemiol **154**(6): 514-520.

Schroder, M. and R. J. Kaufman (2005). "ER stress and the unfolded protein response." Mutat Res **569**(1-2): 29-63.

Schwarz, D. S. and M. D. Blower (2016). "The endoplasmic reticulum: structure, function and response to cellular signaling." Cell Mol Life Sci **73**(1): 79-94.

Sellers, E. A., H. J. Dean, L. A. Shafer, P. J. Martens, W. Phillips-Beck, M. Heaman, H. J. Prior, A. B. Dart, J. McGavock, M. Morris, A. A. Torshizi, S. Ludwig and G. X. Shen (2016). "Exposure to Gestational Diabetes Mellitus: Impact on the Development of Early-Onset Type 2 Diabetes in Canadian First Nations and Non-First Nations Offspring." Diabetes Care **39**(12): 2240-2246.

Sferruzzi-Perri, A. N., J. A. Owens, K. G. Pringle and C. T. Roberts (2011). "The neglected role of insulin-like growth factors in the maternal circulation regulating fetal growth." J Physiol **589**(Pt 1): 7-20.

Shao, H., Y. Lan, Y. Qian, R. Chen, L. Peng, Y. Hua and X. Wang (2022). "Effect of later cord clamping on umbilical cord blood gas in term neonates of diabetic mothers: a randomized clinical trial." BMC Pediatr **22**(1): 111.

Shashikadze, B., F. Flenkenthaler, J. B. Stockl, L. Valla, S. Renner, E. Kemter, E. Wolf and T. Frohlich (2021). "Developmental Effects of (Pre-)Gestational Diabetes on Offspring: Systematic Screening Using Omics Approaches." Genes (Basel)

12(12).

Shashikadze, B., L. Valla, S. D. Lombardo, C. Prehn, M. Haid, F. Riols, J. B. Stockl, R. Elkhateib, S. Renner, B. Rathkolb, J. Menche, M. Hrabe de Angelis, E. Wolf, E. Kemter and T. Frohlich (2023). "Maternal hyperglycemia induces alterations in hepatic amino acid, glucose and lipid metabolism of neonatal offspring: Multi-omics insights from a diabetic pig model." Mol Metab **75**: 101768.

Sheffield, J. S., E. L. Butler-Koster, B. M. Casey, D. D. McIntire and K. J. Leveno (2002). "Maternal diabetes mellitus and infant malformations." Obstet Gynecol **100**(5 Pt 1): 925-930.

Sibiak, R., K. Ozegowska, E. Wender-Ozegowska, P. Gutaj, P. Mozdziak and B. Kempisty (2022). "Fetomaternal Expression of Glucose Transporters (GLUTs)-Biochemical, Cellular and Clinical Aspects." Nutrients **14**(10).

Silverman, B. L., B. E. Metzger, N. H. Cho and C. A. Loeb (1995). "Impaired glucose tolerance in adolescent offspring of diabetic mothers. Relationship to fetal hyperinsulinism." Diabetes Care **18**(5): 611-617.

Soltesz, G., D. Harris, I. Z. Mackenzie and A. Aynsley-Green (1985). "The metabolic and endocrine milieu of the human fetus and mother at 18-21 weeks of gestation. I. Plasma amino acid concentrations." Pediatr Res **19**(1): 91-93.

Steel, J. M., S. D. Johnstone and J. E. Corrie (1984). "Early assessment of gestation in diabetics." Lancet **2**(8409): 975-976.

Steinberg, M. S. (1963). "Reconstruction of tissues by dissociated cells. Some morphogenetic tissue movements and the sorting out of embryonic cells may have a common explanation." Science **141**(3579): 401-408.

Steinberg, M. S. (2007). "Differential adhesion in morphogenesis: a modern view." Curr Opin Genet Dev **17**(4): 281-286.

Supale, S., N. Li, T. Brun and P. Maechler (2012). "Mitochondrial dysfunction in pancreatic beta cells." Trends Endocrinol Metab **23**(9): 477-487.

Supek, F., M. Bosnjak, N. Skunca and T. Smuc (2011). "REVIGO summarizes and visualizes long lists of gene ontology terms." PLoS One **6**(7): e21800.

Szklarczyk, D., J. H. Morris, H. Cook, M. Kuhn, S. Wyder, M. Simonovic, A. Santos, N. T. Doncheva, A. Roth, P. Bork, L. J. Jensen and C. von Mering (2017). "The STRING database in 2017: quality-controlled protein-protein association networks, made broadly accessible." Nucleic Acids Res **45**(D1): D362-D368.

Szlapinski, S. K., R. T. King, G. Retta, E. Yeo, B. J. Strutt and D. J. Hill (2019). "A mouse model of gestational glucose intolerance through exposure to a low protein diet during fetal and neonatal development." J Physiol **597**(16): 4237-4250.

Tabelow, K., J. D. Clayden, P. L. de Micheaux, J. Polzehl, V. J. Schmid and B. Whitcher (2011). "Image analysis and statistical inference in neuroimaging with R." Neuroimage **55**(4): 1686-1693.

Talchai, C., S. Xuan, H. V. Lin, L. Sussel and D. Accili (2012). "Pancreatic beta cell dedifferentiation as a mechanism of diabetic beta cell failure." Cell **150**(6): 1223-1234.

Taricco, E., T. Radaelli, G. Rossi, M. S. Nobile de Santis, G. P. Bulfamante, L. Avagliano and I. Cetin (2009). "Effects of gestational diabetes on fetal oxygen and glucose levels in vivo." BJOG **116**(13): 1729-1735.

Tarry-Adkins, J. L. and S. E. Ozanne (2011). "Mechanisms of early life programming: current knowledge and future directions." Am J Clin Nutr **94**(6 Suppl): 1765S-1771S.

Tellez, N., M. Vilaseca, Y. Marti, A. Pla and E. Montanya (2016). "beta-Cell dedifferentiation, reduced duct cell plasticity, and impaired beta-cell mass

regeneration in middle-aged rats." Am J Physiol Endocrinol Metab **311**(3): E554-563.

Teraoku, H. and S. Lenzen (2017). "Dynamics of Insulin Secretion from EndoC-betaH1 beta-Cell Pseudoislets in Response to Glucose and Other Nutrient and Nonnutrient Secretagogues." J Diabetes Res **2017**: 2309630.

Thomas, F., B. Balkau, F. Vauzelle-Kervroedan and L. Papoz (1994). "Maternal effect and familial aggregation in NIDDM. The CODIAB Study. CODIAB-INSERM-ZENECA Study Group." Diabetes **43**(1): 63-67.

Thong, E. P., E. Codner, J. S. E. Laven and H. Teede (2020). "Diabetes: a metabolic and reproductive disorder in women." Lancet Diabetes Endocrinol **8**(2): 134-149.

Thorburn, A. W., B. Gumbiner, F. Bulacan, P. Wallace and R. R. Henry (1990). "Intracellular glucose oxidation and glycogen synthase activity are reduced in non-insulin-dependent (type II) diabetes independent of impaired glucose uptake." J Clin Invest **85**(2): 522-529.

Tobin, J. D., J. F. Roux and J. S. Soeldner (1969). "Human fetal insulin response after acute maternal glucose administration during labor." Pediatrics **44**(5): 668-671.

Tritschler, S., M. Thomas, A. Bottcher, B. Ludwig, J. Schmid, U. Schubert, E. Kemter, E. Wolf, H. Lickert and F. J. Theis (2022). "A transcriptional cross species map of pancreatic islet cells." Mol Metab **66**: 101595.

Tyanova, S., T. Temu and J. Cox (2016). "The MaxQuant computational platform for mass spectrometry-based shotgun proteomics." Nat Protoc **11**(12): 2301-2319.

Vaiserman, A. and O. Lushchak (2019). "Developmental origins of type 2 diabetes: Focus on epigenetics." Ageing Res Rev **55**: 100957.

Walani, S. R. and J. Biermann (2017). "March of Dimes Foundation: leading the way to birth defects prevention." Public Health Rev **38**: 12.

Wang, Q., J. Jokelainen, J. Auvinen, K. Puukka, S. Keinanen-Kiukaanniemi, M. R. Jarvelin, J. Kettunen, V. P. Makinen and M. Ala-Korpela (2019). "Insulin resistance and systemic metabolic changes in oral glucose tolerance test in 5340 individuals: an interventional study." BMC Med **17**(1): 217.

Wang, Q., A. M. Ratchford, M. M. Chi, E. Schoeller, A. Frolova, T. Schedl and K. H. Moley (2009). "Maternal diabetes causes mitochondrial dysfunction and meiotic defects in murine oocytes." Mol Endocrinol **23**(10): 1603-1612.

Wang, X., R. Misawa, M. C. Zielinski, P. Cowen, J. Jo, V. Periwai, C. Ricordi, A. Khan, J. Szust, J. Shen, J. M. Millis, P. Witkowski and M. Hara (2013). "Regional differences in islet distribution in the human pancreas--preferential beta-cell loss in the head region in patients with type 2 diabetes." PLoS One **8**(6): e67454.

Wang, Y., K. K. Danielson, A. Ropski, T. Harvat, B. Barbaro, D. Paushter, M. Qi and J. Oberholzer (2013). "Systematic analysis of donor and isolation factor's impact on human islet yield and size distribution." Cell Transplant **22**(12): 2323-2333.

Wang, Z., N. W. York, C. G. Nichols and M. S. Remedi (2014). "Pancreatic beta cell dedifferentiation in diabetes and redifferentiation following insulin therapy." Cell Metab **19**(5): 872-882.

Wawrusiewicz-Kurylonek, N., B. Telejko, M. Kuzmicki, A. Sobota, D. Lipinska, J. Pliszka, B. Raczkowska, P. Kuc, R. Urban, J. Szamatowicz, A. Kretowski, P. Laudanski and M. Gorska (2015). "Increased Maternal and Cord Blood Betatrophin in Gestational Diabetes." PLoS One **10**(6): e0131171.

Whaley, W. H., F. P. Zuspan and G. H. Nelson (1966). "Correlation between maternal and fetal plasma levels of glucose and free fatty acids." Am J Obstet Gynecol **94**(3): 419-421.

Whitticar, N. B., E. W. Strahler, P. Rajan, S. Kaya and C. S. Nunemaker (2016). "An Automated Perifusion System for Modifying Cell Culture Conditions over Time." Biol Proced Online **18**: 19.

Wilson, J. D., D. P. Dhall, C. J. Simeonovic and K. J. Lafferty (1986). "Induction and management of diabetes mellitus in the pig." Aust J Exp Biol Med Sci **64 (Pt 6)**: 489-500.

Wittert, G. and M. Grossmann (2022). "Obesity, type 2 diabetes, and testosterone in ageing men." Rev Endocr Metab Disord **23(6)**: 1233-1242.

Wolf, E., C. Braun-Reichhart, E. Streckel and S. Renner (2014). "Genetically engineered pig models for diabetes research." Transgenic Res **23(1)**: 27-38.

Wolf, F. A., P. Angerer and F. J. Theis (2018). "SCANPY: large-scale single-cell gene expression data analysis." Genome Biol **19(1)**: 15.

Wolock, S. L., R. Lopez and A. M. Klein (2019). "Scrublet: Computational Identification of Cell Doublets in Single-Cell Transcriptomic Data." Cell Syst **8(4)**: 281-291 e289.

Wright, E. C., J. R. Miles, C. A. Lents and L. A. Rempel (2016). "Uterine and placenta characteristics during early vascular development in the pig from day 22 to 42 of gestation." Anim Reprod Sci **164**: 14-22.

Wu, L., W. Nicholson, S. M. Knobel, R. J. Steffner, J. M. May, D. W. Piston and A. C. Powers (2004). "Oxidative stress is a mediator of glucose toxicity in insulin-secreting pancreatic islet cell lines." J Biol Chem **279(13)**: 12126-12134.

Wu, Y., B. Liu, Y. Sun, Y. Du, M. K. Santillan, D. A. Santillan, L. G. Snetselaar and W. Bao (2020). "Association of Maternal Prepregnancy Diabetes and Gestational Diabetes Mellitus With Congenital Anomalies of the Newborn." Diabetes Care **43(12)**: 2983-2990.

Yang, P., Z. Zhao and E. A. Reece (2007). "Involvement of c-Jun N-terminal kinases activation in diabetic embryopathy." Biochem Biophys Res Commun **357**(3): 749-754.

Yang, X., J. Leng, H. Liu, L. Wang, W. Li, W. Li, X. Yang, M. Liu and G. Hu (2021). "Maternal gestational diabetes and childhood hyperlipidemia." Diabet Med **38**(11): e14606.

Yeap, B. B. and G. A. Wittert (2022). "Testosterone, Diabetes Risk, and Diabetes Prevention in Men." Endocrinol Metab Clin North Am **51**(1): 157-172.

Yoshioka, M., T. Kayo, T. Ikeda and A. Koizumi (1997). "A novel locus, Mody4, distal to D7Mit189 on chromosome 7 determines early-onset NIDDM in nonobese C57BL/6 (Akita) mutant mice." Diabetes **46**(5): 887-894.

Young, T. K., P. J. Martens, S. P. Taback, E. A. Sellers, H. J. Dean, M. Cheang and B. Flett (2002). "Type 2 diabetes mellitus in children: prenatal and early infancy risk factors among native Canadians." Arch Pediatr Adolesc Med **156**(7): 651-655.

Yuksel, M. A., M. Oncul, A. Tuten, M. Imamoglu, A. S. Acikgoz, M. Kucur and R. Madazli (2014). "Maternal serum and fetal cord blood irisin levels in gestational diabetes mellitus." Diabetes Res Clin Pract **104**(1): 171-175.

Zangen, S. W., S. Ryu and A. Ornoy (2006). "Alterations in the expression of antioxidant genes and the levels of transcription factor NF-kappa B in relation to diabetic embryopathy in the Cohen diabetic rat model." Birth Defects Res A Clin Mol Teratol **76**(2): 107-114.

Zappia, L. and A. Oshlack (2018). "Clustering trees: a visualization for evaluating clusterings at multiple resolutions." Gigascience **7**(7).

Zhang, C., T. Moriguchi, M. Kajihara, R. Esaki, A. Harada, H. Shimohata, H. Oishi, M. Hamada, N. Morito, K. Hasegawa, T. Kudo, J. D. Engel, M. Yamamoto and S.

Takahashi (2005). "MafA is a key regulator of glucose-stimulated insulin secretion." Mol Cell Biol **25**(12): 4969-4976.

Zhang, C. and S. Rawal (2017). "Dietary iron intake, iron status, and gestational diabetes." Am J Clin Nutr **106**(Suppl 6): 1672S-1680S.

Zhang, T., D. H. Kim, X. Xiao, S. Lee, Z. Gong, R. Muzumdar, V. Calabuig-Navarro, J. Yamauchi, H. Harashima, R. Wang, R. Bottino, J. C. Alvarez-Perez, A. Garcia-Ocana, G. Gittes and H. H. Dong (2016). "FoxO1 Plays an Important Role in Regulating beta-Cell Compensation for Insulin Resistance in Male Mice." Endocrinology **157**(3): 1055-1070.

Zhao, Z., P. Yang, R. L. Eckert and E. A. Reece (2009). "Caspase-8: a key role in the pathogenesis of diabetic embryopathy." Birth Defects Res B Dev Reprod Toxicol **86**(1): 72-77.

Zhu, H., S. S. Luo, Y. Cheng, Y. S. Yan, K. X. Zou, G. L. Ding, L. Jin and H. F. Huang (2021). "Intrauterine Hyperglycemia Alters the Metabolomic Profile in Fetal Mouse Pancreas in a Gender-Specific Manner." Front Endocrinol (Lausanne) **12**: 710221.

Zhu, Z., X. Chen, Y. Xiao, J. Wen, J. Chen, K. Wang and G. Chen (2019). "Gestational diabetes mellitus alters DNA methylation profiles in pancreas of the offspring mice." J Diabetes Complications **33**(1): 15-22.

X. INDEX OF FIGURES

| | |
|---|-----|
| Figure 1: Methods used in this work..... | 40 |
| Figure 2: Piglet's pancreas anatomy..... | 46 |
| Figure 3: Pancreas assessment for vibratome cutting..... | 52 |
| Figure 4: Preparation and mounting of the chambers using the pancreatic tissue slices..... | 54 |
| Figure 5: Body weight and organ weight..... | 64 |
| Figure 6: Oral glucose tolerance test (OGTT)..... | 67 |
| Figure 7: <i>In situ</i> GSIS on pancreatic tissue slices..... | 72 |
| Figure 8: Pre-ranked enrichment analysis using STRING with gene sets according to gene ontology (GO) biological process databases..... | 73 |
| Figure 9: Quantitative proteome analysis of spleen side pancreas from hyperglycemia exposed and WT piglets..... | 74 |
| Figure 10: Quantitative proteome analysis of duodenum side pancreas tissue from hyperglycemia exposed and WT piglets..... | 75 |
| Figure 11: Distribution of cell type..... | 76 |
| Figure 12: Distribution based on PHG and PNG group that shows a good separation between the two group and the cells type % in the group..... | 76 |
| Figure 13: Volcano plot showing the upregulated and downregulated genes expressed in PHG vs. PNG..... | 77 |
| Figure 14: Key genes for the assessment of expression pattern..... | 78 |
| Figure 15: Dot-Plot visualization; β -cell signature markers..... | 78 |
| Figure 16: Dot-Plot visualization; β -cell growth factors..... | 79 |
| Figure 17: Dot-Plot visualization; Insulin synthesis genes..... | 79 |
| Figure 18: Dot-Plot visualization; Insulin secretion genes..... | 80 |
| Figure 19: Dot-Plot visualization; ER stress genes..... | 80 |
| Figure 20: Bar diagrams show the percentage of the number of apoptotic and not-apoptotic cells in the PNG vs. PHG..... | 80 |
| Figure 21: Representative image of 2-hormonal staining on pancreatic paraffin slides in the PNG vs. PHG..... | 82 |
| Figure 22: Relative distribution n of islets size..... | 83 |
| Figure 23: Schematic representation underlying mechanism of offspring β -cell dedifferentiation when exposed to maternal diabetes..... | 100 |

XI. INDEX OF TABLES

| | |
|--|-----|
| Table 1: Clinical-chemical parameters..... | 41 |
| Table 2: primer sequence for the PCR reaction..... | 43 |
| Table 3: Master mix components per PCR reaction..... | 43 |
| Table 4: PCR reaction conditions for <i>INS^{C94Y}</i> | 44 |
| Table 5: PCR reaction conditions for <i>INSeGFP</i> and NEO..... | 44 |
| Table 6: Organ list collected during the dissection..... | 47 |
| Table 7: Deparaffinization and rehydration of paraffin sections..... | 48 |
| Table 8: Abs list for the proliferation markers staining..... | 49 |
| Table 9: Pregnancy rate..... | 62 |
| Table 10: PHG piglets' born from diabetic mothers exhibiting malformations.... | 63 |
| Table 11: percentage of the absolute and relative organs weight of the PHG piglets compared to PNG group..... | 65 |
| Table 12: Clinical-chemical parameters in blood serum of neonatal piglets developed in mothers with normal (PNG) or high (PHG) blood glucose levels.... | 68 |
| Table 13: Clinical-chemical parameters in blood serum of sows during the delivery..... | 70 |
| Table 14: Endocrine clusters splenic part..... | 82 |
| Table 15: Proteome results pancreas spleen..... | 148 |
| Table 16: Proteome results pancreas duodenal..... | 150 |
| Table 17: First 100 genes upregulated in the PHG vs.PNG..... | 151 |
| Table 18: First 100 genes downregulated in the PHG vs.PNG..... | 153 |

XII. ANNEX

Proteomic list of the significantly increased or decreased proteins in pancreas splenic part and duodenal part.

Table 15: Pancreas spleen

| Gene | Protein accession | l2fc | P value | FDR | Sign. | Abundance change |
|--------------|-------------------|-------|---------|-------|-------|------------------|
| SST | NP_001009583 | 1.35 | 9E-08 | 3E-06 | + | Increase |
| LOC100515185 | XP_003122092 | 1.28 | 1E-04 | 2E-03 | + | Increase |
| HMGGA2 | XP_005664014 | 1.26 | 2E-05 | 4E-04 | + | Increase |
| AGR2 | XP_005667717 | 1.04 | 1E-04 | 2E-03 | + | Increase |
| LOC100515741 | XP_013853463 | 0.97 | 2E-16 | 2E-14 | + | Increase |
| LOC110255172 | XP_020922490 | 0.94 | 1E-08 | 4E-07 | + | Increase |
| CDK3 | XP_003131249 | 0.92 | 3E-04 | 3E-03 | + | Increase |
| CD36 | XP_020957938 | 0.90 | 1E-05 | 3E-04 | + | Increase |
| FABP4 | NP_001002817 | 0.85 | 0E+00 | 0E+00 | + | Increase |
| SERPINA3-2 | NP_998952 | 0.82 | 3E-03 | 2E-02 | + | Increase |
| INS | NP_001103242 | 0.81 | 3E-07 | 8E-06 | + | Increase |
| CTRL | XP_020949776 | 0.80 | 2E-10 | 8E-09 | + | Increase |
| GSTA1 | NP_999554 | 0.76 | 9E-04 | 9E-03 | + | Increase |
| MAPRE2 | XP_020951924 | 0.74 | 5E-03 | 3E-02 | + | Increase |
| LOC102167522 | XP_020940820 | 0.71 | 2E-04 | 3E-03 | + | Increase |
| PSAT1 | XP_020920809 | 0.71 | 8E-14 | 7E-12 | + | Increase |
| ACADSB | XP_001926332 | 0.68 | 0E+00 | 0E+00 | + | Increase |
| SYCN | XP_003355940 | 0.67 | 4E-03 | 3E-02 | + | Increase |
| STAT5A | XP_020921906 | 0.66 | 5E-03 | 4E-02 | + | Increase |
| MECR | NP_001231011 | 0.66 | 5E-03 | 3E-02 | + | Increase |
| NME4 | XP_020941258 | 0.65 | 3E-03 | 2E-02 | + | Increase |
| PCK2 | NP_001155225 | 0.63 | 0E+00 | 0E+00 | + | Increase |
| BPHL | NP_001230414 | 0.62 | 3E-10 | 2E-08 | + | Increase |
| COL4A2 | XP_020921568 | 0.61 | 1E-04 | 1E-03 | + | Increase |
| HERPUD1 | XP_020949558 | 0.61 | 1E-04 | 2E-03 | + | Increase |
| LOC110261434 | XP_020953497 | 0.61 | 4E-10 | 2E-08 | + | Increase |
| ACADL | NP_999062 | 0.61 | 7E-05 | 1E-03 | + | Increase |
| NCCRP1 | XP_020950022 | -0.59 | 2E-13 | 1E-11 | + | decrease |

| | | | | | | |
|---------------------|--------------|-------|-------|-------|---|----------|
| RPL18A | XP_020939193 | -0.63 | 6E-03 | 4E-02 | + | decrease |
| ENO3 | NP_001037992 | -0.63 | 1E-04 | 2E-03 | + | decrease |
| TMED5 | NP_001230624 | -0.63 | 1E-03 | 1E-02 | + | decrease |
| GCG | XP_005671940 | -0.63 | 0E+00 | 0E+00 | + | decrease |
| SNRPD1 | XP_020951826 | -0.64 | 5E-05 | 8E-04 | + | decrease |
| CBR1 | NP_999238 | -0.64 | 0E+00 | 0E+00 | + | decrease |
| APOC3 | XP_020957907 | -0.67 | 5E-05 | 8E-04 | + | decrease |
| SYNPO2 | XP_020956358 | -0.67 | 6E-04 | 6E-03 | + | decrease |
| HSPB1 | NP_001007519 | -0.70 | 0E+00 | 0E+00 | + | decrease |
| ORM1 | XP_005660429 | -0.72 | 0E+00 | 0E+00 | + | decrease |
| LOC106504545 | XP_020955331 | -0.72 | 3E-04 | 4E-03 | + | decrease |
| PNLIP | NP_001171383 | -0.72 | 2E-13 | 2E-11 | + | decrease |
| LOC100521789 | XP_020945783 | -0.75 | 0E+00 | 0E+00 | + | decrease |
| SPINK1 | XP_003354394 | -0.78 | 5E-09 | 2E-07 | + | decrease |
| RPL35 | NP_999491 | -0.85 | 9E-04 | 9E-03 | + | decrease |
| JCHAIN | XP_003357009 | -0.87 | 1E-03 | 1E-02 | + | decrease |
| RPL34 | XP_013834419 | -0.88 | 3E-06 | 7E-05 | + | decrease |
| ADA | XP_020933637 | -0.89 | 3E-06 | 7E-05 | + | decrease |
| PLS3 | XP_001925971 | -0.89 | 8E-05 | 1E-03 | + | decrease |
| CAND2 | XP_020925016 | -0.92 | 1E-03 | 1E-02 | + | decrease |
| RPL18 | XP_020950359 | -0.94 | 2E-08 | 7E-07 | + | decrease |
| RPL6 | NP_001038007 | -0.97 | 0E+00 | 0E+00 | + | decrease |
| PDIA2 | XP_020942596 | -1.01 | 8E-04 | 8E-03 | + | decrease |
| RPL4 | XP_005659919 | -1.02 | 0E+00 | 0E+00 | + | decrease |
| RPL19 | XP_003131557 | -1.02 | 4E-07 | 1E-05 | + | decrease |
| RPL24 | XP_003132745 | -1.03 | 8E-05 | 1E-03 | + | decrease |
| RPL8 | XP_005655354 | -1.08 | 7E-16 | 7E-14 | + | decrease |
| SORT1 | XP_013852742 | -1.12 | 5E-04 | 5E-03 | + | decrease |
| TDH | XP_020927752 | -1.15 | 3E-07 | 1E-05 | + | decrease |
| RPL14 | XP_020923829 | -1.16 | 4E-05 | 7E-04 | + | decrease |
| SYCP2 | XP_020933812 | -1.17 | 6E-05 | 9E-04 | + | decrease |
| SDSL | XP_020928520 | -1.22 | 3E-04 | 3E-03 | + | decrease |
| PNLIPRP2 | NP_001177220 | -1.26 | 0E+00 | 0E+00 | + | decrease |
| RPL7A | XP_020926795 | -1.32 | 0E+00 | 0E+00 | + | decrease |
| LOC100038328 | XP_020937734 | -1.35 | 4E-05 | 7E-04 | + | decrease |
| ALG1 | XP_013851121 | -1.38 | 1E-04 | 2E-03 | + | decrease |
| LOC100152327 | NP_001230248 | -1.41 | 0E+00 | 0E+00 | + | decrease |

| | | | | | | |
|---------------------|--------------|-------|-------|-------|---|----------|
| USH2A | XP_020919951 | -1.43 | 2E-05 | 4E-04 | + | decrease |
| LOC100525572 | XP_020945289 | -1.59 | 2E-05 | 4E-04 | + | decrease |
| LOC396781 | NP_998993 | -1.62 | 0E+00 | 0E+00 | + | decrease |

Table 16: Pancreas duodenal

| Gene | Protein accession | l2fc | P value | FDR | Sign. | Abundance change |
|---------------------|--------------------------|-------------|----------------|------------|--------------|-------------------------|
| HMGN3 | XP_005659480 | 1.70 | 5E-04 | 1E-02 | + | increase |
| LOC110255172 | XP_020922490 | 1.25 | 2E-09 | 3E-07 | + | increase |
| FABP4 | NP_001002817 | 1.21 | 0E+00 | 0E+00 | + | increase |
| LOC100515185 | XP_003122092 | 1.03 | 9E-04 | 2E-02 | + | increase |
| SELENOH | NP_001171877 | 0.91 | 5E-04 | 1E-02 | + | increase |
| LOC100515741 | XP_013853463 | 0.83 | 9E-09 | 9E-07 | + | increase |
| SCGN | NP_001070692 | 0.78 | 7E-15 | 2E-12 | + | increase |
| LOC110261434 | XP_020953497 | 0.77 | 9E-10 | 1E-07 | + | increase |
| ACADL | NP_999062 | 0.72 | 1E-03 | 2E-02 | + | increase |
| SST | NP_001009583 | 0.72 | 2E-04 | 4E-03 | + | increase |
| PCK2 | NP_001155225 | 0.66 | 0E+00 | 0E+00 | + | increase |
| ACADSB | XP_001926332 | 0.64 | 4E-16 | 1E-13 | + | increase |
| PSAT1 | XP_020920809 | 0.62 | 1E-04 | 3E-03 | + | increase |
| TDH | XP_020927752 | -0.65 | 2E-03 | 4E-02 | + | decrease |
| PPY | XP_013836362 | -0.66 | 2E-04 | 4E-03 | + | decrease |
| SOD3 | NP_001072156 | -0.66 | 9E-04 | 2E-02 | + | decrease |
| CLU | XP_020927747 | -0.76 | 3E-12 | 7E-10 | + | decrease |
| LIMA1 | NP_001108148 | -0.76 | 2E-03 | 4E-02 | + | decrease |
| PNLIPRP2 | NP_001177220 | -0.79 | 2E-14 | 6E-12 | + | decrease |
| ADA | XP_020933637 | -0.87 | 5E-06 | 3E-04 | + | decrease |
| FAM50A | XP_020936411 | -0.96 | 1E-04 | 3E-03 | + | decrease |
| LOC100038328 | XP_020937734 | -1.08 | 1E-04 | 3E-03 | + | decrease |
| LOC100152327 | NP_001230248 | -1.09 | 9E-14 | 2E-11 | + | decrease |
| USH2A | XP_020919951 | -1.16 | 5E-04 | 1E-02 | + | decrease |
| ENAH | XP_020920069 | -1.18 | 3E-03 | 5E-02 | + | decrease |
| LOC396781 | NP_998993 | -1.26 | 0E+00 | 0E+00 | + | decrease |

First 100 Single cell RNA sequencing genes upregulated and downregulated in the β -cells of the PHG group compared to the PNG group.

Table 17: First 100 genes upregulated in the PHG vs. PNG

| names | logfc | logexprs | pvals_adj | log_pvals_adj |
|--------------------|----------|----------|-----------|---------------|
| CLEC3B | 4.230699 | 2.8903 | 3.33E-32 | 31.47721 |
| TENM1 | 3.591512 | 3.531667 | 6.27E-34 | 33.20239 |
| PPP1R16B | 3.388894 | 2.567133 | 4.03E-30 | 29.39449 |
| SLC18A1 | 3.258686 | 3.369335 | 1.37E-32 | 31.86349 |
| NEUROG3 | 3.100637 | 4.682485 | 5.1E-37 | 36.29281 |
| RBP4 | 2.755953 | 6.850883 | 7E-36 | 35.15479 |
| ssc-mir-670 | 2.68421 | 3.24218 | 6.1E-29 | 28.21449 |
| SMOC2 | 2.47925 | 3.623264 | 3.92E-31 | 30.40631 |
| ALDOB | 2.468825 | 7.482541 | 3.96E-34 | 33.4027 |
| KCNJ2 | 2.356714 | 2.742325 | 4.23E-26 | 25.37361 |
| SERPIND1 | 2.290419 | 3.850219 | 1.4E-29 | 28.85302 |
| LHFPL3 | 2.290393 | 2.746967 | 1.96E-24 | 23.70807 |
| CCDC3 | 2.251988 | 4.288777 | 4.78E-33 | 32.32045 |
| STK33 | 2.122843 | 4.00985 | 2.87E-29 | 28.542 |
| TSPAN2 | 2.072036 | 2.376227 | 4.27E-22 | 21.36999 |
| KAZN | 2.033264 | 5.423855 | 8.09E-37 | 36.09187 |
| PFKFB3 | 2.00546 | 3.615962 | 2.86E-28 | 27.54307 |
| FN1 | 1.961151 | 5.726308 | 4.97E-37 | 36.30336 |
| IER5L | 1.925375 | 2.598948 | 6.4E-24 | 23.19348 |
| ITPRID2 | 1.891308 | 2.636061 | 1.27E-23 | 22.89666 |
| PLA2G1B | 1.88589 | 4.954073 | 2.43E-31 | 30.6145 |
| CCND1 | 1.873318 | 4.40249 | 8.37E-31 | 30.07716 |
| LEPR | 1.852607 | 4.853647 | 3.26E-32 | 31.48681 |
| SLC25A29 | 1.847863 | 4.692328 | 2.15E-32 | 31.66854 |
| HSPA6 | 1.839099 | 5.402723 | 4.85E-33 | 32.31423 |
| ACKR3 | 1.83663 | 4.185058 | 2.97E-28 | 27.52763 |
| CSMD3 | 1.831094 | 3.436843 | 8.03E-26 | 25.09543 |
| RNF128 | 1.81423 | 3.10895 | 8.64E-25 | 24.06346 |
| PCDH9 | 1.813768 | 7.016085 | 1.94E-39 | 38.71194 |
| PIZO1 | 1.799019 | 3.097367 | 1.99E-25 | 24.70189 |
| FLRT1 | 1.771503 | 3.974827 | 2.67E-29 | 28.57421 |
| KCNN2 | 1.763937 | 2.404234 | 4.7E-22 | 21.3283 |
| RYR2 | 1.754848 | 3.828452 | 1.08E-27 | 26.96825 |
| RABEPK | 1.663111 | 5.801435 | 2.15E-35 | 34.66713 |
| IGF2R | 1.659694 | 5.308757 | 3.22E-34 | 33.49191 |
| EPAS1 | 1.645797 | 3.711617 | 8.03E-26 | 25.09543 |
| KCNN3 | 1.643256 | 3.074706 | 6.67E-24 | 23.17581 |
| PLCL1 | 1.63719 | 2.842428 | 2.28E-19 | 18.64231 |
| GABBR2 | 1.609047 | 3.999807 | 1.14E-27 | 26.94347 |

| | | | | |
|-----------------|----------|----------|----------|----------|
| ITGBL1 | 1.59193 | 5.71226 | 2.55E-35 | 34.59294 |
| DUSP2 | 1.559793 | 3.012453 | 3.7E-21 | 20.43153 |
| MGAT3 | 1.543393 | 5.237811 | 9.88E-33 | 32.00503 |
| SYNPO | 1.528158 | 3.451115 | 8.22E-25 | 24.08502 |
| SLC25A21 | 1.515214 | 3.65952 | 2.36E-25 | 24.62631 |
| DNAJB1 | 1.51339 | 9.170067 | 3.65E-43 | 42.4382 |
| PTPRU | 1.510908 | 2.918494 | 4.18E-22 | 21.37851 |
| GP2 | 1.510261 | 2.504302 | 1.68E-20 | 19.7742 |
| ADGRF5 | 1.49768 | 2.381595 | 4.02E-20 | 19.39558 |
| KLF15 | 1.457362 | 2.492716 | 6.36E-20 | 19.19633 |
| GLRA3 | 1.449577 | 4.334909 | 9.18E-27 | 26.0371 |
| SLC8A3 | 1.411219 | 2.924293 | 2.94E-20 | 19.53189 |
| DPP6 | 1.407504 | 2.851554 | 2.23E-20 | 19.65115 |
| ARHGAP24 | 1.40184 | 5.830279 | 1.37E-33 | 32.86202 |
| CTPS1 | 1.397649 | 2.30538 | 6.99E-19 | 18.15561 |
| ALG8 | 1.39349 | 5.912588 | 2.32E-34 | 33.6341 |
| GADD45B | 1.391177 | 3.984668 | 1.2E-24 | 23.91928 |
| SHISAL1 | 1.389865 | 3.36241 | 2.32E-23 | 22.63414 |
| ATP2A3 | 1.358212 | 5.09656 | 3.12E-30 | 29.50548 |
| KCNT2 | 1.353702 | 4.375682 | 6.18E-27 | 26.20872 |
| SNORA81 | 1.351748 | 4.788179 | 1.62E-28 | 27.79027 |
| GLP1R | 1.347055 | 2.860381 | 1.52E-20 | 19.81898 |
| MAGI2 | 1.3413 | 4.753427 | 7.53E-29 | 28.12345 |
| PTPRD | 1.32318 | 6.114763 | 5.68E-35 | 34.24592 |
| ADGRB3 | 1.316744 | 4.84165 | 1.86E-25 | 24.72965 |
| FOXP2 | 1.31513 | 3.857109 | 1.36E-24 | 23.86514 |
| TMCC3 | 1.314938 | 3.632925 | 3.48E-23 | 22.45887 |
| TLE4 | 1.27849 | 2.427868 | 7.36E-19 | 18.13329 |
| DLL1 | 1.273903 | 3.338008 | 1.71E-21 | 20.76672 |
| AMIGO2 | 1.269375 | 5.738373 | 3.08E-32 | 31.51155 |
| DISP3 | 1.266833 | 5.348542 | 9.77E-31 | 30.01022 |
| HSPH1 | 1.260128 | 6.968718 | 1.25E-36 | 35.90155 |
| IGFBP1 | 1.258356 | 3.22741 | 2.93E-21 | 20.53279 |
| HTR2A | 1.256693 | 2.579946 | 6.06E-19 | 18.21739 |
| KIAA0930 | 1.251544 | 6.043241 | 2.27E-33 | 32.64405 |
| IFI6 | 1.243345 | 6.004592 | 8.36E-30 | 29.07755 |
| COL16A1 | 1.242529 | 3.528475 | 3.29E-22 | 21.48239 |
| DDIT3 | 1.221839 | 4.519535 | 2.45E-24 | 23.61072 |
| PDLIM1 | 1.210507 | 3.659949 | 3.08E-22 | 21.51085 |
| KHDRBS3 | 1.210128 | 3.03189 | 5.97E-20 | 19.22404 |
| NPAS4 | 1.204885 | 6.995708 | 3.17E-32 | 31.49899 |
| SYNJ2 | 1.19071 | 2.347662 | 3.57E-16 | 15.44752 |
| DPYSL3 | 1.18982 | 3.446577 | 7.83E-22 | 21.10614 |
| KCNB1 | 1.187194 | 4.378371 | 4.93E-26 | 25.30718 |
| PRKCA | 1.172726 | 6.708946 | 3.08E-36 | 35.51078 |
| A1CF | 1.171787 | 6.209182 | 1.64E-33 | 32.78439 |

| | | | | |
|-----------------|----------|----------|----------|----------|
| SLC16A3 | 1.161611 | 2.853988 | 6.79E-19 | 18.16807 |
| TMEM179 | 1.159582 | 5.187929 | 3.62E-29 | 28.44188 |
| C1orf21 | 1.158321 | 3.671876 | 1.61E-21 | 20.79223 |
| SLC36A1 | 1.147335 | 3.538855 | 4.98E-21 | 20.30301 |
| ACTRT3 | 1.139778 | 2.403254 | 9.37E-17 | 16.02841 |
| PDE9A | 1.127694 | 2.708322 | 3.88E-18 | 17.41104 |
| EPHA3 | 1.124071 | 2.899606 | 4.03E-18 | 17.39459 |
| ADAMTSL4 | 1.122968 | 2.99486 | 2.74E-16 | 15.56222 |
| EGFR | 1.116382 | 4.090148 | 1.53E-23 | 22.81513 |
| SLC10A1 | 1.107889 | 4.254268 | 9E-25 | 24.04581 |
| PRKD1 | 1.107329 | 2.359469 | 4.81E-15 | 14.31762 |
| KCNG2 | 1.096798 | 3.577826 | 4.3E-21 | 20.36638 |
| PLXNA4 | 1.090409 | 3.974074 | 3.56E-23 | 22.44857 |
| CEBPA | 1.087577 | 2.633923 | 2.24E-17 | 16.64993 |
| ZNF483 | 1.08324 | 4.057451 | 1.26E-23 | 22.8996 |

Table 18: First 100 genes downregulated in the PHG vs. PNG

| names | logfc | logexprs | pvals_adj | log_pvals_adj |
|-----------------|----------|----------|-----------|---------------|
| CDH17 | -0.88728 | 2.58978 | 6.7E-12 | 11.17378 |
| RPS3A | -0.88812 | 10.30699 | 2.69E-39 | 38.57089 |
| INA | -0.89013 | 3.340901 | 1.91E-13 | 12.71836 |
| SNTB1 | -0.89378 | 2.336769 | 8.53E-13 | 12.06902 |
| HADH | -0.89962 | 8.547736 | 6.15E-34 | 33.21085 |
| GPATCH11 | -0.90147 | 5.974116 | 2.24E-27 | 26.64955 |
| PSME1 | -0.9021 | 5.086617 | 4.52E-24 | 23.34472 |
| ARPC5 | -0.90787 | 5.500655 | 9.43E-26 | 25.02561 |
| PLS3 | -0.91001 | 3.111045 | 1.62E-15 | 14.79 |
| ROM1 | -0.91134 | 2.842402 | 3.78E-14 | 13.42222 |
| CD247 | -0.91369 | 4.343675 | 4.03E-20 | 19.39484 |
| SLC2A2 | -0.91644 | 7.340356 | 3.74E-31 | 30.42728 |
| RACK1 | -0.91838 | 9.763996 | 1.37E-38 | 37.86417 |
| DHRS4 | -0.92239 | 2.384148 | 2.01E-12 | 11.69607 |
| CYRIA | -0.924 | 3.21961 | 3.07E-16 | 15.51263 |
| APEX1 | -0.92436 | 4.26272 | 1.22E-19 | 18.91226 |
| SNCG | -0.92824 | 3.238877 | 9.79E-16 | 15.00923 |
| RPS4X | -0.93494 | 10.33094 | 1.94E-39 | 38.71194 |
| PSMB8 | -0.93705 | 3.315556 | 5.72E-15 | 14.24289 |
| PRXL2B | -0.9412 | 4.609724 | 3.36E-22 | 21.47331 |
| ST8SIA5 | -0.94298 | 2.819035 | 1.65E-14 | 13.78174 |
| MAP4K1 | -0.95357 | 2.160865 | 8.04E-13 | 12.09471 |
| TES | -0.95557 | 2.899605 | 9.25E-15 | 14.03401 |

| | | | | |
|------------------|----------|----------|----------|----------|
| COX7C | -0.96275 | 7.178196 | 1.86E-31 | 30.73008 |
| TNFRSF11A | -0.96662 | 4.274279 | 3.39E-21 | 20.46982 |
| ASIC1 | -0.96808 | 3.918211 | 1.5E-19 | 18.82285 |
| TFF2 | -0.97199 | 2.344586 | 8.11E-13 | 12.09114 |
| CRYBA2 | -0.97221 | 6.854855 | 8.24E-32 | 31.08384 |
| PLPPR4 | -0.97393 | 2.686736 | 6.43E-14 | 13.19191 |
| TRIB2 | -0.97437 | 5.236696 | 1.66E-24 | 23.78049 |
| WFDC1 | -0.97507 | 5.210097 | 8.42E-25 | 24.0747 |
| HEBP1 | -0.97636 | 3.671179 | 2.91E-18 | 17.53605 |
| GBA3 | -0.977 | 6.130973 | 7.3E-29 | 28.13654 |
| RARRES2 | -0.97801 | 5.529417 | 6.18E-27 | 26.20872 |
| ENTPD3 | -0.98032 | 4.363835 | 7.11E-22 | 21.14833 |
| AARD | -0.98139 | 5.751599 | 1.54E-26 | 25.81335 |
| EFEMP2 | -0.98524 | 2.478795 | 1.33E-13 | 12.8777 |
| CNTN4 | -0.99405 | 4.785563 | 1.56E-23 | 22.80695 |
| PIK3IP1 | -1.00351 | 3.749657 | 5.14E-19 | 18.28939 |
| C1orf194 | -1.00413 | 4.254023 | 6.17E-22 | 21.21003 |
| ANXA2 | -1.00884 | 9.37683 | 1.77E-36 | 35.75186 |
| ZFY | -1.01428 | 4.006881 | 6.49E-20 | 19.1877 |
| CEACAM16 | -1.01947 | 2.287112 | 1.54E-13 | 12.81382 |
| TSTD1 | -1.02914 | 4.900044 | 4.3E-24 | 23.36686 |
| MKRN2OS | -1.03055 | 3.186632 | 2.71E-17 | 16.56772 |
| CASP3 | -1.03736 | 3.354574 | 4.97E-17 | 16.30346 |
| ACVR1C | -1.04092 | 3.47668 | 4.95E-18 | 17.30558 |
| PTER | -1.04333 | 2.456115 | 1.21E-13 | 12.91666 |
| GLIPR2 | -1.05682 | 3.527885 | 1.54E-18 | 17.81216 |
| JUP | -1.05757 | 4.034189 | 3.23E-20 | 19.4904 |
| PLA2G10 | -1.06682 | 2.656444 | 8.15E-16 | 15.08873 |
| CFAP300 | -1.07018 | 2.761667 | 5.68E-16 | 15.2455 |
| ZNF467 | -1.07187 | 3.289023 | 4.96E-18 | 17.30453 |
| ESM1 | -1.07907 | 7.797595 | 1.65E-34 | 33.78288 |
| SMAD9 | -1.08289 | 4.255607 | 1.27E-21 | 20.89614 |
| ENTPD5 | -1.08642 | 4.540023 | 5.06E-24 | 23.29597 |
| PROS1 | -1.10305 | 3.134636 | 6.58E-18 | 17.18207 |
| FEV | -1.11051 | 3.28578 | 2.12E-17 | 16.67448 |
| NFIX | -1.11327 | 3.283657 | 1.05E-17 | 16.97793 |
| CRACR2B | -1.1196 | 2.566437 | 1.94E-15 | 14.7126 |
| HIGD1A | -1.12534 | 6.88973 | 1.43E-33 | 32.84384 |
| EPB41L4A | -1.12713 | 4.132599 | 2.09E-22 | 21.68028 |
| LZTS1 | -1.13905 | 2.599383 | 4.19E-15 | 14.37803 |
| DDAH2 | -1.14113 | 3.800651 | 3.2E-21 | 20.49533 |
| NR1D1 | -1.15248 | 3.660699 | 2.75E-20 | 19.56014 |
| LYPD6B | -1.15598 | 4.34066 | 1.72E-22 | 21.76342 |
| SLC38A2 | -1.16185 | 4.521077 | 2.7E-24 | 23.56819 |
| TMEM141 | -1.1874 | 5.801254 | 3.49E-30 | 29.4576 |
| DCX | -1.19843 | 5.389401 | 1.11E-27 | 26.95314 |

| | | | | |
|----------------------------|----------|----------|----------|----------|
| ABRACL | -1.20216 | 3.030198 | 4.23E-18 | 17.37336 |
| GABRD | -1.20661 | 2.410296 | 5.41E-16 | 15.26644 |
| RND3 | -1.22057 | 4.311487 | 9.78E-24 | 23.00978 |
| MAMDC2 | -1.2277 | 3.480921 | 2.26E-19 | 18.64617 |
| OR51E1 | -1.23953 | 3.821675 | 4.19E-22 | 21.37827 |
| CD82 | -1.27889 | 2.320351 | 1.12E-15 | 14.95001 |
| RPL36A- HNRNPH2 | -1.28794 | 8.551686 | 1.07E-39 | 38.96993 |
| ADRA2A | -1.2971 | 3.455201 | 4.72E-20 | 19.32639 |
| RSPH9 | -1.3047 | 3.17516 | 4.23E-19 | 18.37393 |
| CLRN3 | -1.32311 | 3.961523 | 2.81E-23 | 22.55097 |
| TEF | -1.3294 | 4.639092 | 1.53E-26 | 25.81431 |
| PCDH7 | -1.34614 | 3.200948 | 3.63E-19 | 18.44049 |
| TNFAIP8 | -1.35894 | 2.921744 | 1.57E-18 | 17.8049 |
| CALML4 | -1.36227 | 5.568856 | 2.66E-31 | 30.57589 |
| SLIT3 | -1.40107 | 2.854988 | 5.76E-19 | 18.2393 |
| ATP6V1D | -1.42818 | 6.717596 | 2.27E-36 | 35.64437 |
| LYL1 | -1.49824 | 2.664101 | 2.93E-18 | 17.53328 |
| CIART | -1.54204 | 3.818136 | 6.5E-24 | 23.18681 |
| IFITM3 | -1.56332 | 7.155524 | 3.59E-31 | 30.44522 |
| MGAM | -1.56582 | 3.429148 | 8.11E-23 | 22.09124 |
| AP1S2 | -1.57796 | 6.951142 | 1.7E-37 | 36.77041 |
| SPON1 | -1.63432 | 3.139629 | 4.24E-21 | 20.37288 |
| DBP | -1.69719 | 5.462463 | 3.47E-31 | 30.46006 |
| LRRN3 | -1.72587 | 5.94403 | 5.21E-35 | 34.28328 |
| NUPR1 | -1.83217 | 4.887647 | 1.57E-30 | 29.80333 |
| PRSS35 | -1.84195 | 4.033065 | 2.55E-27 | 26.59311 |
| FAM13C | -1.91229 | 3.362718 | 1.85E-23 | 22.73362 |
| FRZB | -1.95495 | 3.4978 | 1.24E-24 | 23.90593 |
| CDA | -2.1481 | 6.21477 | 3.33E-39 | 38.47746 |
| NRXN3 | -2.181 | 3.287481 | 2.95E-25 | 24.53028 |
| LSM6 | -2.23399 | 6.955934 | 1.06E-41 | 40.97434 |
| MFAP2 | -2.36575 | 2.896124 | 6.25E-24 | 23.20405 |
| CALB1 | -2.60929 | 5.782667 | 2.92E-38 | 37.53533 |

